

NUMERICAL SIMULATION OF THE PERFORMANCE OF HORIZONTAL DRAINS FOR
SUBSURFACE SLOPE STABILIZATION

BY

MARIE LEONY PATHMANATHAN

A thesis submitted in partial fulfillment of
the requirements for the degree of

MASTER OF SCIENCE IN CIVIL ENGINEERING

WASHINGTON STATE UNIVERSITY
Department of Civil and Environmental Engineering

May 2009

To the Faculty of Washington State University:

The members of the Committee appointed to examine the thesis of MARIE LEONY
PATHMANATHAN find it satisfactory and recommend that it be accepted.

Dr. Balasingam Muhunthan

Dr. Akram Hossain

Dr. William F. Cofer

ACKNOWLEDGEMENTS

My utmost gratitude goes to my advisor, Dr. Balasingam Muhunthan for allowing me to join his team, for his guidance, kindness, and most of all, for his patience. My thanks and appreciation also goes to my thesis committee members, Dr. William Cofer and Dr. Akram Hossain. I am greatly indebted to my family friends Dr. Nirmala Gnanapragasam, Dr. Nadarajah Sivanewaran and Dr. Navaratnarajah Sasiharan for exhorting me to pursue a graduate degree in geotechnical engineering. I thank my friends in Pullman for the memorable time.

I wouldn't be performing this work without my family's continuous support. First, I have to thank my husband, Priyatharshan. His continuous encouragement and support cannot be described by a word. I thank all my family members for their continuous support and interest in whatever I have pursued. Their love and prayers gave me the strength. Especially, I would like to thank my parents, brother and sister for their unconditional loves and prayers.

Special thanks are extended to the Department of Civil and environmental engineering, Washington State University and Washington State Department of Transportation pooled fund research for assisting me with funds to complete the research and my Masters.

This work would not have been completed without the help and support of many individuals. I would like to thank everyone who has helped me along the way. Particularly: Tom Badger, Washington State Department of Transportation, chief Geologist for providing continuous help throughout this research; Dr. Roger Beckie for giving me the valuable guidance; Dr. Adrian Rodriguez-Marek for his support and friendship as a professor in Geotechnical engineering division; Dr. Sadiq Zarrouk for his valuable help with TOUGH2 simulation software; Dr. Karsten Pruess for TOUGH2 software support; Tom Weber for assisting me with computing resources; Vicki Ruddick for the assistance on administrative work.

NUMERICAL SIMULATION OF THE PERFORMANCE OF HORIZONTAL DRAINS FOR THE SUBSURFACE SLOPE STABILIZATION

Abstract

By Marie Leony Pathmanathan, M.S.
Washington State University
May 2009

Chair: Balasingam Muhunthan

Numerous slope failures are caused by heavy rainfall. During these rainfall periods, the ground water table rises up contributing to an increase in porewater pressure and a reduction in slope stability. Therefore, lowering of the ground water table is important for reducing the pore water pressure and increasing the stability of the slope. Installing horizontal drains is a very efficient and cost effective method for lowering the ground water table. The horizontal drains method has a well established theory, but there seems to be limited resources available for designing horizontal drains. The objective of this research is to develop design charts for optimal design of subsurface drainage systems. A finite difference based numerical simulator called TOUGH2 was used to model selected sites in the state of Washington. Simulated pressure values were matched to the site instrumentation data. The failure surface was located using XSTABL. A parametric study was conducted on a model slope to find optimal design parameters such as number of drains, elevation of drains, and spacing between drains.

The study showed that the anisotropic permeability ratio is an important soil parameter in influencing the horizontal drain performance because it changes the profile of phreatic surfaces very much. It was found that slopes with higher ratios of permeability stabilized quicker than those with lower ratios of permeability. The study found that drains installed along the toe of the slide give more stability than those installed in higher elevations. The stability of the slope also increased with increasing length of drains and decreased when drains are spaced at larger intervals. Charts quantifying the changes have been developed. The length of drain extending longer than its intersection with the critical failure surface is found not to provide an increase in factor of safety.

TABLE OF CONTENTS

	Page
ACKNOWLEDGEMENTS.....	iii
ABSTRACT	iv
LIST OF TABLES	viii
LIST OF FIGURES	ix
CHAPTER ONE: INTRODUCTION.....	1
1.1. Background.....	1
1.2. Objectives	4
1.3. Organization of Thesis	4
CHAPTER TWO: LITERATURE REVIEW.....	5
2.1. Introduction	5
2.2. Hutchinson (1977)	6
2.3. Lau and Kenney (1983).....	7
2.4. Cai et al. (1998)	8
2.5. Rahardjo et al. (2002).....	10
CHAPTER THREE: FIELD PERFORMANCE OF SELECTED SITES	13
3.1. SR 101 MP 69.8 – South of Aberdeen, Washington	15
3.2. SR 101 MP 184 –Washington (Bogachiel Slide)	21
3.3. SR 101 MP 322, Lilliwaup, Washington	25
3.4. SR 101 MP 326 – Lilliwaup, Washington	29
3.5. SR 530 – Skaglund Hill Landslide, Washington.....	31
3.6. Route 80 California – Redtop Landslide.....	36
3.7. Summary	42
CHAPTER FOUR: TOUGH2 COMPUTER CODE.....	43
4.1. Introduction	43
4.2. Flow equations.....	44
4.3. Space and time discretization	46
4.4. Initial and Boundary conditions.....	47

4.5.	Solution of Linear Equations.....	47
4.6.	TOUGH2 Architecture.....	48
4.7.	Data Input and Initialization.....	49
4.8.	Equation-Of-State Modules.....	51
4.9.	Supporting Tools.....	52
CHAPTER FIVE: VERIFICATION OF NUMERICAL SIMULATION OF FLOW PATTERN AND SLOPE STABILITY ANALYSIS.....		54
5.1.	Introduction	54
5.2.	MP69.8 Site Geometry.....	54
5.3.	TOUGH2 model	55
5.4.	Simulation of Water Level	56
5.5.	Slope failure analysis	59
5.6.	Equivalent Slope Stability Model Using XSTABL.....	60
5.7.	Summary of verification results.....	62
CHAPTER SIX: PARAMETRIC STUDY AND DESIGN CHARTS.....		64
6.1.	Introduction	64
6.2.	Model geometry and TOUGH2 simulations	65
6.3.	Parametric Study.....	69
6.4.	Stability Calculations using XSTABL.....	71
6.5.	Design Charts	74
CHAPTER SEVEN: CONCLUSIONS AND DISCUSSIONS.....		79
7.1.	Conclusions	79
7.2.	Recommendations.....	81
REFERENCES		82

LIST OF TABLES

	Page
Table 2-1: Hydraulic properties of soils (Cai et al. 1998).....	9
Table 3-1: Description of data	14
Table 5-1: Soil properties at SR 101 MP 69.8 site	60
Table 6-1: Different horizontal drain arrangements and groundwater conditions	70
Table 6-2: FOS, Difference in FOS (ΔF) for different horizontal drain arrangements	73
Table 6-3. FOS for different slope angles	74

LIST OF FIGURES

	Page
Figure 2.1: Finite element mesh for the selected model (Cai et al. 1998)	9
Figure 2.2: Profiles of selected slopes (Rahardjo et al., 2002).....	11
Figure 2.3: Drain locations, finite element mesh for the selected slope (Rahardjo et al., 2002) .	12
Figure 3.1: Directory structure of instrumented data in compact disk.....	15
Figure 3.2: Plan of slide area at SR 101 MP 69.8 (Kleinfelder 2006)	16
Figure 3.3: Cross-section of slide area at SR 101 MP 69.8 (Kleinfelder 2006).....	17
Figure 3.4: Site plan with emergency drains at SR 101 MP 69.8 (Kleinfelder 2006).....	17
Figure 3.5: Selected stabilization option at SR 101 MP 69.8 (Kleinfelder 2006)	18
Figure 3.6: Cross-section of slide area with selected stabilization option at SR 101 MP 69.8 (Kleinfelder 2006).....	18
Figure 3.7: Boring locations at SR 101 MP 69.8 (Kleinfelder 2006)	20
Figure 3.8: Inclinator plot at SR 101 MP 69.8.....	20
Figure 3.9: Piezometer and rain data Vs time at SR 101 MP 69.8	21
Figure 3.10: Landslide plan with horizontal drains at SR 101 MP 184 (WSDOT 2007)	22
Figure 3.11: Boring locations at SR 101 MP 184 (WSDOT 2007)	24
Figure 3.12: Piezometer and rainfall data Vs time at SR 101 MP 184.....	24
Figure 3.13: Inclinator data vs time at SR 101 MP 184	25
Figure 3.14: SR 101 MP 322, site plans (Golder, 2000).....	26
Figure 3.15: Boring locations at SR 101 MP 322 (WSDOT).....	27
Figure 3.16: SR 101 MP 322, piezometer chart	28
Figure 3.17: SR 101 MP 322, inclinometer charts.....	28
Figure 3.18: SR 101 MP 326, site plan (WSDOT 2007)	29
Figure 3.19: Piezometer plots at SR 101 MP 326.....	30
Figure 3.20: SR 101 MP 326, inclinometer charts.....	31
Figure 3.21 Site plan of SR 530, skaglund hill (Landau 1993)	32
Figure 3.22: Horizontal drain layout of SR 530, Skaglund hill (Landau 1993)	33
Figure 3.23: Cross-sectional view of subsurface conditions (Landau 1993)	34
Figure 3.24: Boring plan at SR 530 skaglund hill (Landau 1993).....	35

Figure 3.25: Ground waterlevel & rainfall during february 2006 to june 2006 at SR 530 MP 36.5 (WSDOT, instrumentation)	35
Figure 3.26: Cumulative displacement from february 2006 to march 2006 at SR 530 MP 36.5 (WSDOT, instrumentation)	36
Figure 3.27: Site plan at r 80 Redtop landslide (CALTRANS 2001)	37
Figure 3.28: Site plan at r 80 Redtop landslide (CALTRANS 2007)	38
Figure 3.29: Site plan, cross section of R 80 Redtop landslide (CALTRANS 2001)	39
Figure 3.30: Profile of shaft in landslide, (b)–shaft detail at R 80 redtop landslide (CALTRANS 2001)	41
Figure 3.31: Piezometer elevation and horizontal ground movement vs time from november 1998 to march 2005 at r80, redtop landslide (CALTRANS 2007)	42
Figure 4.1: Space discretization and geometry data in the integral finite difference method (Pruess, 1999)	46
Figure 4.2: Modular “MULKOM” architecture of TOUGH2 (Pruess, 1999)	49
Figure 5.1: Model geometry of SR 101 MP 69.8	55
Figure 5.2: Simulated initial phreatic surface and piezometric data before installed the drains ...	56
Figure 5.3: Porewater pressure contour (in kPa) for SR 101 MP 69.8	57
Figure 5.4: Velocity vector plot for SR 101 MP 69.8	57
Figure 5.5: Overlay of groundwater levels from simulations and field at SR 101 MP 69.8	58
Figure 5.6: XSTABL input geometry	59
Figure 5.7: Identified field failure surface (Kleinfelder 2006)	60
Figure 5.8: Identified larger failure surface from XSTABL	61
Figure 5.9: Identified smaller failure surface from XSTABL	61
Figure 5.10 Improved FOS after installing horizontal drains for failure planes.	62
Figure 6.1: Geometry, cross-section with initial phreatic surface	66
Figure 6.2: Mesh geometry of the selected model	67
Figure 6.3: Modeled phreatic surfaces for the slope with no drains	68
Figure 6.4: Two dimensional distribution of porewater pressure (in kpa) of model with $k_h/k_v = 5$	68
Figure 6.5: Cross section of slope with drain location and variables	69
Figure 6.6: Drain location along the width of slope	69

Figure 6.7: Average porewater pressure (in kPa) distribution of slope with drain $k_h/k_v = 5$	71
Figure 6.8: Identified failure surface for selected model	72
Figure 6.9: Minimum safety factor for critical surface against elevation of drains.....	74
Figure 6.10: Minimum safety factor for critical surface against length of drains	75
Figure 6.11: Minimum safety factor for critical surface against spacing between drains	75
Figure 6.12: Minimum safety factor for critical surface against slope angle	76
Figure 6.13: Increase in FOS ratio Versus Elevation of drains	76
Figure 6.14: Increase in FOS ratio Versus Length of drains	77
Figure 6.15: Increase in FOS Versus Spacing between drains.....	77

CHAPTER ONE

INTRODUCTION

1.1. Background

Rapidly rising groundwater level leads in most cases to slope failures. Thus, to improve the stability, water level should be lowered. Surface drains such as trenches are sufficient to improve the stability when the failure planes are shallow. The horizontal drains method is a cost effective and widely used method to draw down the water table for deep-seated failures. Though commonly termed “horizontal drain method”, drains are installed in a slightly upward direction to facilitate drainage by gravity. The typical drains are 2 to 4 inches (50 to 100mm) in diameter and are installed on hill slopes extending to 200 to 300 feet (60 to 90m) in length. First a hole is drilled on the slope, and then a perforated PVC pipe is inserted through the hole.

While horizontal drains have been used in an ad hoc manner throughout civilization, the first documented case of the use of horizontal drains in North America was in California. Stanton (1948) reported the successful use of horizontal drains to stabilize a large number of slides by the California Division of Highways. Since then a number of published case histories from many countries have shown the effectiveness of horizontal drains to stabilize slopes and embankments under a variety of geological and hydrological conditions (Smith and Stafford 1957; Tong and Maher 1975; Hutchinson 1977; Lamb 1980, Mallawaratchie et al. 1996; Santi et al. 2001 and Tsao et al. 2005).

Early installations generally consisted of perforated steel pipes without filters that were prone to both corrosion and siltation. Thus, Smith and Stafford (1957) recommended that the 6m length of drain nearest to the outlet should be galvanized and non-perforated to slow down

corrosion and hinder choking of the pipe by roots. More recently perforated plastic PVC pipes have been used with filters formed of porous concrete, resin bonded sand or synthetic filter fabrics (Hutchinson 1977). In jointed rock and residual soil masses, the use of impermeable inverts has been advocated (Choi 1974).

In many projects, site constraints and the depth of water-bearing deposits below existing site grades prevent the use of conventional subsurface drainage methods and a common problem with slotted PVC pipes is the required periodic maintenance to remove soil clogs. The use of geotextile prevents the clogging of the drain.

This study is focused on the performance of horizontal drains. Effectiveness of the horizontal drainage system is a function of many factors including the drain location, length and spacing, as well as soil properties and slope geometry. Typically, effectiveness is described in terms of the increase in slope factor of safety as compared to factor of safety without horizontal drains. Most design of horizontal drains is governed by local experience, with the quantity of water discharge as the main criterion of success. However, many field case studies as well as analytical models have demonstrated that the change in flow pattern, resulting in the change in pressure distribution is critical for the success of stabilization. Especially in clay slopes, the reduction of pore water pressures may be achieved with very small yield of water.

Even though horizontal drains have been used for long time, limited research effort has been made on improving slope stability using subsurface drainage. Principles, design, and maintenance documentation for horizontal drains or subsurface drainage were not fully realized. Drains are installed roughly to prevent damage from landslides for a short period of time,

resulting in various levels of success. Design of drainage is mostly based on empirical and subjective methods.

The need for a rational design method for drains has been noted by several researchers and various charts and diagrams have been developed (Choi, 1974; Kenney et al. 1977). These design charts have yet to be calibrated against field experience. In recent years various numerical models have been used to study the flow pattern when the horizontal drain is present (Chen et al., 2003; Crenshaw and Santi, 2004; Samani et al., 2005).

There have been a few studies made that describe the different parameters controlling the horizontal drainage systems. Martin et al (1994) have suggested that a small number of drains installed at appropriate locations in accordance with a well-conceived conceptual ground water model may be more effective than a large number of drains installed at uniform spacing over the slope. Field monitoring of two residual soil slopes in Singapore complemented with a parametric study on drain position by Rahardjo et al. (2002) confirmed this finding.

This study first presents a detailed examination of the field performance of horizontal drains on some selected slopes in the states of Washington (WA) and California (CA). It includes the site location, details of the project, geotechnical and geologic records, drain location, instrumentation details, and performance data. The sites are used for further examination using an advanced numerical model. The finite difference computer code TOUGH2 V2.0 (Pruess et al. 1999) is used in the simulation. The model is verified on a well instrumented slope in Washington State and then used to make a parametric study to elicit information on system performance.

1.2. Objectives

The specific objectives of this study are to:

1. Document and examine the field performance of selected sites in Washington and California. Identify key geologic and geotechnical variables controlling horizontal drain performance.
2. Numerically simulate groundwater flow for slopes with horizontal drains. Verify the numerical results with existing field records.
3. Perform a parametric study on variables that affect system performance, and
4. Develop design charts for design of subsurface drainage system.

1.3. Organization of Thesis

This thesis is organized into seven chapters. Chapter 2 provides a literature review of horizontal drains and factors influencing their performance. Chapter 3 describes the field performance of selected sites. Background of each site such as geology, hydrology, geometry, and horizontal drain details are provided in this chapter. Chapter 4 gives the details of TOUGH2 and numerical flow analysis. The basic theory and methodology used in TOUGH2 is discussed followed by the procedure used in the numerical simulations. Chapter 5 gives details of the numerical modeling of flow pattern and verification on site data. One site was selected to verify the model. Field recorded piezometric and failure surface data are matched with numerical models. Chapter 6 presents a detail of the parametric study and results. The parametric study was conducted for key factors which influence the performance of drains such as elevation, spacing, and the length of drains. Finally, conclusions drawn from this study and recommendations for future research in this area are given in Chapter 7.

CHAPTER TWO

LITERATURE REVIEW

2.1. Introduction

Horizontal drains are the common means of subsurface drainage. The method entails the installation of small diameter pipe drains within a slope usually by helical auger or rotary drill to reduce ground-water pressures. The main success of a horizontal drain is dependent on how much pore water pressure is reduced (Nonveiller 1970, Kenney et al. 1976) on slope.

In many projects, site constraints and the depth of water-bearing deposits below existing site grades prevent the use of conventional subsurface drainage methods. Santi et al. (2001) demonstrated successful installation of horizontal wick drains using conventional construction equipment. Wick drains are flat geotextile-covered plastic channels which have been used since the 1970s' to accelerate consolidation and settlement in vertical installation. The use of geotextile prevents the clogging of the drain, a common problem with slotted PVC pipes which require periodic maintenance to remove soil clogs. Bahner and Jackson (2007) have reported the improvement of the stability of 6 to 37 m tall bluffs around the Lake Michigan shoreline using wick drains. The installation of wick drains was done horizontally using their patented system involving horizontal directional drilling (HDD) methods. Horizontal drilling forms part of a suite of "trenchless" technologies that are increasingly used in urban areas to construct new utilities or to renovate existing water, sanitary drainage, electricity or gas or networks. Their impact on surface sites is minimal, thereby reducing inconveniences caused to users in comparison with the work carried out using "trenching" techniques. Such innovative excavation

equipment of trenchless techniques could be adapted to provide more effective, efficient installation and function of subsurface drainage systems within marginally stable slopes.

There have been a few studies which have attempted to describe in part many parameters controlling the horizontal drainage system to evaluate the feasibility of using a system of horizontal drains to lower ground water levels in hillsides. Monitoring of horizontal drain systems has generally been confined to measurement of drain discharge. The important effects of horizontal drainage on pore water pressures have been measured rather rarely. Some case studies where measurements of pore water pressure were made show the system to be over designed (East 1974). There is thus a great need for documenting case records of well instrumented and monitored horizontal drain installations.

Groundwater flow analysis using a numerical model is a frequently used tool in practice. A number of computer programs have been developed over the years with various capacities of groundwater flow applications. They include, TRUST (Narasimhan, 1975); TOUGH2 Version 2.0 (Pruess, 1999); MODFLOW 2000 (USGS); Seep3D (Geo-Slope International, 2007); FEFLOW Version 5 (WASY GmbH, 2006); and PetraSim 4 (Thunderhead Engineering, 2007).

The section below gives details of a selected group of studies on horizontal drains. These include field instrumented studies as well as numerical simulations.

2.2. Hutchinson (1977)

Hutchinson (1977) studied the effectiveness of corrective measures in relation to geological conditions and types of slope movement. Various types of corrective measures were reviewed. It included modification of slope profile by cuts and fills, drainage, and restraining structures. The study here is focused on drainage using horizontal drains and trenches.

This comprehensive study also describes the history and case records of the horizontal drain method. It shows that a comprehensive and long term monitoring of various methods (such as stresses, porewater pressures, movement of slides and drain discharges) used in stability improvement is necessary to achieve an efficient method. It shows that for drainage measures, initial groundwater level should at least be measured for one full season and preferably longer. It is also important to measure the variation of permeability with depth, and the permeability ratio k_h/k_v . Drainage is effective not only until the slope settles by consolidation, but also when water flow reaches the steady state. Since it takes a certain period to become effective, the slope should be monitored for the long-term. This helps to find any deterioration by clogging, movements or any other causes which reduce the performance of drains.

2.3. Lau and Kenney (1983)

Lau and Kenney (1983) studied the effectiveness of horizontal drains in clay slopes. The investigation consisted of three parts. First a field test was carried out to check the feasibility of using horizontal drains to lower the groundwater level. The observed groundwater levels were compared with numerical simulations. Subsequently, a parametric study was conducted to identify the factors that influenced the performance of drains.

The groundwater pressures were estimated from the TRUST computer code (Narasimhan, 1975). The phreatic surface was assumed to coincide with the ground surface to facilitate the calculations. Three dimensional groundwater pressures obtained from TRUST output were converted to equivalent two dimensional values to estimate the factor of safety using geotechnical stability analyses. The results showed that the installation of horizontal drains significantly increased the minimum safety factor of the slope.

The influence of the diameter of drains, spacing between drains, length and inclination of drains, and the location of the drains were studied using a parametric study. Three different slopes with different geometry, soil and hydraulic characteristics were selected to study the parameters for different drainage systems. The results showed the improvement of stability of slope primarily depends on the coefficient of consolidation of the soil in the slope, the diameter of drains, spacing, and the inclination and length of the drains with respect to the critical failure surface. Note that the coefficient of consolidation is dependent on the permeability of the material. Slope stability was found to increase with increasing drain diameter or decreasing spacing between drains, and the length of drains had suggested being closer to critical slip surface.

2.4. Cai et al. (1998)

Cai et al. (1998) proposed a numerical method to predict the effects of horizontal drains on groundwater level during rainfall. The scheme was also used to study the effects of the length, spacing and direction angle of horizontal drains on slope stability. For this study, a three dimensional finite element analysis was conducted for transient water flow through saturated-unsaturated soils.

The finite element discretization of the problem with horizontal drains is shown in Fig. 2.1(a), 2.1(b). Three sets of Van Genuchten model parameters of hydraulic characteristics for Glendale Clayey Loam (GCL), Uplands Silty Sand (USS), and Bet Degan Loamy Sand (BLS) as shown in Table 2.1 were used to investigate their influences on the groundwater level and the slope stability.

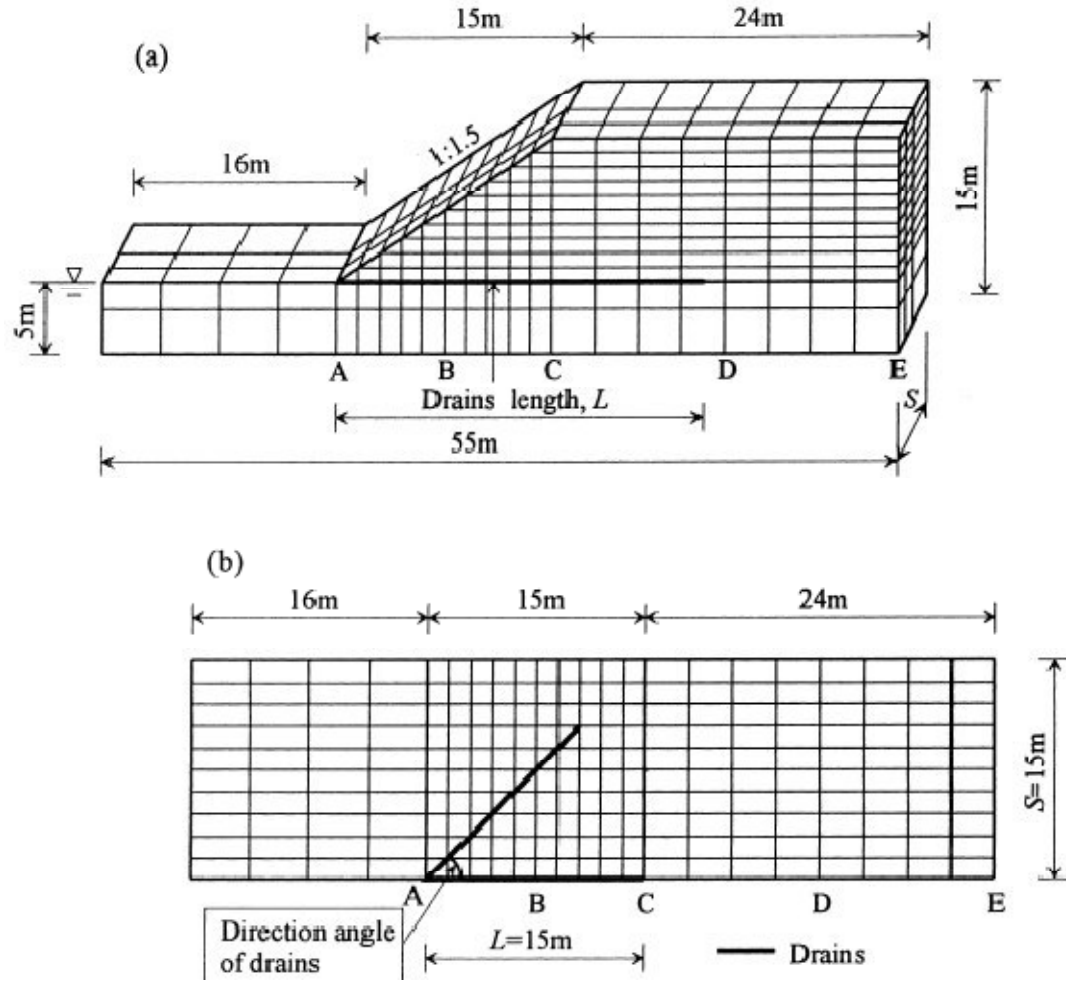


Figure 2.1(a), 2.1(b): (a) – 3D finite element mesh, (b) – 2D finite element mesh on horizontal plane for the selected model (Cai et al. 1998)

SOIL TYPE	α (m^{-1})	n	θ_r	θ_s	$K_s(10^{-4} \text{ cm/s})$
GCL	1.0601	1.3954	0.106	0.469	1.516
USS	7.0870	1.8103	0.049	0.304	18.292
BLS	2.7610	3.0224	0.044	0.375	63.832

Table 2-1: Hydraulic properties of soils (Cai et al. 1998)

Results of the study concluded that the length of drains is more critical than the spacing between drains. When the groundwater level is steady under rainfall, the ratio of rainfall intensity/saturated hydraulic conductivity plays a major role on groundwater level.

2.5. Rahardjo et al. (2002)

Rahardjo et al. (2002) examined the effectiveness of horizontal drains for slope stability for residual slopes under tropical climate. The selected study area is located in a region with heavy rainfalls and higher temperatures. The horizontal drains were used to stabilize unsaturated residual soil slopes. During heavy rainfall matric suction and shear strength decreased rapidly. Horizontal drains are used as a preventive measure to drain away the groundwater in such cases and improve stability.

Their investigation consisted of two instrumented field residual slopes and a parametric study. The slopes selected are shown in Figs. 2.2(a) and 2.2(b). Fig. 2.2(a) displays the cross-section of a slope that was approximately 10m wide, 24m long and with 2:1 slope inclination. Twelve six-meter long horizontal drains were installed in four rows for that slope. Spacing was maintained as two meters while the drain inclined at a 10% gradient. Purple silty clay was underlain by decomposed rock and overlain by orange silty clay. Fig. 2.2 (b) displays the cross-section having a slope inclination of 1:1.75. The soil on the slope was medium stiff clayey silt, silty clay and sandy clay. A horizontal drain of six-meter length was installed in a 3mx3m grid on the slope face. Both slopes were monitored for the effectiveness of horizontal drains with respect to the rainfall.

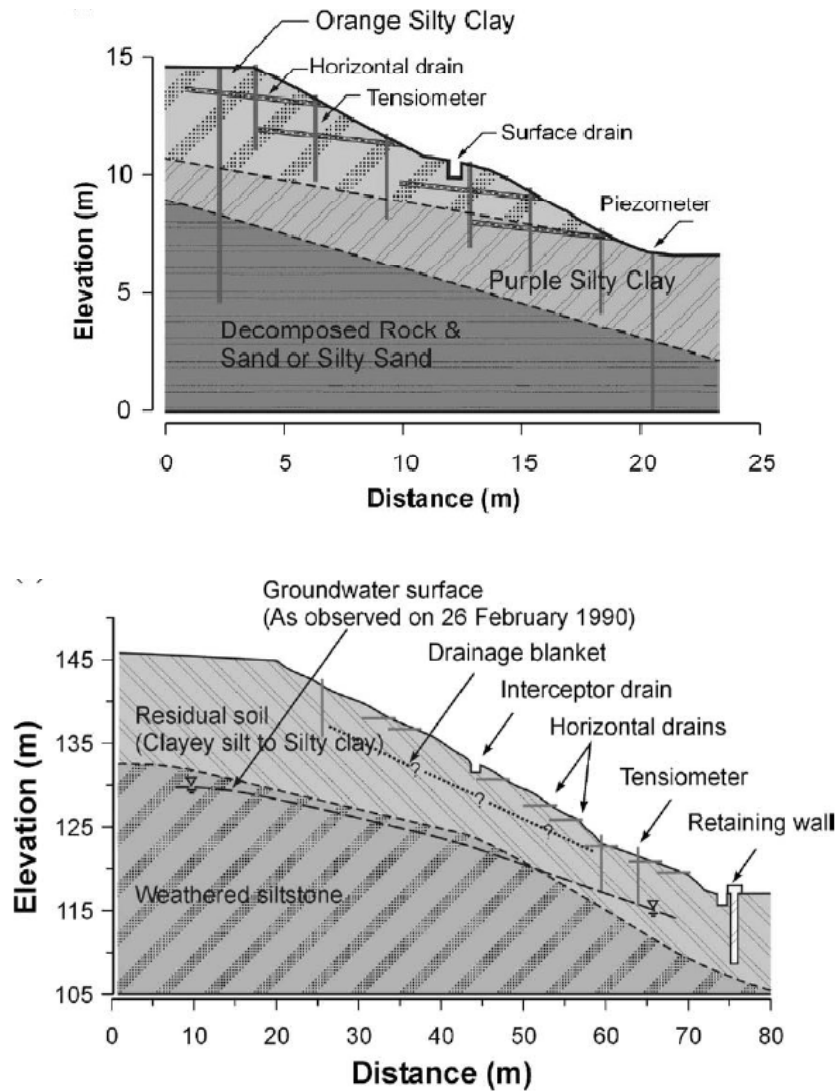


Figure 2.2(a), 2.2(b): (a) – Profile1, (b) – profile2 of selected slopes (Rahardjo et al., 2002)

A numerical analysis of the problem was conducted to study the efficiency of the horizontal drains related with the elevation of drain on the slope. A homogeneous slope (Fig. 2.3(a)) was selected for parametric study. Mesh details are shown in Fig. 2.3(b).

Five cases were considered for the study. The first one was without drains, the second, third, and fourth were cases with individual drain locations of #1, #2, and #3 (Fig. 2.3 (a)) and the fifth case was the combination of all three drains.

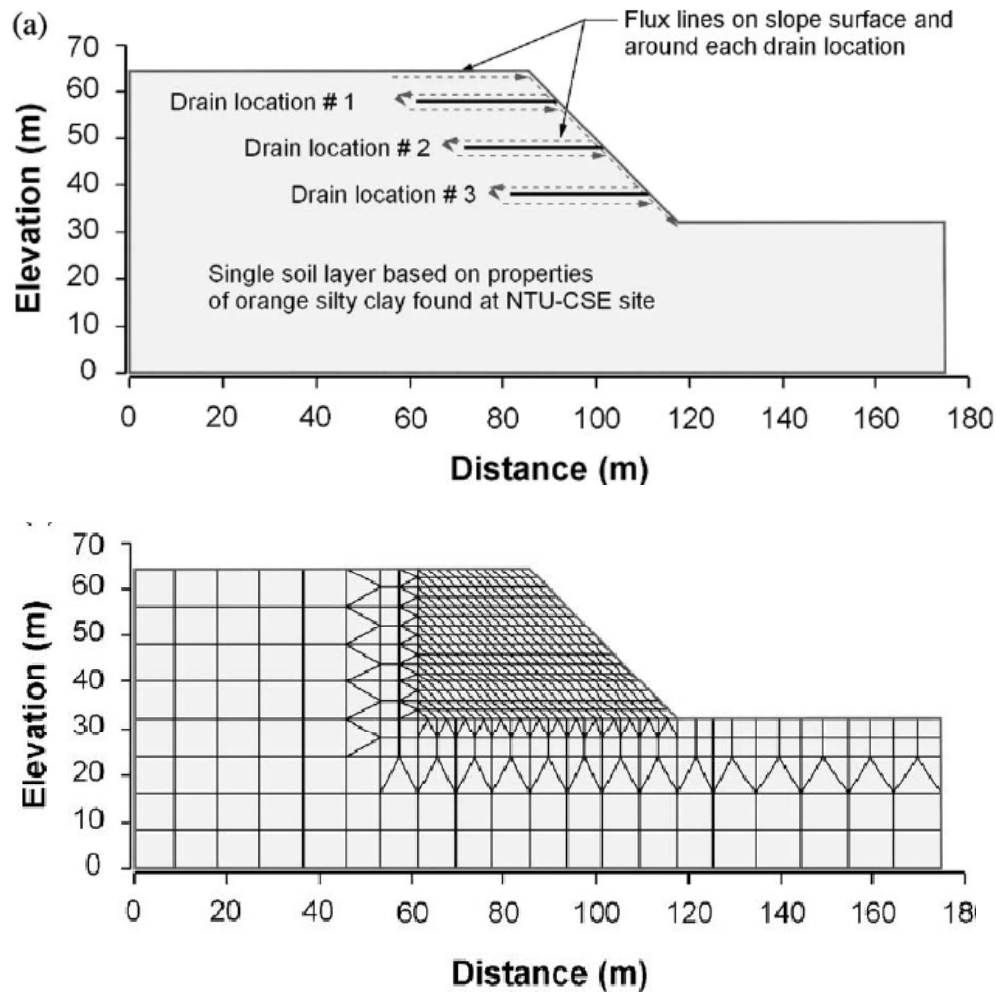


Figure 2.3(a), 2.3(b): (a) – Drain locations, (b) – finite element mesh for the selected slope (Rahardjo et al., 2002)

The results of the numerical simulations showed the bottom most horizontal drain (#3) to be much more efficient in increasing slope stability than the other two drain locations #1, #2. The factor of safety of using the drain at the bottom most case differed only slightly from the case with all drains in operation (case 5). Thus, it appears that drains installed near the toe of slope are as effective as a combination of many levels of drains.

This observation reinforces the findings of Lau and Kenny (1983) and Martin et al. (1994). The drains in the upper region are not significant when the drains were located in the lower region.

CHAPTER THREE

FIELD PERFORMANCE OF SELECTED SITES

In order to study the system variables that influenced the performance of horizontal drains under various geological conditions, the national pooled fund study headed by the state of Washington is in the process of gathering data from a number of state agencies and industry sources. Based on the information collected thus far, this study documents the salient feature of six projects that have used horizontal drains to lower groundwater level and to improve slope stability. Five of these projects were selected from Washington State Department of Transportation (WSDOT) records and one from California Department of Transportation (CALTRANS). The selection was based on the availability of instrumented data that are useful for verification of the numerical analyses. The project locations are as follows:

1. SR 101 MP69.8 (SouthWest, Washington)
2. SR 101 MP184 (Olympic Peninsula, Washington)
3. SR 101 MP322 (Olympic Peninsula, Washington)
4. SR 101 MP326 (Olympic Peninsula, Washington)
5. SR 530-Skaglund Hill (North West, Washington)
6. R 80-Redtop landslide (District 4, California)

Table 3.1 presents a summary of the available data for the following selected projects. They include the site location, the slide name if available, the contractor who performed the geotechnical investigation, the availability of the different reports, and the person who provided most of the information.

The project data that were collected in an electronic format are put together in a Compact Disk (Pathmanathan, 2009) under a directory structure shown in Figure 3.1. This compact disk is available for distribution. The collected data for each project is organized within separate folders having subfolders as follows:

- Boring records : Contains boring logs
- Geotechnical report: Includes geotechnical investigation and evaluation reports.
- Layouts : Figures, layouts, and images
- Instrumentation: Piezometer/inclinometer data and relevant charts.

Region	Projects			Geotechnical investigation	Instrumentation maintained by;	Boring records	Geologic records	Piezometer readings		Inclinometer readings		Drain layout		Contact Person	STATE
	State Route Number	Mile post	Sub name					before	after	before	after	designed	constructed		
South West	SR 101	MP 69.8	-	Kleinfelder	WSDOT	✓	✓	✓	✓	✓		✓		Jeff Young / Bud Savage	WA
Olympic Peninsula	SR 101	MP 184	Bogachiel	WSDOT	WSDOT	✓	✓		✓		✓		✓	Jeff Young / Bud Savage	WA
Olympic Peninsula	SR 101	MP 322	Lilliwaup Slide	Golder	WSDOT	✓	✓		✓		✓	✓		Jeff Young / Bud Savage	WA
Olympic Peninsula	SR 101	MP 326	Lilliwaup Slide	Golder	WSDOT	✓	✓		✓		✓	✓		Jeff Young / Bud Savage	WA
North West	SR 530	MP 36.5	Skaglund Hill	Landau	WSDOT	✓	✓	✓	✓	✓	✓		✓	Todd Mooney/ Steve Lowell	WA
District 4	R 80	KP R16.6	Redtop	CALTRANS	CALTRANS	✓	✓					✓		Todd Mooney/ Steve Lowell	CA

Table 3-1: Description of data

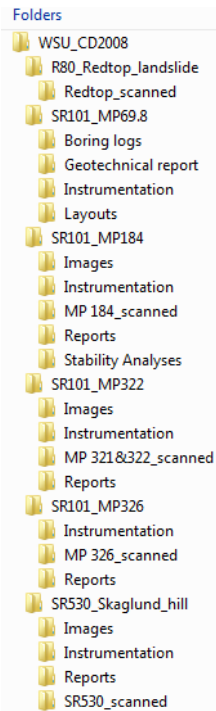


Figure 3.1: Directory structure of instrumented data in compact disk

The important features of the different slides, the associated geological profile, the layout of the drains and details of the instrumentation and the observed pattern of pore pressure changes are described in the following sections.

3.1. SR 101 MP 69.8 – South of Aberdeen, Washington

Description of Slide

This landslide located along SR 101 at MP69.8, south of Aberdeen in the state of Washington is part of an active ancient landslide. It has resulted in numerous cracks along SR 101 that have been frequently occurring for several years in this area. The failure extends to about 250 ft (76m) along SR 101 highway and along upslope of the roadway to a horizontal distance of about 150 ft (45m) and down slope about 300 ft (90m) as illustrated in Figures 3.2

and 3.3. It expands the total elevation difference between the active head scarp area and toe of the landslide to about 110ft (33.5m).

The movement of landslide accelerated after a heavy rain fall during January of 2006, resulting frequent need for maintenance of the highway and traffic speed reduction. WSDOT installed emergency drains in mid January 2006 to slow down the slide movement. The site plan with the layout of the emergency drains is shown in Figure 3.4.

Kleinfelder Inc. performed a detailed geotechnical investigation of this site and recommended horizontal drains at an elevation near the toe of the landslide as shown in Figure 3.5. Since the region in the toe of the slope was found to be over-steepened and unstable, they also recommended re-grading the slope near the toe area (Figure 3.5). The horizontal drain layout as designed by Kleinfelder was installed in summer, 2006. The cross-sectional detail of their implementation is shown in Figure 3.6. The section also shows the layout of two failure surfaces obtained from inclinometer readings.

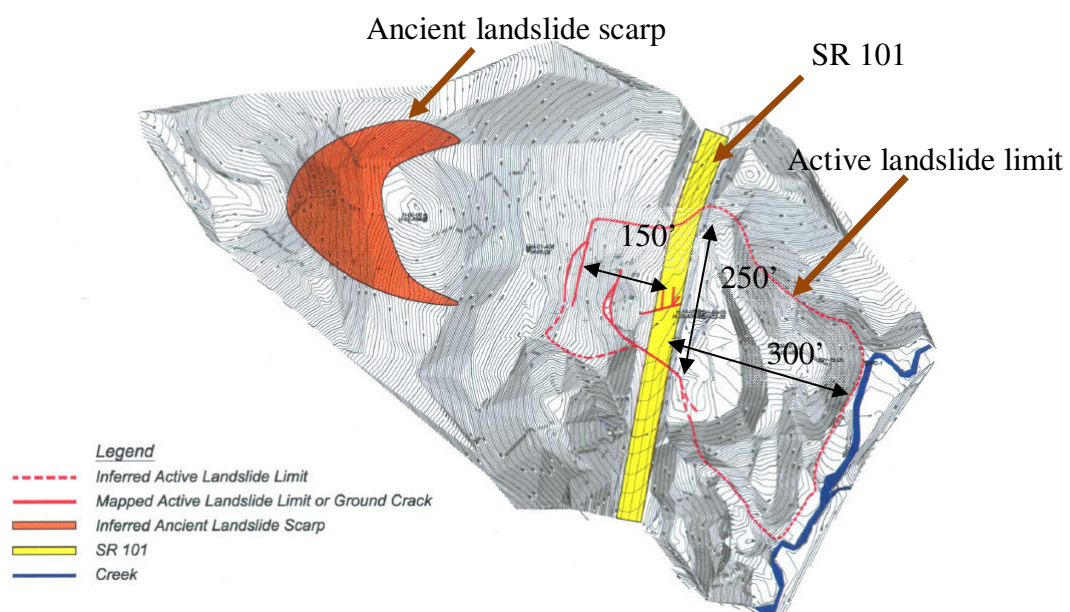


Figure 3.2: Plan of slide area at SR 101 MP 69.8 (Kleinfelder 2006)

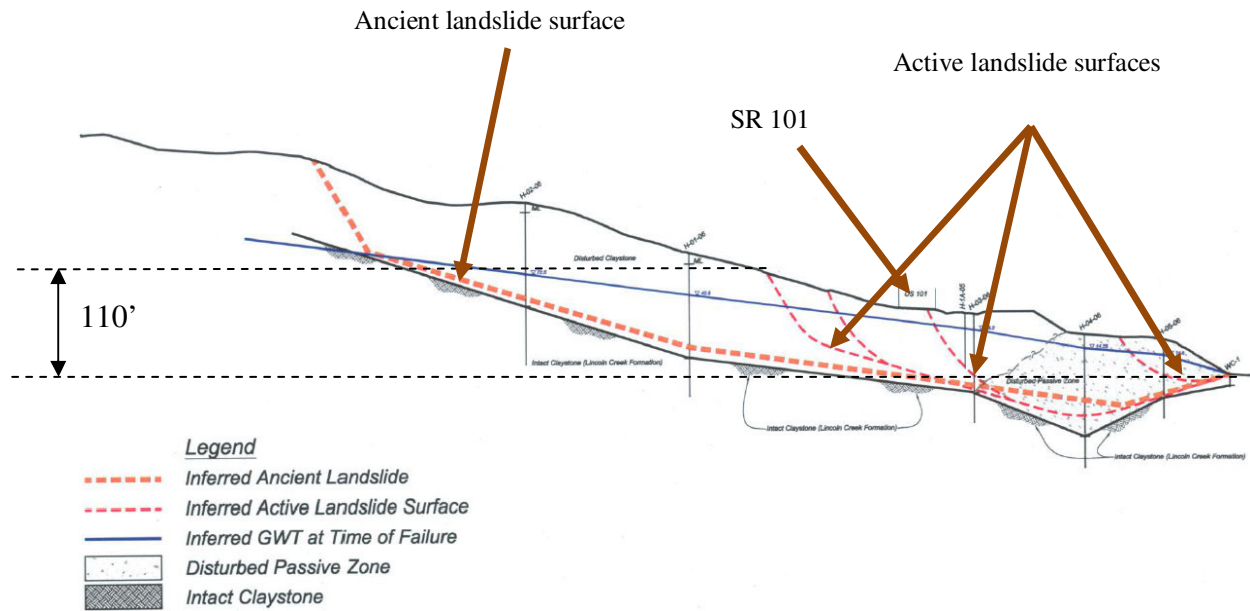


Figure 3.3: Cross-section of slide area at SR 101 MP 69.8 (Kleinfelder 2006)

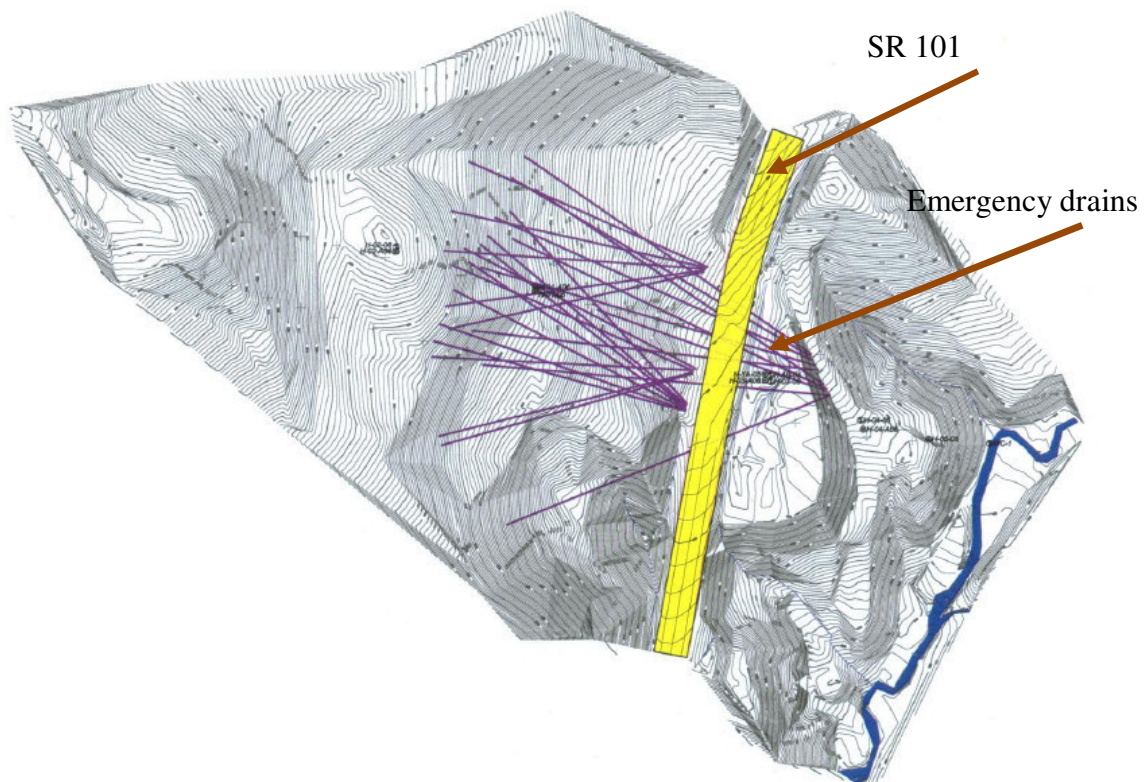


Figure 3.4: Site plan with emergency drains at SR 101 MP 69.8 (Kleinfelder 2006)

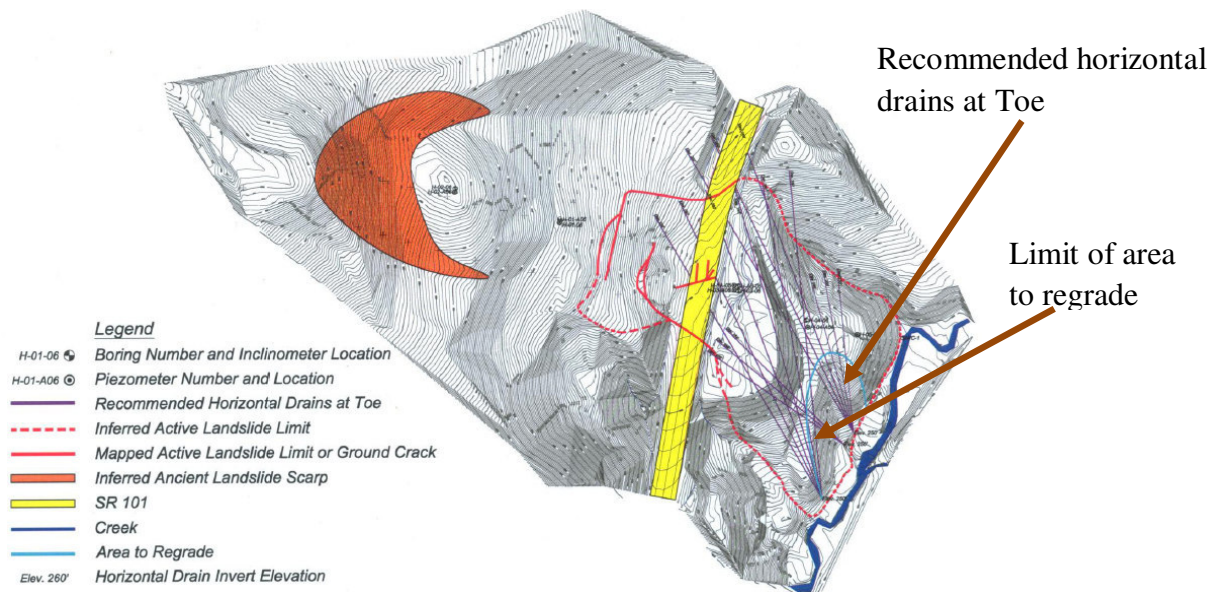


Figure 3.5: Selected stabilization option at SR 101 MP 69.8 (Kleinfelder 2006)

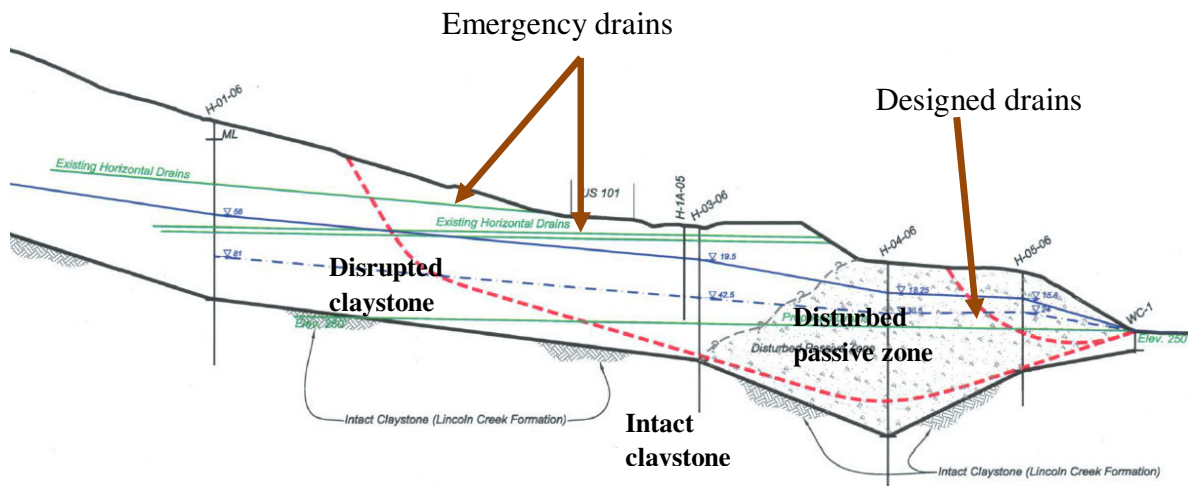


Figure 3.6: Cross-section of slide area with selected stabilization option at SR 101 MP 69.8 (Kleinfelder 2006)

Subsurface Conditions

This project site is located in the active Cascadia Subduction Zone margin. The geotechnical investigations by Kleinfelder concluded that the major geologic units of the site consisted of disturbed claystone and intact claystone of the Lincoln Creek Formation. Figure 3.6 displays the different soil units on site. Deeply weathered marine sedimentary rocks are overlain by varying amounts of landslide debris. A disturbed passive zone is located near the toe area below the highway.

Instrumentation

Washington state department of transportation instrumented this site with five borings constructed in 2006 at locations H-01-06 through H-05-06 as illustrated in Figure 3.7. Inclinerometers were installed on all boring sites (except H-05-06) at depths ranging from 110.5 feet to 136.5 feet (33.7m to 41.6m) below ground surface. These inclinometers were installed within the active landslide limit. These installations were distorted by the continuously moving slide, which started shortly after installation, as shown in Figure 3.8.

Piezometers were installed at H-01-06 through H-05-06 after failure occurred in January of 2006. Groundwater level is a key measurement from the field to evaluate the performance of horizontal drains. Figure 3.9 shows the variation of groundwater level below the soil surface for each Piezometer, with the time period. It also shows the variation of rainfall in inches within the time period. It can be seen that, from February to September 2006, Piezometer readings show a nearly steady state with less than one inch (25.4mm) rainfall. Note that, during this time period, emergency horizontal drains also existed at the project site. It is seen that all the Piezometers readings dropped down significantly after installing horizontal drains (Figure 3.9). An exception

is the case of H2A-06 due to the fact that this Piezometer was located on the upslope area and was not effective in draining water.

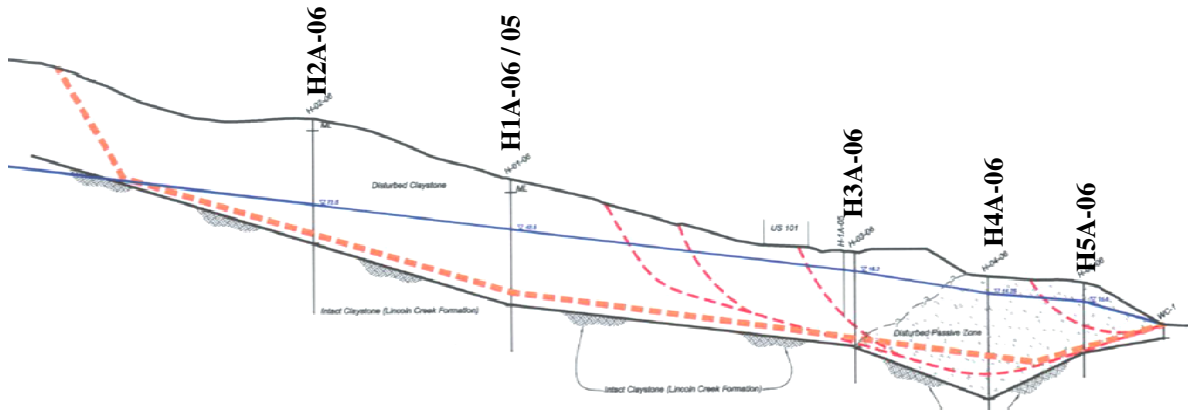


Figure 3.7: Boring locations at SR 101 MP 69.8 (Kleinfelder 2006)

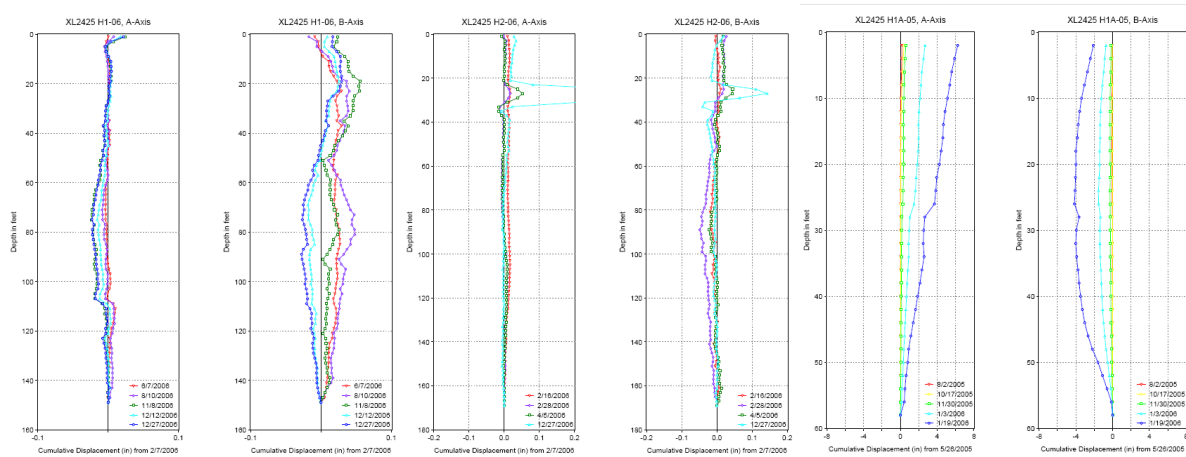


Figure 3.8: Inclinomometer plot at SR 101 MP 69.8

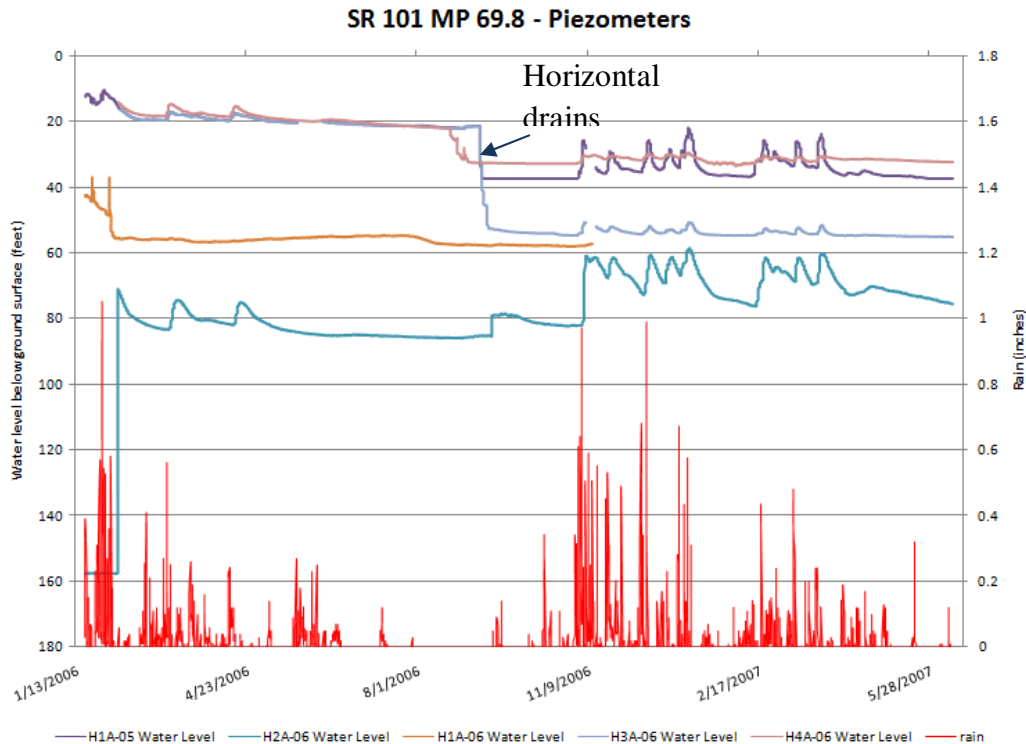


Figure 3.9: Piezometer and rain data Vs Time at SR 101 MP 69.8

3.2. SR 101 MP 184 –Washington (Bogachiel Slide)

Description of Slide

The section near MP 184 along Washington highway SR 101 is another one that has been subjected to ongoing landslide-related impacts since at least 1950. Mostly down slope failures of the highway have occurred from time to time and required regular pavement repairs; several geotechnical investigations; minor upslope realignment; and surface and subsurface drainage improvements.

In late August 2004, during the driest part of the year, a rapidly deforming slump of earth flow occurred, threatening both traveled lanes between Stations 510 and 512 as indicated in

Figure 3.10. Several remedial activities were taken to stabilize this slope and to protect the highway between 2004 and 2006. These included minor upslope realignment and surface and subsurface drainage improvements. Several costly retaining walls and more than 6000 feet (1830m) of horizontal drains were constructed. After completing a soldier pile, tie-back wall in the spring of 2006, no movement or other evidence of distress has been detected within or beneath the wall.

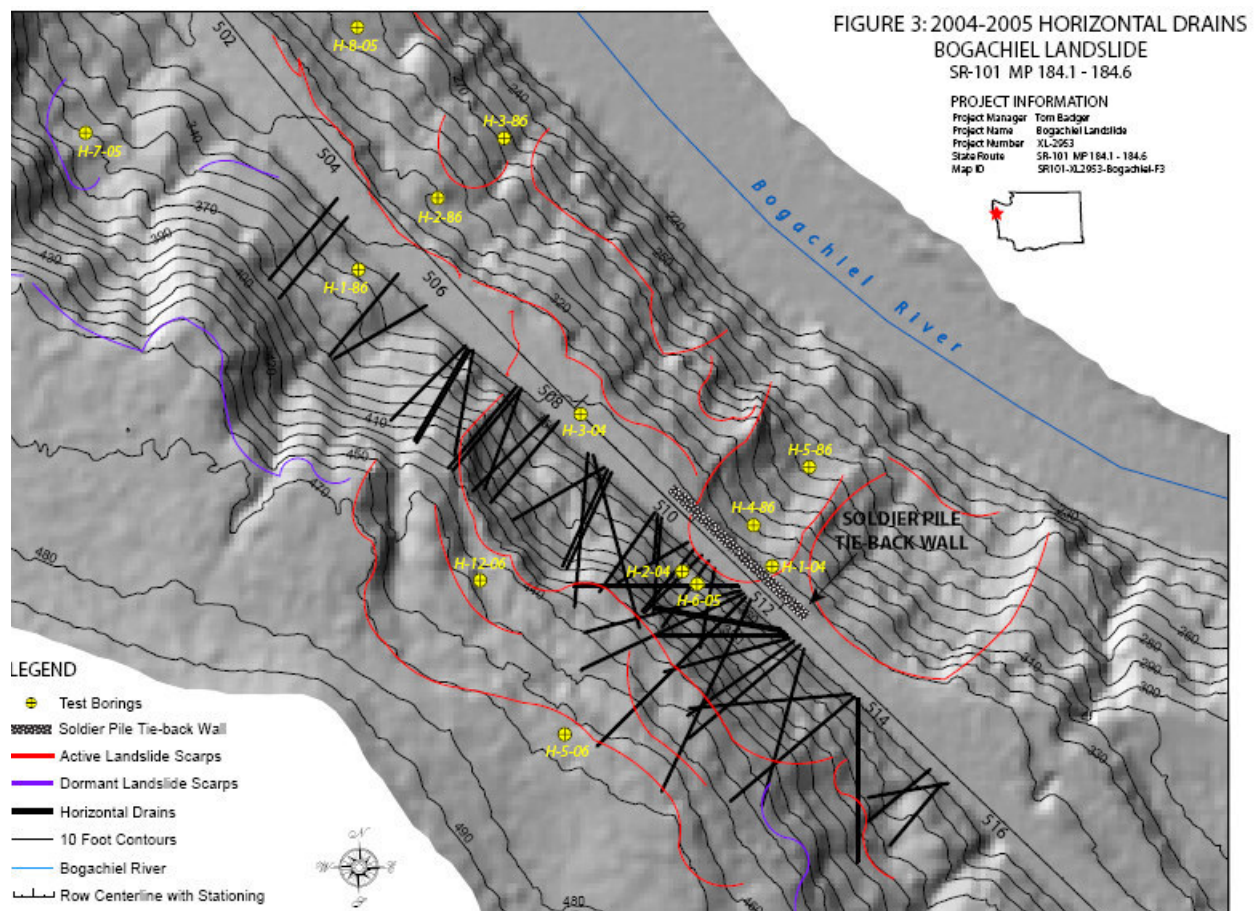


Figure 3.10: Landslide Plan with Horizontal Drains At SR 101 MP 184 (WSDOT 2007)

Subsurface conditions

This project site is also located within the active Cascadia Subduction Zone margin. The major geologic units of the site are disturbed sandstones, siltstones and intact claystone of the Lincoln Creek Formation. Deeply weathered marine sedimentary rocks are overlain by varying amounts of landslide debris.

Instrumentation

This site was instrumented with piezometers and inclinometers during the period between 2004 and 2006. Borings of H-1-04 through H-4-04 were done between September to December in 2004, and H-5-06 through H-12-06 were done between August of 2005 and May 2006. Figure 3.11 shows boring locations. Precipitation was recorded for each four hour interval using a tipping-bucket rain gage which is connected to an electronic data logger. Piezometers and inclinometers were monitored to evaluate groundwater conditions and to characterize the depths, direction, and rates of landslide movement.

The variation of piezometric levels and precipitation data are plotted on the chart shown in Figure 3.12. Most of the piezometers show a relatively stable water level except those at H-5b-06 and H-6c-05. These two piezometers were located on the upslope of area. Thus, the use of horizontal drains did not have as much influence in this zone as expected.

A summary of eight sets of inclinometer data are plotted in Figure 3.13. There is no data available from August to mid-September 2006 due to instrumentation error. The plot shows relatively stable readings.

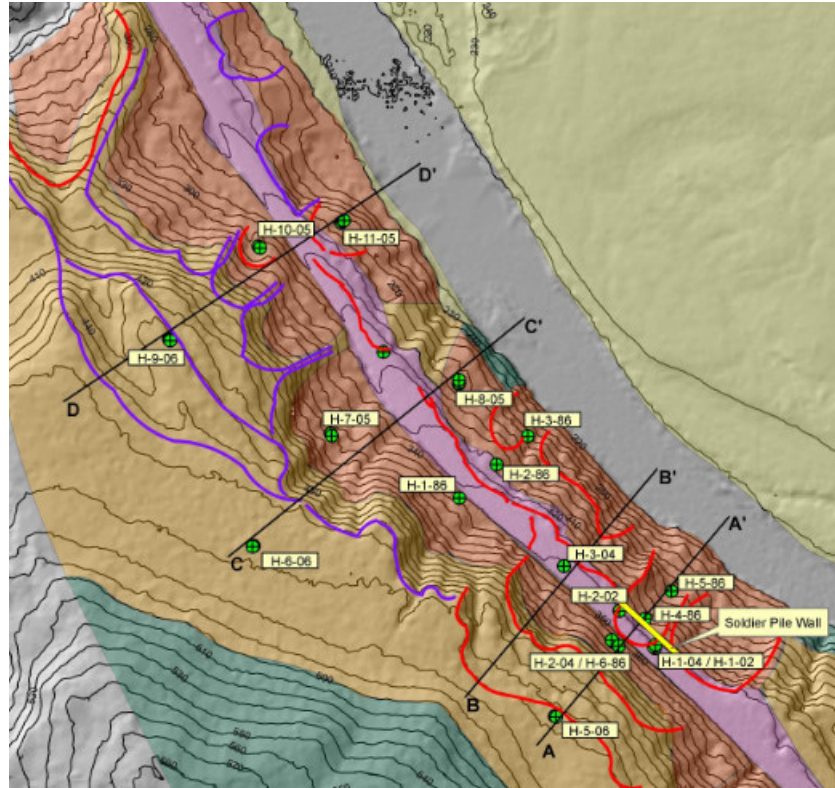


Figure 3.11: Boring locations at SR 101 MP 184 (WSDOT 2007)

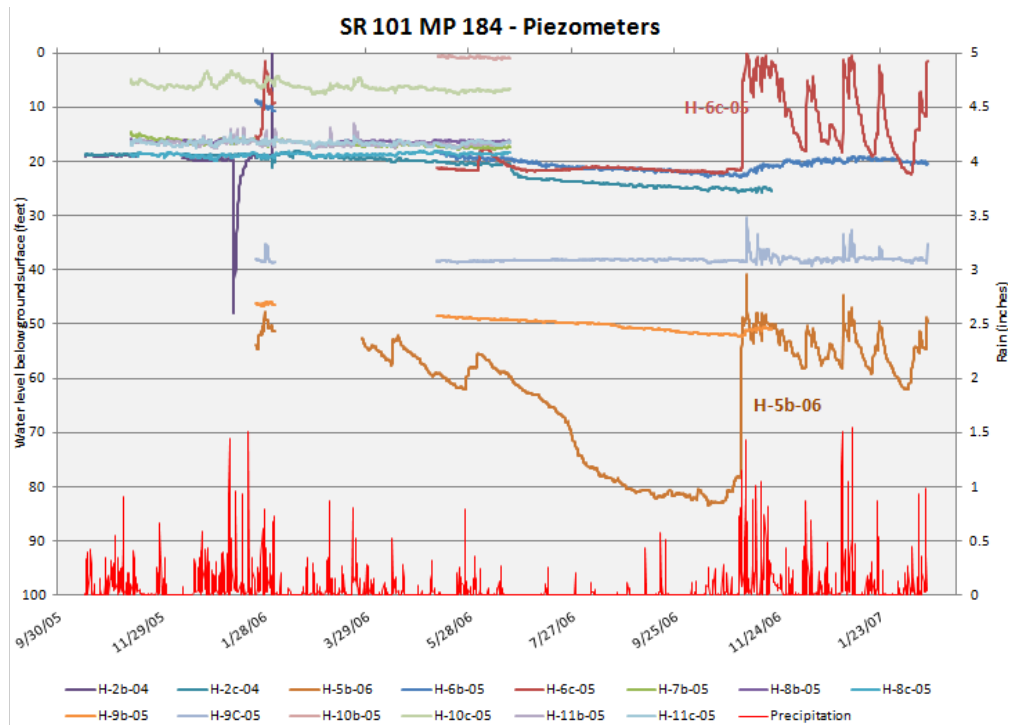


Figure 3.12: Piezometer and Rainfall Data Vs Time at SR 101 MP 184

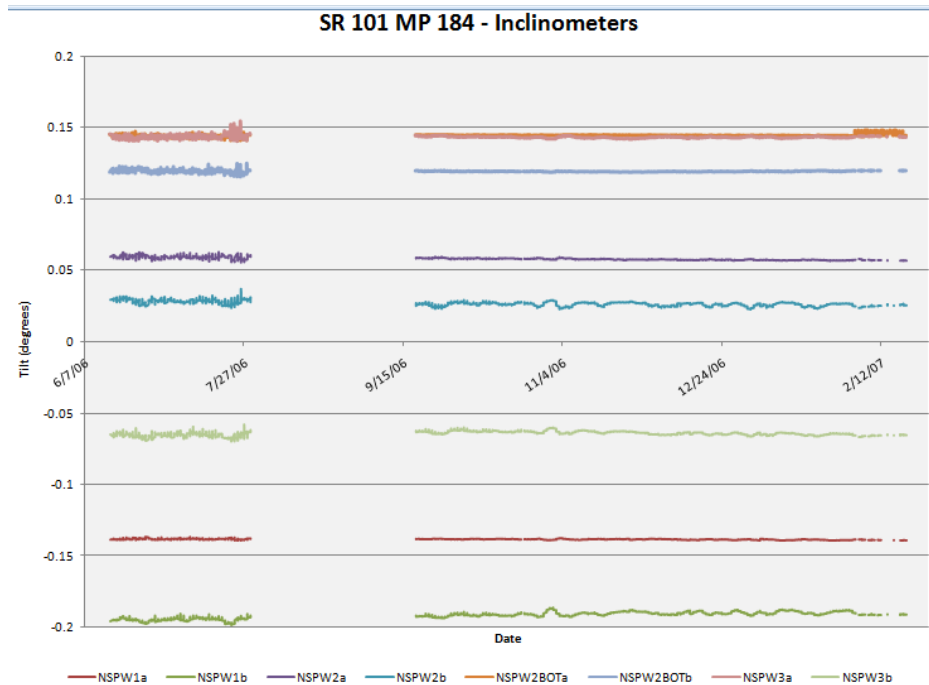


Figure 3.13: Inclinator data Vs time at SR 101 MP 184

3.3. SR 101 MP 322, Lilliwaup, Washington

Description of Slide

The location at MP 322 just north of Eldon, Washington adjacent to Hood Canal along Washington Highway SR 101 is another slope that has encountered stability problems (Figure 3.14). This slide is also part of an ancient landslide. The majority of recent landslides occurred in mid-February to March of 1999. These landslides caused frequent requirements for maintenance of the highway. This slope was studied by Golder Associates Inc. and they made recommendations for remedial actions for stabilization. These involved a combination of drainage, slope surface treatment, and a toe treatment consisting of a fill buttress and/or deep soldier pile tieback retaining wall.

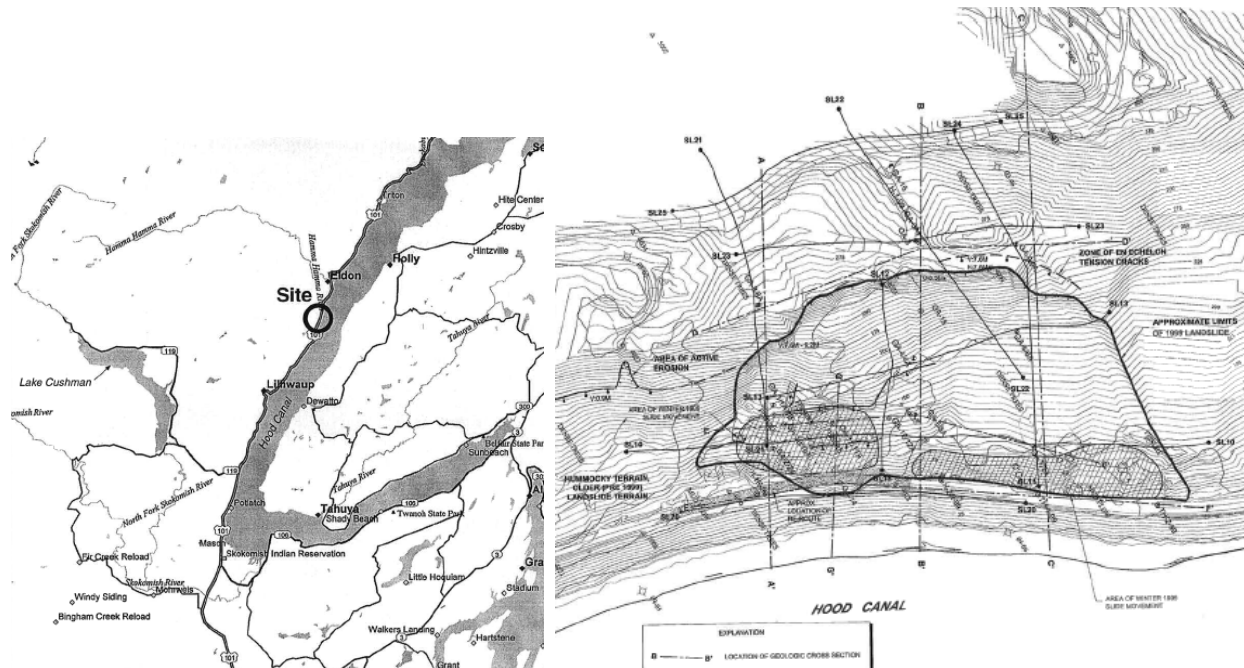


Figure 3.14: SR 101 MP 322, Site Plans (Golder, 2000)

Subsurface conditions

The recent landslide activity at MP322 appears to be located within a larger area of ancient landslide deposits. Boring logs showed the major geologic units of the site to consist of landslide debris, glaciofluvial deposits, and glaciolacustrine deposits. In general, the groundwater levels in the initial set of borings were observed to drop about 5 to 10 feet (1.5 to 3m) from April/May through September 1999. However, there was not a clear relationship between this drop and the flow from the horizontal drains. This lack of correlation could be attributed to the uncertainties about the drain orientation and the limited number of Piezometers near effective drains.

Instrumentation

The WSDOT installed horizontal drains on this site during mid and late 1999. Piezometers and inclinometers were installed at the site after the horizontal drains were installed. Since the instrumentation data is not available before adding horizontal drains, effects of the horizontal drains on groundwater level could not be compared.

Boring locations on the site are shown on Figure 3.15. Summaries of piezometric levels and precipitation are plotted on the chart shown as Figure 3.16. All piezometers showed near stable water levels. Significant movement of the slide is evident from the inclinometer readings shown in Figure 3.17. However, the field study confirmed no movement on the slope. This was due to a problem with the instrument at that time.

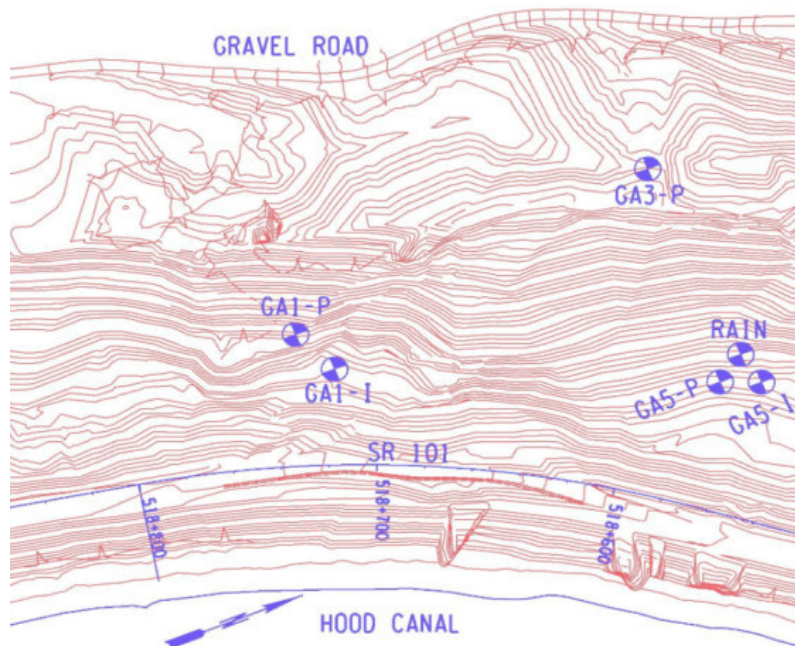


Figure 3.15: Boring locations at SR 101 MP 322 (WSDOT)

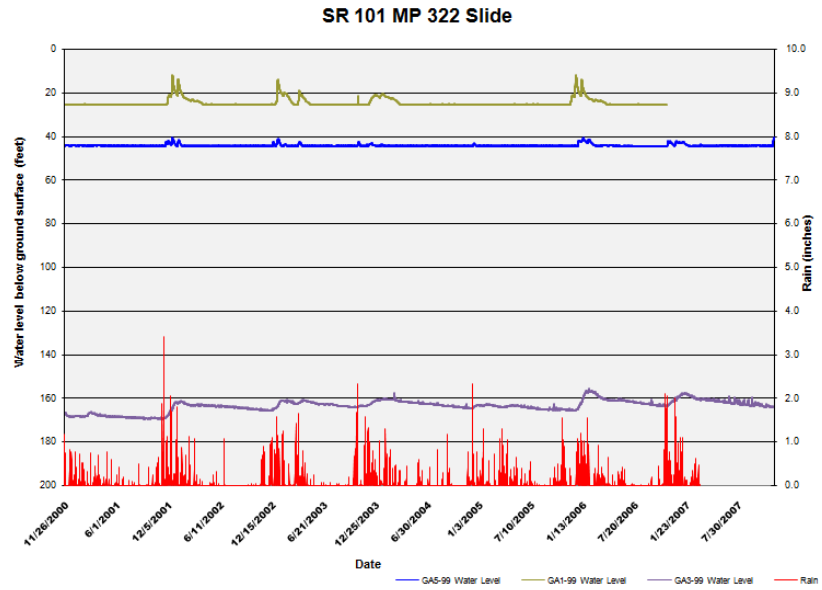


Figure 3.16: SR 101 MP 322, Piezometer Chart

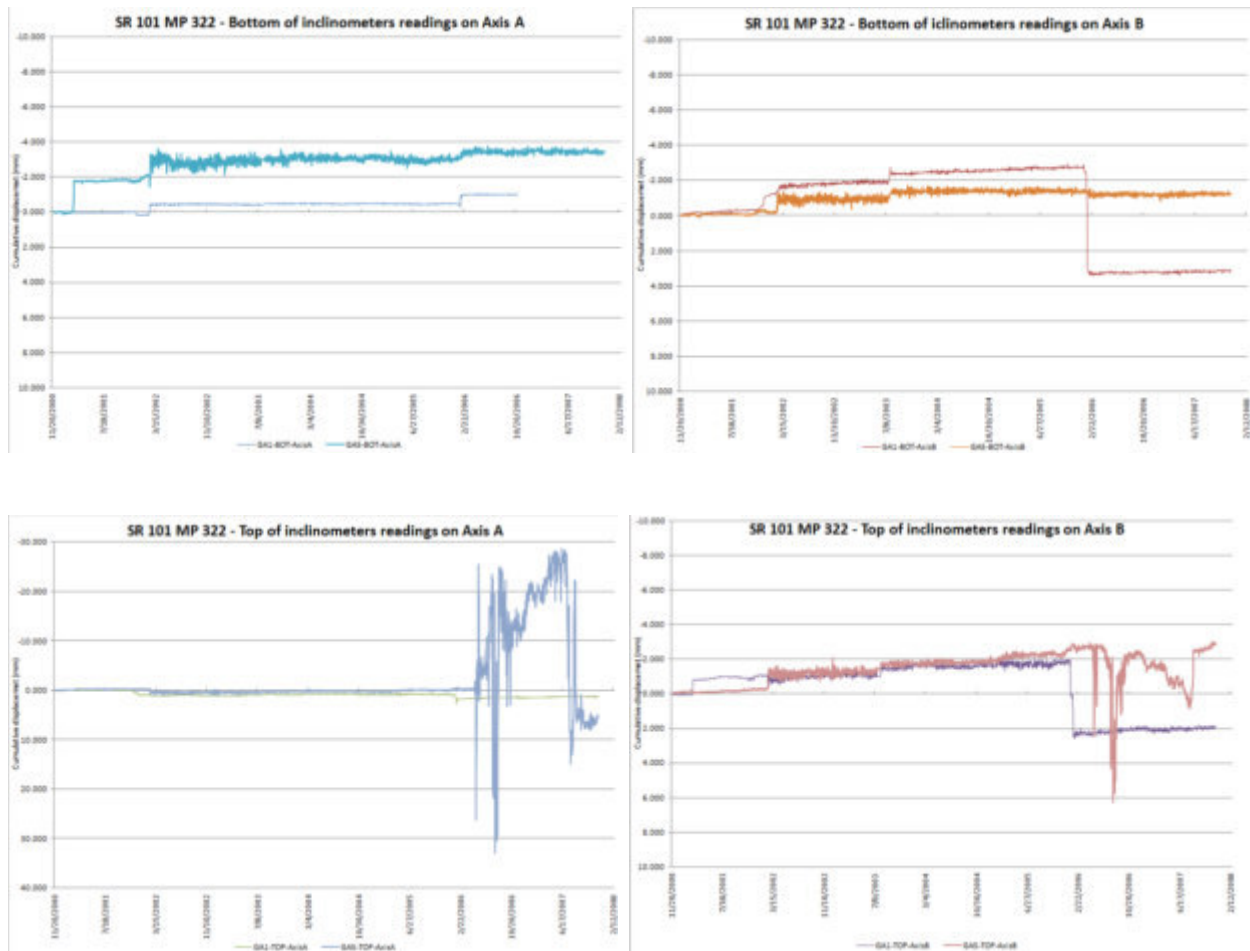


Figure 3.17: SR 101 MP 322, Inclinator Charts

3.4. SR 101 MP 326 – Lilliwaup, Washington

Description of Slide

The location near MP 326 north of Eldon, Washington adjacent to Hood Canal along SR 101 prone to landslide action (Figure 3.18). This slide has become active periodically for many years. Its most recent activity has been between 1995 and 1996. The result required frequent clean up and maintenance. This slide was analyzed by Golder Associates Inc. and remedy actions were recommended to stabilize the slope.

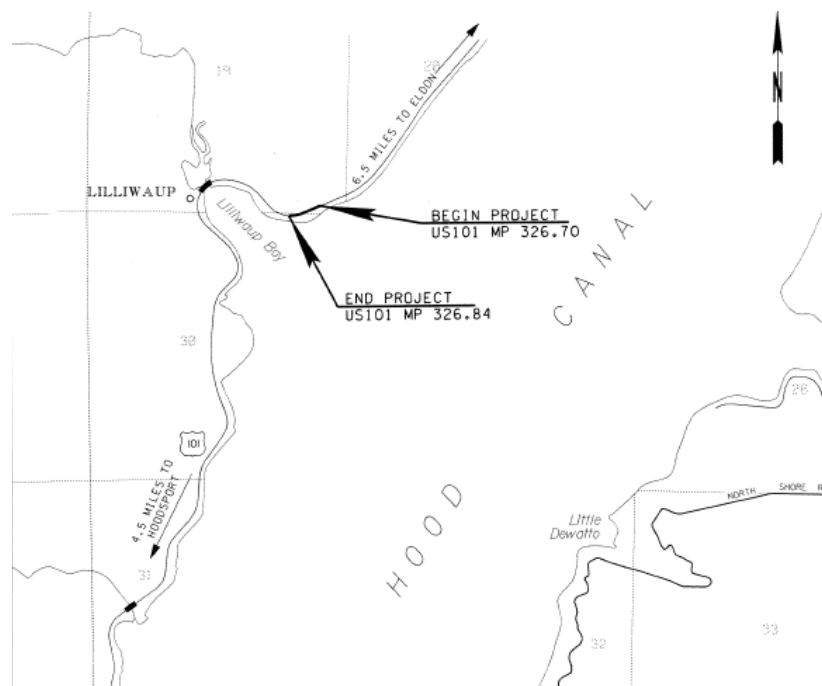


Figure 3.18: SR 101 MP 326, Site Plan (WSDOT 2007)

Subsurface conditions

The subsurface conditions at MP326 site are very similar to those of MP322. It is also part of an ancient landslide with major geologic units that consisted of landslide debris, glaciofluvial deposits and glaciolacustrine deposits.

Instrumentation

The WSDOT has been collecting Piezometer and inclinometer data from this site since November, 2000. A summary of the Piezometer readings and inclinometer readings are plotted in Figures 3.19 and 3.20, respectively. It can be seen that piezometers show a fairly stable water level from 2000 to 2006. Inclinometer readings showed a steady level until June of 2005. After that, a movement was observed on all inclinometers. This may be due to clogging of the drain, vegetation change in the project area, or a problem with the instrument during the time.

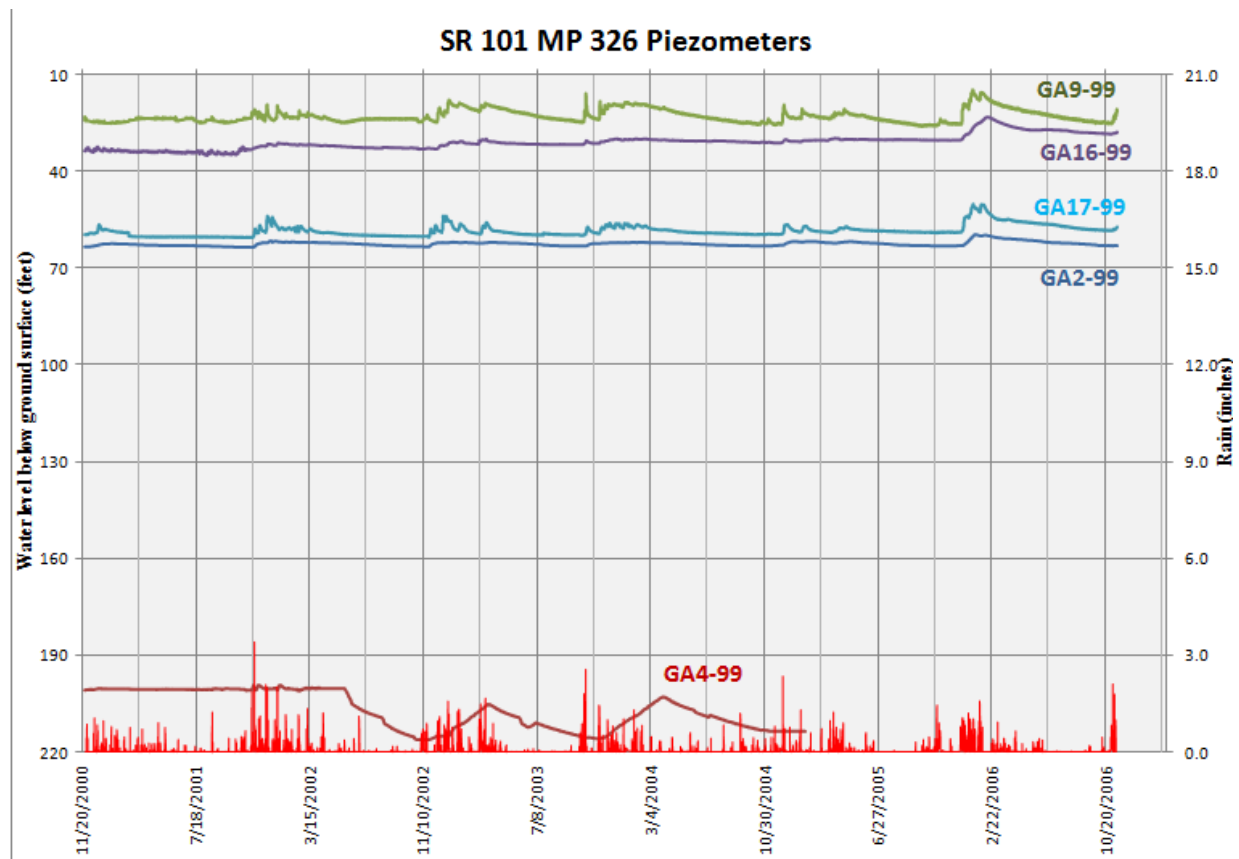


Figure 3.19: Piezometer plots at SR 101 MP 326

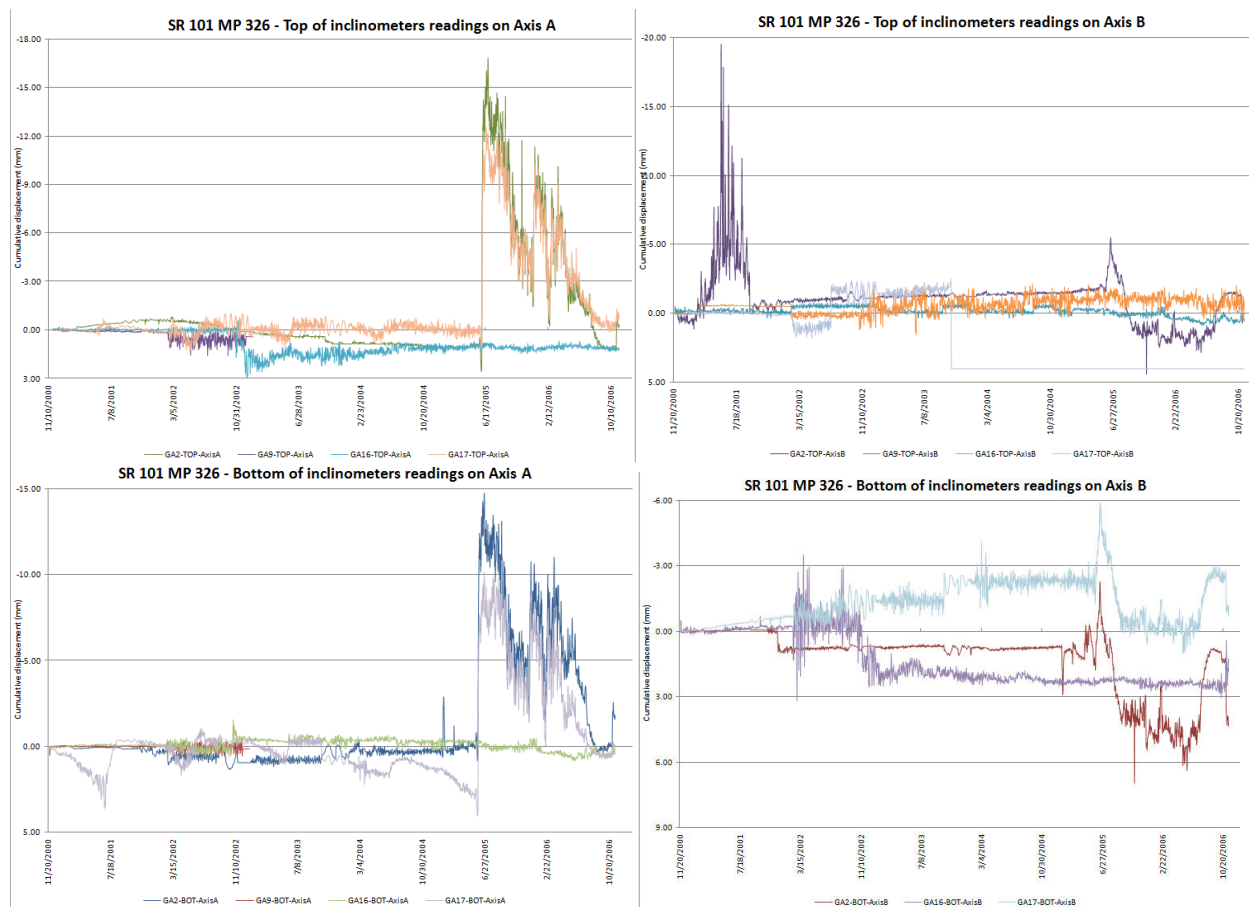


Figure 3.20: SR 101 MP 326, Inclinator Charts

3.5. SR 530 – Skaglund Hill Landslide, Washington

Description of Slide

This slide area spans approximately 3.5 miles (5.6 km) of Washington SR530 highway between mileposts 35.39 and 38.90, as shown in Figure 3.21. The project area is located north of the Folk Stillaguamish river valley. This project area has been impacted by ancient and historically active landslide activity. The western extent of the project is related to human-induced stability issues, whereas the project alignment in the eastern portion of the project has been largely controlled by non geotechnical issues. This highway has needed frequent

maintenance since the 1960's. Realignment of the roadway was recommended to avoid the instability. But, a completely realignment of the highway in this area is not feasible. Landau Associates conducted explorations to characterize the subsurface conditions and recommended design and implementation of horizontal drains, a buttress and a retaining wall. The horizontal drain layout is as shown in Figure 3.22. Landau also conducted supplemental explorations and engineering analyses to address the remaining areas of geotechnical concerns with revised design level information.

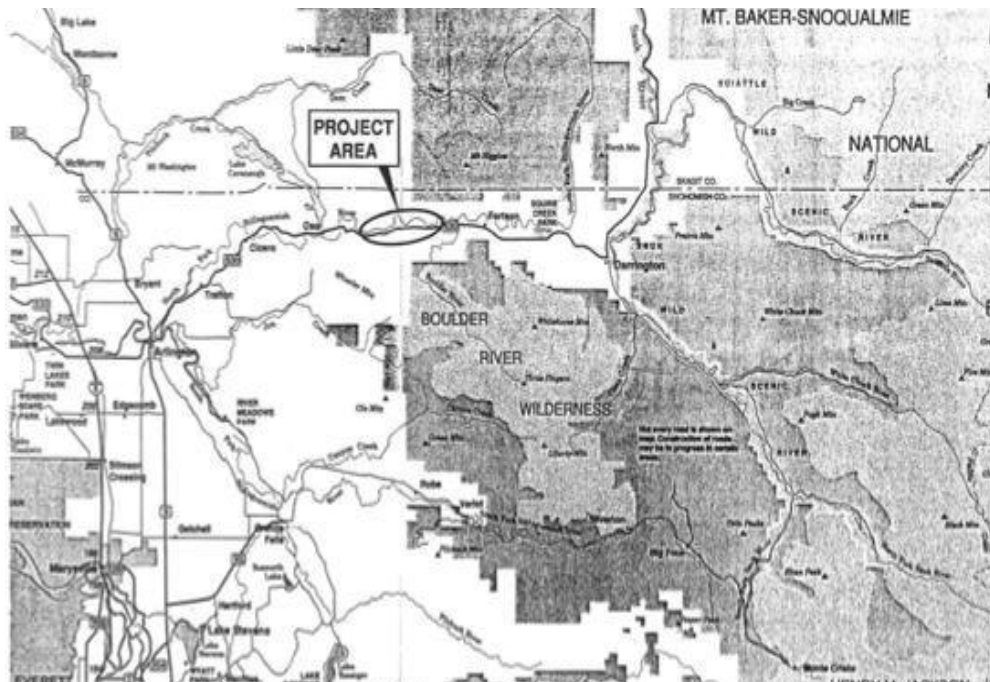


Figure 3.21: Site plan of SR 530, Skaglund Hill (Landau 1993)

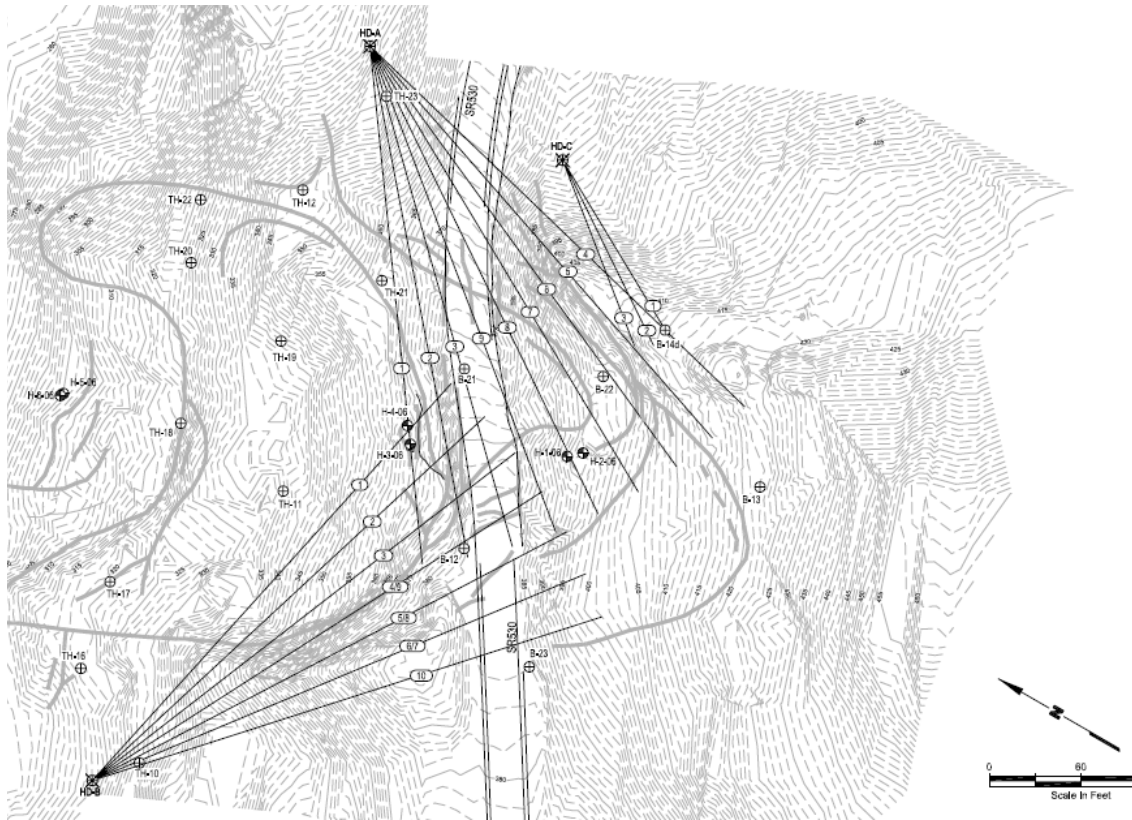


Figure 3.22: Horizontal drain layout of SR 530, Skaglund Hill (Landau 1993)

Subsurface conditions

The North Fork Stillaguamish River valley is near the geologic transition from the Puget Sound Basin to the Cascade Mountains. The topography near the project alignment varies from nearly flat along the river and lake terraces to moderate to steep slopes along valley sidewalls. This area is covered with recent Pleistocene-age soil deposits underlain by metamorphic bedrock. Processes relating to the last period of major glaciations in Washington have influenced the shallow geology in this area. The western portion of the project is generally dominated by grained glacial lacustrine deposits. The eastern portion of the project area is dominated by coarser grained fluvial and glacial deposits

The area receives approximately 60 to 80 inches of precipitation annually and is well vegetated with bush, grasses and several species of conifers and hardwoods. Figure 3.23 shows the cross-sectional view of the site developed from subsurface explorations. A relatively thin top soil layer overlays the native soil of fluvial, glacial and colluvial/mass wasted origin.

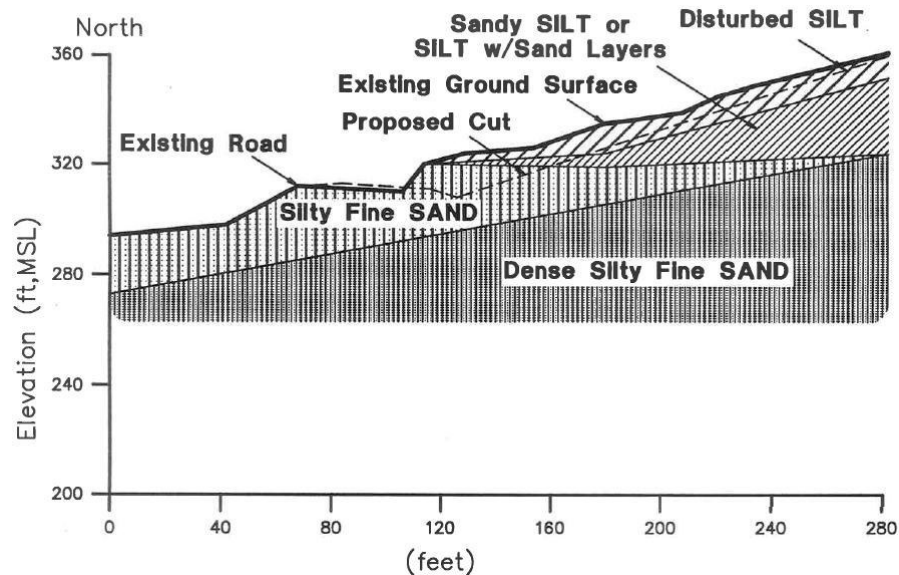


Figure 3.23: Cross-sectional view of subsurface conditions (Landau 1993)

Instrumentation

This site was instrumented with a Piezometer and rain gauges during the period from February 2006 to June 2006. Figure 3.24 shows the boring locations. Piezometer and inclinometer data are shown on Figures 3.25 and 3.26. It can be seen that the ground water level dropped significantly after installation of the drains, while the average rainfall remained almost the same.

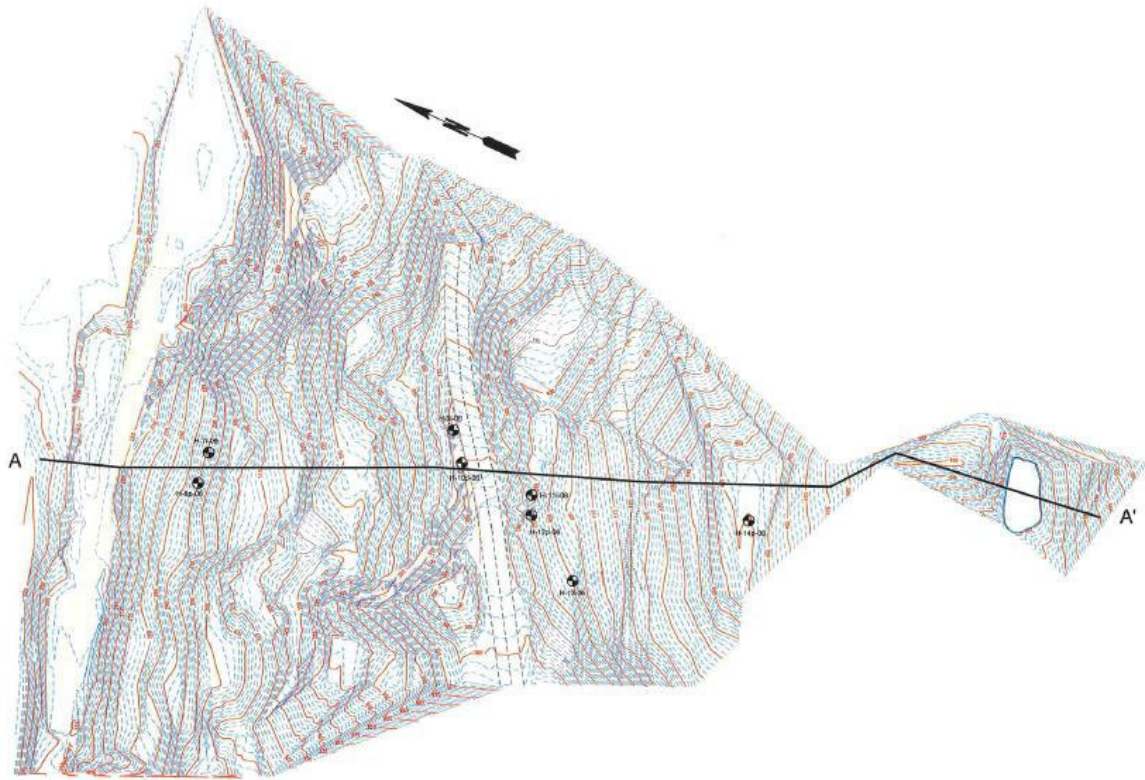


Figure 3.24: Boring plan at SR 530 Skaglund Hill (Landau 1993)

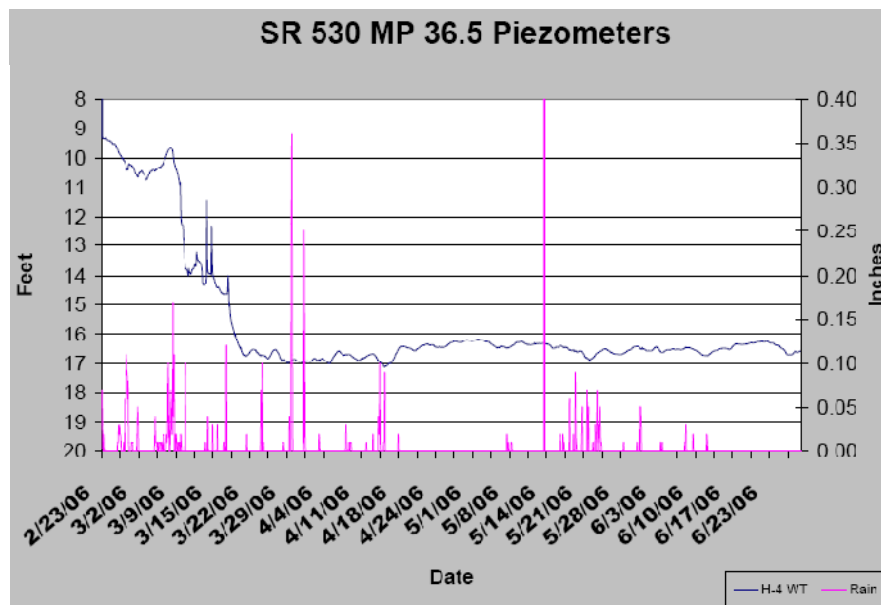


Figure 3.25: Ground Water level & Rainfall during February 2006 to June 2006 at SR 530 MP36.5 (WSDOT, Instrumentation)

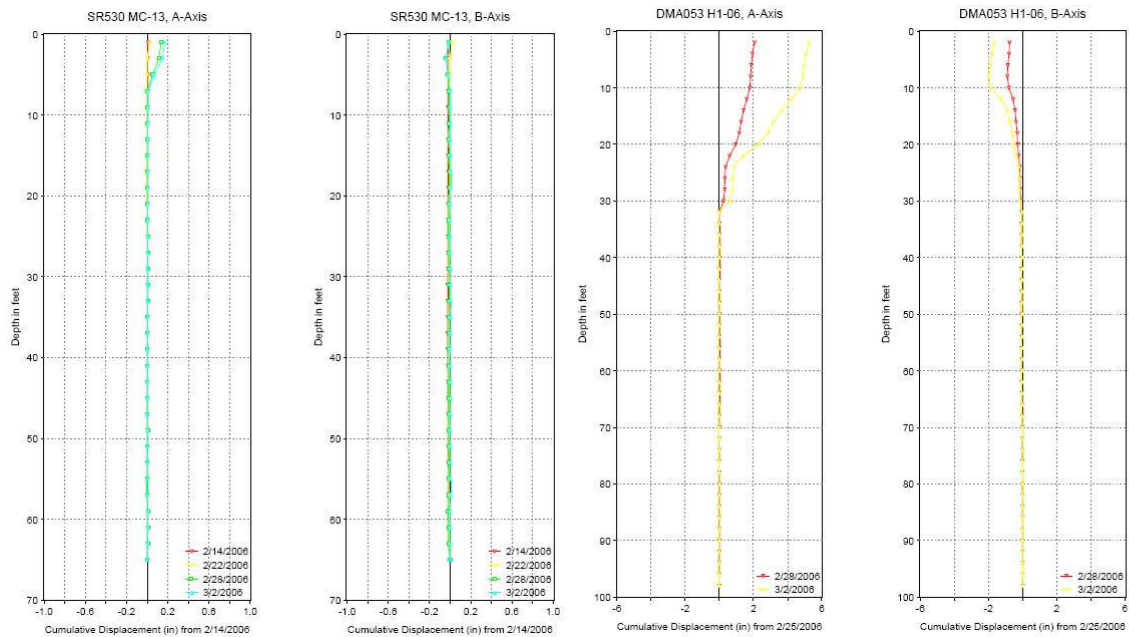


Figure 3.26: Cumulative displacement from February 2006 to March 2006 at SR 530 MP36.5 (WSDOT, Instrumentation)

3.6. Route 80 California – Redtop Landslide

Description of Slide

Redtop landslide at American Canyon is located in Solano County in California. Highway R80 traverses the width of the landslide near interchange R80/680, as shown in Figure 3.27. The active portion of the landslide is 4400ft (1340m) wide and up to 230ft (70m) deep. The landslide extent ranged between 500 and 2600 feet (150 to 790m) in length. The landslide toe is at American Canyon Creek.

This landslide has two contiguous slide masses, as shown in Figure 3.28. One is a small slide on the west side and the other one a much larger slide on the east side. The slide on the west side has required repairs off and on from the early days of the freeway construction in 1969. The larger slide on the east was reactivated in 1994 and in mid-1996. Stabilization measures

were needed for this slide. An approximately 200acre (0.8km²) landslide mass is within a much larger ancient landslide that extends from about American Canyon Creek to the top of the mountain. The difference in elevation between headscarp to toe is about 500 feet (150m) over the distance of 2700 feet (820m). The slope on the opposite side is also underlain by a large landslide complex, which does not influence highway R80.

The highway moved by about five feet (1.5m) south towards American Canyon Creek, resulting in repairs of pavement, median barrier and drainage facilities. Much of this movement occurred between February and July, 1998, when the area received twice the amount of normal rainfall (41 inches (1040mm)).



Figure 3.27: Site Plan at R 80 Redtop landslide (CALTRANS 2001)



Figure 3.28: Site Plan at R 80 Redtop landslide (CALTRANS 2007)

Subsurface conditions

The recent landslide activity at redtop appears to be located within a larger area of ancient landslide deposits. The slope geologic setting map is shown on figures 3.29 (a) and (b). Major geologic units of the site consist of landslide debris overlain by sedimentary rocks.

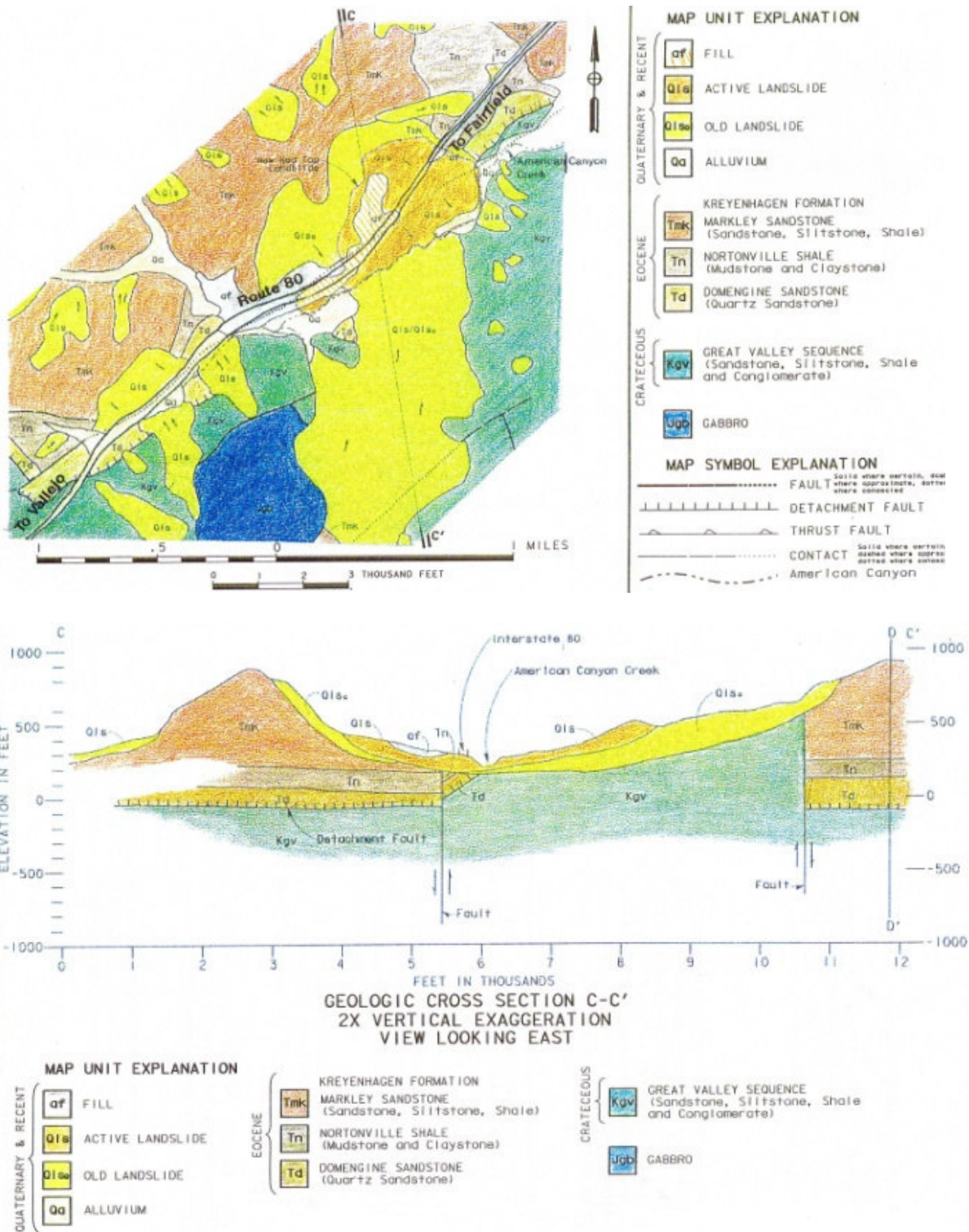
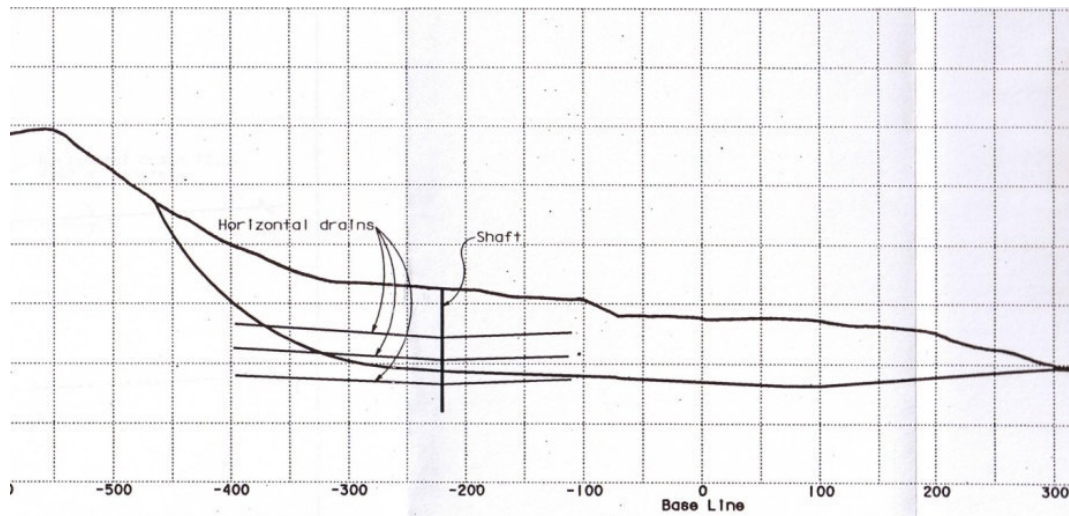


Figure 3.29(a), 3.29(b): (a)-Site Plan, (b)-Site Cross Section of R 80 Redtop landslide (CALTRANS 2001)

Instrumentation

Horizontal drains with eight large diameter (24 inches) pumping wells were constructed to stabilize the slide. The shaft and horizontal drain profile and the shaft detail are shown in figures 3.30(a), (b), respectively. The performance of the pumping wells was monitored using an array of 109 piezometers and survey monitoring of the ground surface. The total pumping rate for 8 wells averaged 70,000 gallons per day ($0.003\text{m}^3/\text{s}$) with surges up to 128,000 gallons per day ($0.005\text{m}^3/\text{s}$). Piezometer elevation data and horizontal ground movement data are shown in Figures 3.31. Since horizontal drains were installed and pumping from shaft was started, the groundwater level has lowered by about 12m and no ground movement has been observed for one year. The instrumentation data shows that the system improved the stability of slope.



PROFILE OF SHAFT IN LANDSLIDE

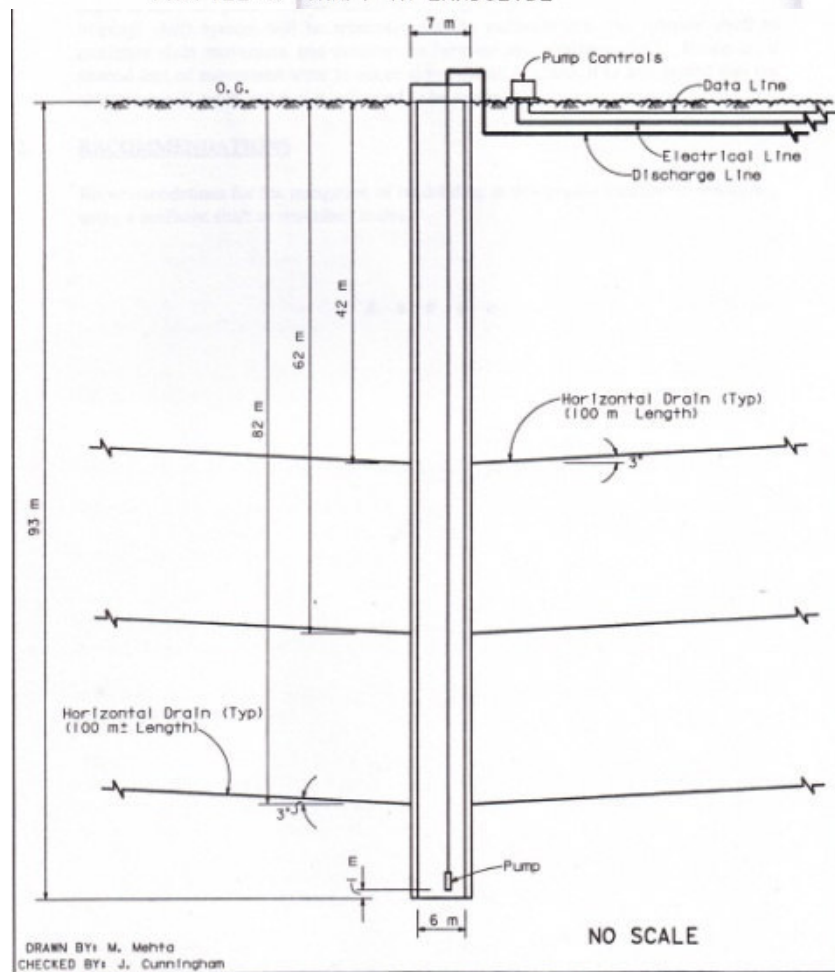


Figure 3.30(a), 3.30(b): (a)-Profile of shaft in landslide, (b)-Shaft detail at R80 Redtop landslide (CALTRANS 2001)

Horizontal Movement at GPS Monument MP07 in relation to Piezometric Head Elevation at Piezometer P-33c November 1998 to March 2005

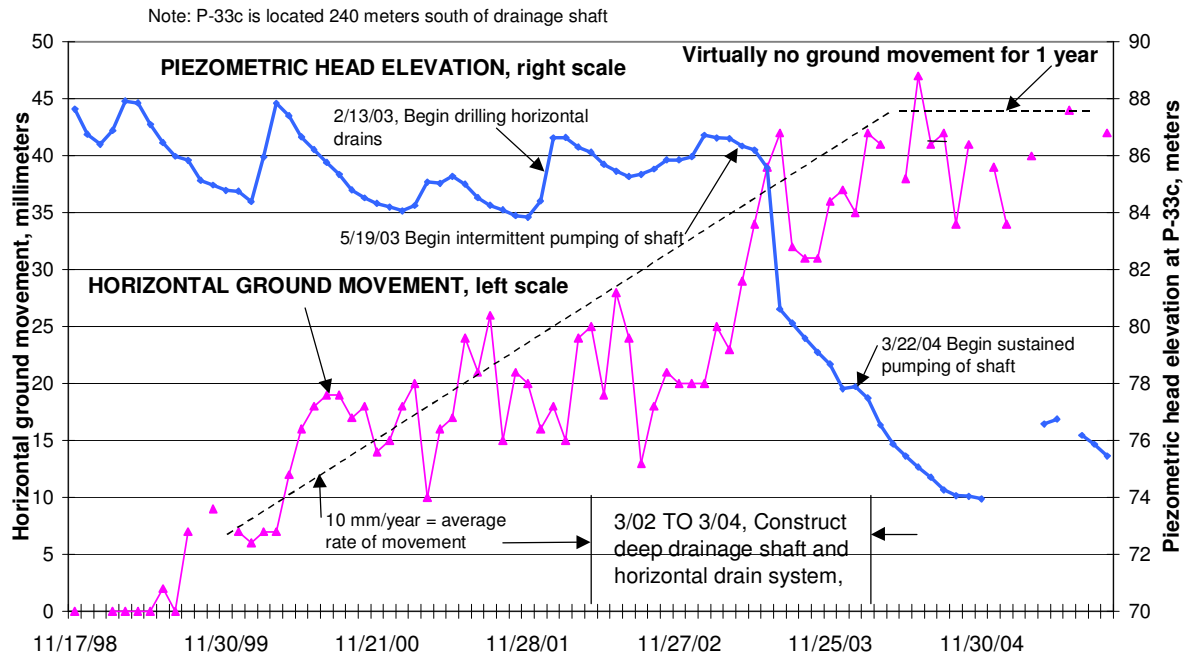


Figure 3.31: Piezometer elevation and Horizontal ground movement Vs Time from November 1998 to March 2005 at R80, Redtop landslide (CALTRANS 2007).

3.7. Summary

An examination of the field records associated with the case studies presented show that in all cases the installation of drains resulted in lowering the ground water level and increasing stability. The level of the lowered ground water table remained relatively constant even with varying amounts of rainfall. Thus, it can be concluded that the horizontal drains performed well on these sites regardless of the different nature of geological characteristics and soil profile.

Based on the available information, the site at SR 101 MP 69.8 was the only one with sufficient data (before and after installation of drains) for verification using numerical simulations. Thus, this site was selected to verify the numerical model.

CHAPTER FOUR

TOUGH2 COMPUTER CODE

4.1. Introduction

Field instrumentation consisting of piezometers, discharge measuring devices, and inclinometers provide us with valuable information on the performance of horizontal drains in slope stability remediation as described in the last chapter. However, they are costly in terms of construction and maintenance costs and also limited to the field conditions on which they are installed. On the other hand, advances in ground water flow models and associated numerical computer codes provide us with the ability to simulate the performance of horizontal drains. Once a numerical code is verified based on some field case records, it can be used to perform parametric studies to elicit information on the effect of system variables on horizontal drain performance.

A number of numerical codes are extant in the literature. Based on a careful review of this software, the computer code TOUGH2 (Transport of Unsaturated Groundwater and Heat) was chosen for use in this study. TOUGH2 was developed by the Lawrence Berkeley National Laboratory and is the most updated version of the TRUST code used by Lau and Kenney (1983) in their study. It is a general purpose numerical code for solving non-isothermal flows of multi-component, multiphase fluids in multi-dimensional porous and fractured media. TOUGH2 Version 2.0 (Pruess, 1999) is a new and improved version of TOUGH2 for simulating fluid flow and heat transfer in porous media. At the core of TOUGH2 is a solver for energy and mass balance equations of a multi-dimensional model. TOUGH2 was designed for applications in

geothermal reservoir engineering, environmental assessment, nuclear waste disposal, and variably saturated zone hydrology.

TOUGH2 can flexibly describe the flow in porous and fractured media in one, two or three dimensional geometries. It uses the integral finite difference method for space discretization of the flow system. It is a general purpose tool with a variety of programming and computing options available to choose from. The code allows defining boundaries with time-dependent or time-independent conditions. Its capability to define sinks and sources can be effectively used to model rainfall infiltration with either a fixed data or time dependant tabular format. It also allows varying parameters and controlling accuracy such as permeability, porosity and time steps. TOUGH2's capability to do averaging and/or interpolation makes it easy to use with limited data points from the field. On the negative side, TOUGH2 is a code based simulator written in the standard FORTRAN language with command line and file based inputs and outputs.

4.2. Flow equations

TOUGH2 solves Mass and Energy balance equations in their general form as in Equation 4.1.

$$\frac{d}{dt} \int_{V_n} M^k dV_n = \int_{\Gamma_n} F^k \cdot n d\Gamma_n + \int_{V_n} q^k dV_n \quad (4.1)$$

\uparrow
 Mass
 accumulation

\uparrow
 Mass flux

\uparrow
 Sinks & sources

where the mass or energy accumulation is the volume integration over an arbitrary volume V_n of the flow system under study, bounded by the closed surface Γ_n .

Mass or Energy accumulation is in the left hand side of the equation, where M is the accumulation term representing mass or energy per volume, and $\kappa = 1, 2, \dots, NK$ represents mass component labels such as water, air, H_2 etc. For the heat component, $\kappa = NK+1$. F denotes mass or heat flux flowing into the considered Volume, V_n , through the surface element, Γ_n , in a direction normal to the surface. The area vector normal to the surface is denoted by “ n ”. The last volume integral of this equation accounts for all the sinks and sources of the mass components in the considered volume, V_n . “ q ” denotes the sinks and sources.

Equation 4.1 can be converted to a partial differential equation by applying Gauss’ divergence theorem as:

$$\frac{\partial M^\kappa}{\partial t} = -\text{div}F^\kappa + q^\kappa \quad (4.2)$$

Equation 4.2 is the general form commonly used as the starting point for deriving finite difference or finite element discretization approaches.

For an approximate description of seepage of water in an unsaturated zone, phase change effects can be neglected. The gas phase can be assumed as passive with negligible gas pressure gradients for a liquid phase flow equation. For an almost isothermal condition, the liquid phase density and viscosity can be neglected, as appropriate. Under the above assumptions, Equation 4.2 simplifies to Richards’ equation (1931):

$$\frac{\partial \theta}{\partial t} = -\text{div}[K\nabla h] \quad (4.3)$$

where θ is the specific volumetric moisture content and K is the hydraulic conductivity.

4.3. Space and time discretization

Space is discretized using the “integral finite difference method” (Edwards, 1972; Narasimhan and Witherspoon, 1976) by introducing appropriate volume averages as:

$$\int_{V_n} M dV = V_n M_n \quad (4.4)$$

where M is a volume-normalized extensive quantity, and M_n is the average value of M over V_n .

The surface integrals are approximated as a discrete sum of averages over surface segments A_{nm} as:

$$\int_{\Gamma_n} \mathbf{F}^K \cdot \mathbf{n} d\Gamma = \sum_m A_{nm} F_{nm} \quad (4.5)$$

where F_{nm} is the average value of the (inward) normal component of F over the surface segment A_{nm} between volume elements V_n and V_m .

The discretization approach used in the integral finite difference method and the definition of the geometric parameters are illustrated in Figure 4.1. D_m , D_n are the distances from nodal points to the surface boundary.

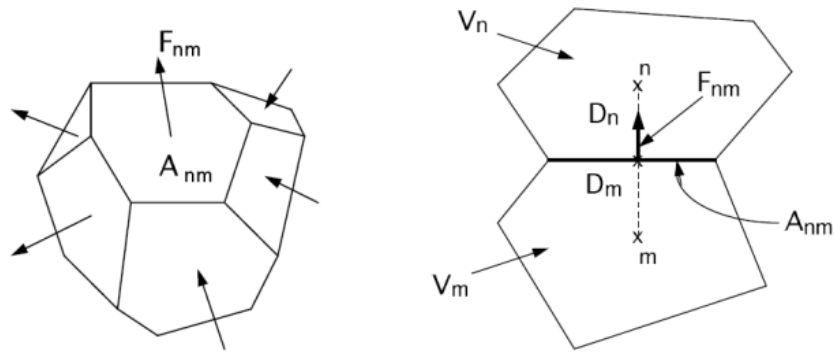


Figure 4.1: Space discretization and geometry data in the integral finite difference method (Pruess, 1999)

By substituting equations 4.4 and 4.5 into the governing equation 4.1, a set of first-order ordinary differential equations in time are obtained as:

$$\frac{dM_n^k}{dt} = \frac{1}{V_n} \sum_m A_{nm} F_{nm}^k + q_n^k \quad (4.6)$$

Equation 4.6 is solved at new time level $t^{k+1} = t^k + \Delta t$ to reach numerical stability. This approach is called “fully implicit”; since all unknown thermodynamic parameters are defined at time level t^{k+1} .

4.4. Initial and Boundary conditions

Before simulating groundwater flow, all of the elements must be initialized. Initial groundwater level and water saturation are defined at this stage.

Boundary conditions can be classified as Dirichlet conditions or Neumann conditions. For the Dirichlet condition, thermodynamic conditions, such as pressure and temperature are prescribed while for the Neumann condition, fluxes, such as mass and heat crossing boundary surfaces are prescribed. Boundary conditions also can be classified as time-dependent conditions or time-independent conditions.

4.5. Solution of Linear Equations

Evaluating the thermo-physical properties for all grid blocks, assembling the vector of residuals and a Jacobian matrix, and solving the linear equation system at each Newton-Raphson iteration step consumes an enormous amount of computing resources. TOUGH2 provides a choice of direct or iterative methods for linear equation solution as detailed by Moridis and Pruess (1998). Linear equation solvers based on direct methods are more robust but consume huge storage requirements and require much execution time, which increases proportionally with

the cube of the problem size. Iterative solvers are more problem specific and less predictable than direct solvers. Iterative solvers have much lower memory and computing power requirements. Iterative solvers are the method of choice for large problems with several thousand three dimensional grid blocks or more. Special care must be taken while using iterative solvers to ensure convergence, which may be affected by numerical properties such as many zeros on the main diagonal, a large numerical range of matrix elements or almost linearly dependent rows or columns. The off-diagonal elements in the Jacobian matrix are proportional to time step size. If they become too large to be differentiated after numerical round off, convergence of the linear equation system may no longer be achieved. In such situations a somewhat reduced time step must be used to achieve convergence.

4.6. TOUGH2 Architecture

TOUGH2 was developed according to the “MULKOM” modular architecture (Fig. 4.2), in which the main flow and transport module can interface with different fluid property modules. This Modular Architecture gives TOUGH2 the flexibility to handle a wide variety of multi-component, multiphase flow systems. The nature and properties of specific fluid mixtures enter the governing equations only through thermophysical parameters, such as fluid density, viscosity, enthalpy, etc., which are provided by an appropriate “EOS” (Equation-Of-State) module.

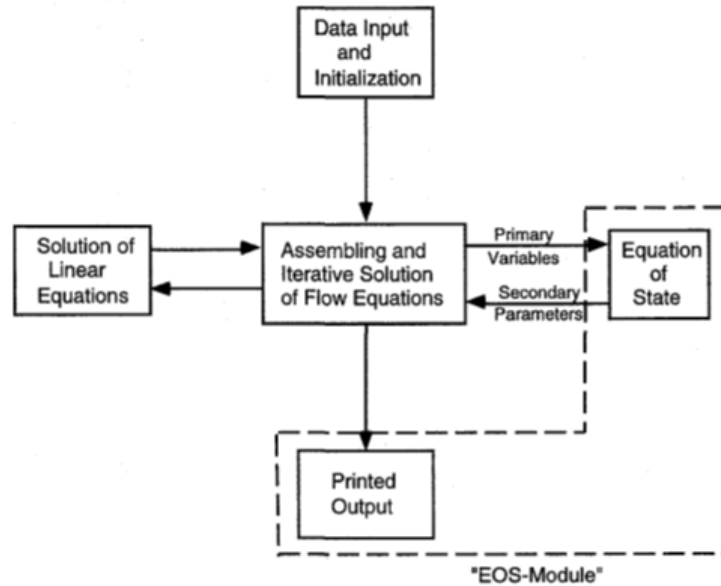


Figure 4.2: Modular “MULKOM” architecture of TOUGH2 (Pruess, 1999)

4.7. Data Input and Initialization

TOUGH2 requires specification of space-discretized geometry, and various program options, computational parameters, and time-stepping information. Most of these necessary input data are supplied to TOUGH2 in the form of ASCII text formatted files, which can be either directly provided by the user, or can be generated internally from data provided in a file named “INPUT”. Records such as thermophysical properties of the fluid may be defined in this file. Each record in the “INPUT” file can be up to 80 characters long. Input parameters are defined in SI units. The initialization stage also can generate a variety of computational grids or meshes. Other FILES often used to define the inputs are:

- a) MESH: Geometry of the considered system is defined in this file.
- b) GENER: This file defines sources and sinks.
- c) INCON: This file defines the initial conditions.

Geometry

TOUGH2 requires specification of space-discretized geometry. Geometry definition can be either regular or irregular shapes. TOUGH2 offers a way for defining flow system geometry by means of a special program module called MESHMaker. MESHMaker can generate two-dimensional radially symmetric (R-Z) meshes and XYZ for one-, two-, and three-dimensional Cartesian grids to define simplified geometries. The three-dimensional rectilinear XYZ option was involved for this horizontal drain study. MESHMaker on simplified geometries dramatically reduces the manual work to define meshes. On the other hand, TOUGH2 can also handle complex irregular geometry inputs. However generating the meshes for complex systems is extremely time consuming and should be done with the aid of third party tools such as Wingridder™ (Lehua Pan, 2008).

Initial and boundary conditions of flow system

Thermodynamic conditions, such as pressure and temperature on the boundary are made by assigning very large volumes to grid blocks on or near the boundary so that their thermodynamic conditions do not change. Time-independent Dirichlet conditions are accomplished in TOUGH2 input with the simple selection of “active” and “inactive” elements in the MESH definition. Defining inactive elements makes the thermodynamic conditions of that cell remain unchanged and removes it from the flow equations resulting significant reduction of computational overhead.

Neumann conditions can be specified in TOUGH2 by time-dependent (in tabular format) rates or time-independent (fixed) rates.

Sinks and Sources

The GENER record in the input file defines the Sinks and Sources in the system. Water taken away from the system is defined as Production with a value for q which is less than zero or negative. Water flow into the system is defined as Injection with the variable q set to a positive number. Injection could be a constant rate or a time varying rate, such as rainfall over a period of time.

Program options

Computer program options are another set of critical inputs to control the simulation. Parameters to set the accuracy level of the outputs and time steps can be defined. Simulation termination criteria could be either the number of iterations to run, a time period to run, or a certain accuracy to reach. Generally, simulation time is traded off with simulation accuracy. Constants such as gravity can also be defined in the INPUT file. Output formats can also be controlled through the setting of various records.

4.8. Equation-Of-State Modules

TOUGH2 comes with a package of ten equation-of-state (EOS) modules, each targeting different applications. All EOS modules are partitioned into two main blocks, Equation of state and printed output. This type of modularization provides flexibility and convenience in the choice of primary variables.

Each Equation of State block functions in conjunction with flow equations. Flow equations interface with the EOS modules by providing primary variables and getting back secondary parameters (Figure 4.2). In this study, the EOS9 module was selected for the

simulation of saturated groundwater flow. EOS9 handles the variably saturated flow of water component in an isothermal condition. Thus, there is no heat balance equation needed, and only the water mass balance equation is solved for each grid block. Richard's equation for unsaturated flow is used to describe the flow model in EOS9. EOS9 gets Pressure (P_{liq}) for saturated conditions and Water saturation (S_{liq}) for unsaturated conditions as primary variables from the flow equation and returns secondary parameters of the solution, mainly pressure diffusivity and flow velocity at specified grid locations.

TOUGH2 produces a self explanatory text file output during the simulation run. Most of the contents of this printed output can be controlled by the user by setting a variety of parameters. Various PARAMETER settings, problem size, dependent arrays, and disk files in use are some of the information written during the initialization phase to the standard output file. Output generally includes time-stepping information, and a complete element-by-element report of thermodynamic state variables and other important parameters for each iteration. Depending on user settings, additional optional outputs may be printed, such as mass and heat flow rates and velocities and on diffusive fluxes of components in phases.

4.9. Supporting Tools

Extreme care must be taken to compile the code for our application and to format the inputs in the TOUGH2 specific format. There are several supporting packages commercially available to format input and output of TOUGH2. Since none of the supporting packages were purchased with TOUGH2 in this study, all of the pre and post processing of data were done using a tool set developed using PERL and MATLAB. This tool set helps to efficiently run TOUGH2 while minimizing the chances of errors.

While initializing TOUGH2 data, large text files need to be edited for adding initial and boundary conditions. This process requires a considerable amount of time to do manually. Thus, scripts written in PERL were used for this purpose.

TOUGH2 generates a less than user friendly output file as a text file. A Perl script was developed to scan through this output file and to extract the final iteration results in a format which is readily accessible by Excel or MATLAB for post processing. Formatted output was written to a text based comma separated values (CSV) format file. In order to visualize the output in a three-dimensional graphical format, a script was written in MATLAB. These made it easier to observe changes in the flow pattern and the pore-pressures of a given problem.

CHAPTER FIVE

VERIFICATION OF NUMERICAL SIMULATION OF FLOW PATTERN AND SLOPE STABILITY ANALYSIS

5.1. Introduction

The numerical simulation of the ground water flow using TOUGH2 was verified using the field performance data from the Washington Department of Transportation project site near SR 101 MP 69.8 (section 3.1). As highlighted before, this site is located in the western part of Washington State. The landslide on this site is a part of ancient landslides, reactivated recently after having heavy rainfall. The main geologic units of the site consist of deeply weathered marine sedimentary rocks overlain by various landslide deposits. Horizontal drains were installed to improve the stability of the slope by lowering the groundwater level. The site was instrumented with Piezometers and inclinometers to monitor the performance of drains.

The results of ground water flow analysis were input into the slope stability program XSTABL (Sharma, 1996). This program was to develop the potential slip surface, and it was compared with the actual surface observed from field records (Figure. 3.6)

5.2. MP69.8 Site Geometry

A schematic of the cross section of the model developed for TOUGH2 analysis based on field records is as shown in Figure 5.1 (See also Fig. 3.6). A three dimensional model was created for the slope with dimensions of 185meters long, 50meters wide, and 65meters deep. These dimensions were chosen so as to accommodate the limitation of the computational storage

and time. The values were chosen after repeated trials so as to not affect the final results of the simulation.

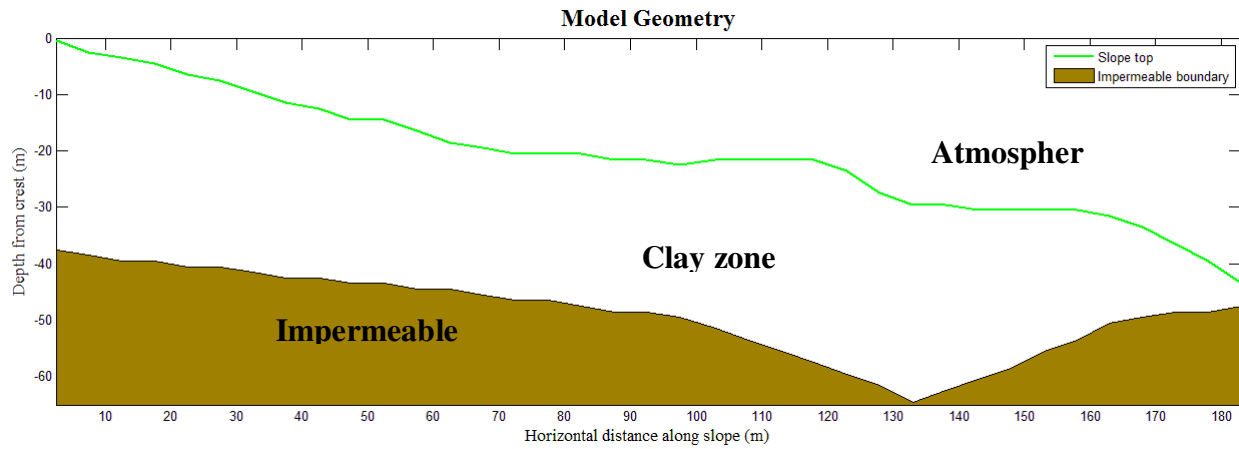


Figure 5.1: Model Geometry of SR 101 MP 69.8

Model parameters were assigned based on field geotechnical investigations. The model was divided as three major domains named as clay, impermeable and atmosphere. The clay zone, defined as a low permeable material, the impermeable zone, and the atmosphere zone, defined as boundary with no water flow into the impermeable Lincoln Creek Formation.

5.3. TOUGH2 model

This site geometry was modeled using EOS9 module of TOUGH2 and assigned with initial and boundary conditions to be solved by the EOS9 module for saturated water flow. The model was initialized with the groundwater level at the river level. Infiltration was applied continuously along the slope face while maintaining a constant discharge to the river. Atmosphere was modeled with 100% porosity to define the boundaries. The impermeable Lincoln Creek Formation was modeled as a material with very small permeability ($1 \times 10^{-15} \text{ m}^2 = 1 \text{ mD}$) to define the lower boundary. The river level at the toe of the slope was defined as a constant pressure boundary. Infiltration was assigned on the slope as a time dependent Neumann

boundary with flux flow into the permeable region. Porosity was assigned as 60% for clay and 35% for impermeable zone. Absolute permeability values for clay in the x, y and z directions were assumed to be $3 \times 10^{-12} \text{ m}^2$, $3 \times 10^{-12} \text{ m}^2$ and $1 \times 10^{-12} \text{ m}^2$, respectively. Also, absolute permeability values were assumed in the x, y and z directions for rock as $3 \times 10^{-15} \text{ m}^2$, $3 \times 10^{-15} \text{ m}^2$ and $1 \times 10^{-15} \text{ m}^2$, respectively and for air as $3 \times 10^{-11} \text{ m}^2$, $3 \times 10^{-11} \text{ m}^2$ and $1 \times 10^{-11} \text{ m}^2$, respectively. EOS9 assumes isothermal conditions and default thermo physical parameters were used (heat conductivity = $2.51 \text{ W/m}^\circ\text{C}$ and specific heat = $920 \text{ J/kg}^\circ\text{C}$). Steady state conditions were modeled for infinite time. Initial flow calculation was allowed until reaching a convergence rate of $1 \times 10^{-5} \text{ N/m}^2$.

5.4. Simulation of Water Level

The water level before installation of the drains was modeled and numerically simulated in TOUGH2 with boundary conditions, permeability values, and infiltration. The simulated water level is as shown in Figure 5.2. This simulated water level values are compared with those from field Piezometer readings, as shown on the same figure.

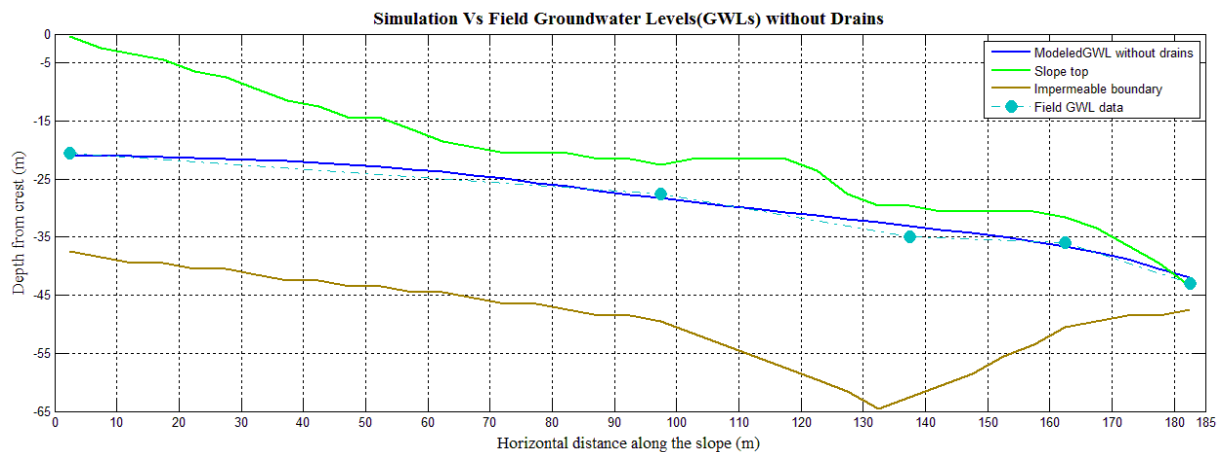


Figure 5.2: Simulated initial phreatic surface and piezometric data before installed the drains

It can be seen that, except for some minor mismatches, the prediction matches the field data well. The mismatches may be due to the idealized assumptions (cracks non-homogeneous soil properties, vegetations etc.) used in the simulation model. In comparison to the model geometry, these differences are small enough to be neglected and within the accuracy range of the scope of this research.

The pore water pressure distribution across a typical cross-section of the slope and the resultant velocity-vector plot are shown in Figures 5.3 and 5.4, respectively. Water level and porewater pressure contours correlate to the velocity vector plot.

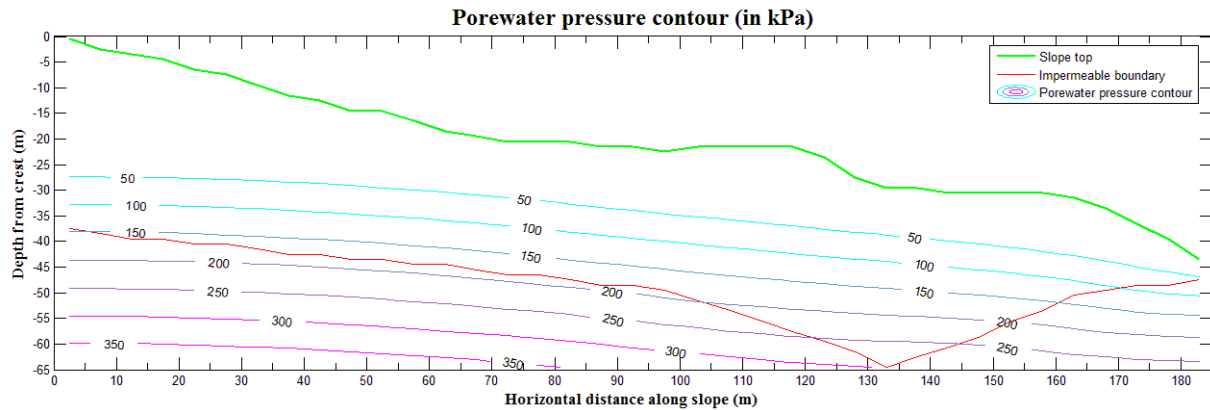


Figure 5.3: Porewater pressure contour (in kPa) for SR 101 MP 69.8

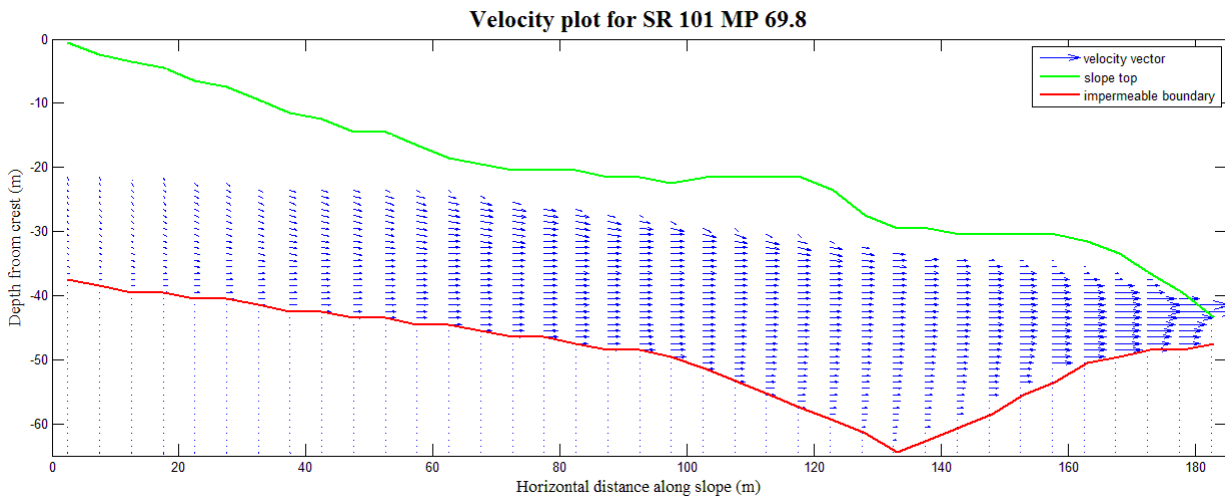


Figure 5.4: Velocity vector plot for SR 101 MP 69.8

The initial ground water level was used as the initial condition to simulate the changes that occur as a result of the installation of the horizontal drains. The location of the drain is as shown in Figure 5.5. Drain elements are assumed to be time independent boundary conditions with zero pressure head (Cai et al., 1998). Also it was assumed to be continuously flowing water with no blocks along the drain. With the above assumptions, drains were added to the model and initialized as atmospheric pressure at each drain element.

Then, the slope was modeled for the transient state with a limited time period. The average groundwater level was calculated after adding horizontal drains and compared to the results with field Piezometer data. A two dimensional overlay of simulated groundwater levels and Piezometer data before and after installing the drains are shown in figure 5.5. Blue and cyan lines represent simulated groundwater levels, blue and cyan markers represent field Piezometer data and the red dotted line represents the horizontal drain.

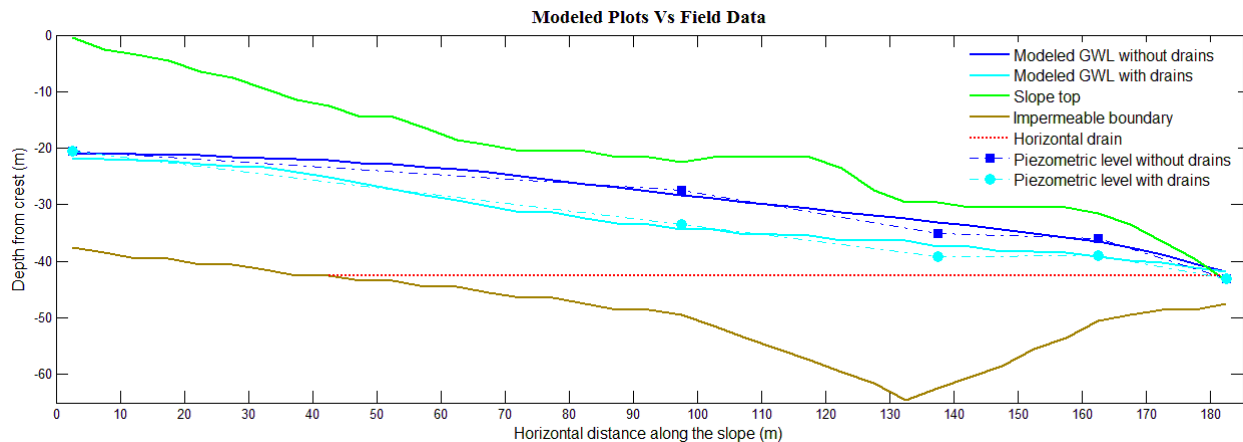


Figure 5.5: Overlay of groundwater levels from simulations and field at SR 101 MP
69.8

When comparing the groundwater levels after installing the horizontal drains, simulation results are well matched with the four Piezometer locations. The Piezometer reading at 137.5m along the horizontal distance shows the only visible mismatch. It could be due to imperfections

in the field drains such as bends, blocks, cracks, etc., or due to inhomogeneous soil. We can ignore that field data since the other four fitted well.

5.5. Slope failure analysis

The ground water data from TOUGH2 was input into XSTABL to evaluate the stability of the slope before and after installation of the drains. The cross-sectional geometry of the site with the soil and impermeable boundaries was defined in XSTABL as shown in figure 5.6. The slide zone is overlain by a clay zone in the upslope, a passive block in the down slope, and it is underlain by impermeable rock.

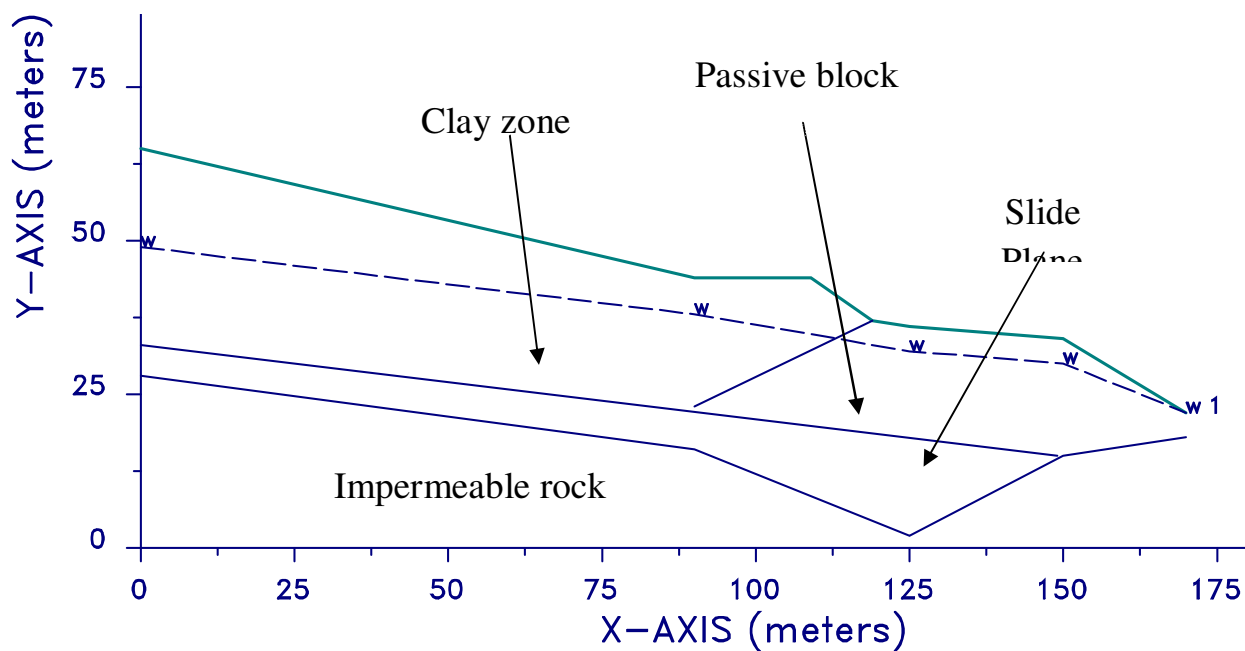


Figure 5.6: XSTABL input geometry

Soil properties such as cohesion and friction angle were taken from Kleinfelder's data and assigned to XSTABL input as described in Table 5.1.

	Unit Weight (lb/Cu.Ft)	Cohesion (psf)	Friction Angle (⁰)
Clay Zone	130	0	28
Passive Block	120	0	28
Impermeable Rock	130	2500	35
Slide Plane	110	0	12.5

Table 5-1: Soil properties at SR 101 MP 69.8 site

5.6. Equivalent Slope Stability Model Using XSTABL

Failure planes identified from field measurements are shown on Figure 5.7. It was assumed that two types of failure modes exist. One is the larger failure which is a noncircular failure plane cracking above the highway SR101. The other one is the failure of the lower block near the toe of the slope. Subsequently, after the failure of this lower block, the adjacent upper block loses its lateral support and moves towards its failed surface.

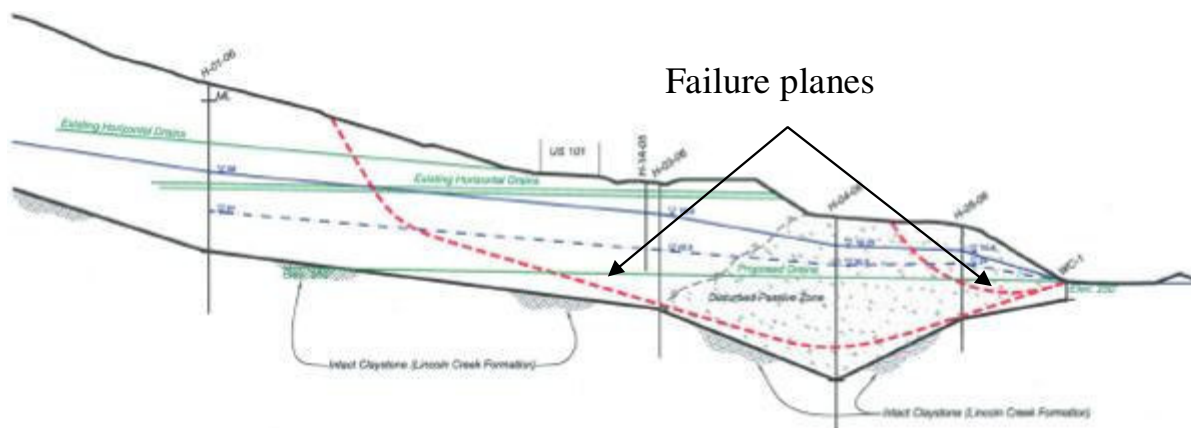


Figure 5.7: Identified field failure surface (Kleinfelder 2006)

Both of the failure surfaces were analyzed for Factor of Safety (FOS) equal one using the search option in XSTABL. Figure 5.8 and figure 5.9 show the output plots from XSTABL for

larger and smaller failure surfaces, respectively. These plots are well matched to the failure planes from field data (see Fig. 5.7).

MP698_36 11-05-** 19:20

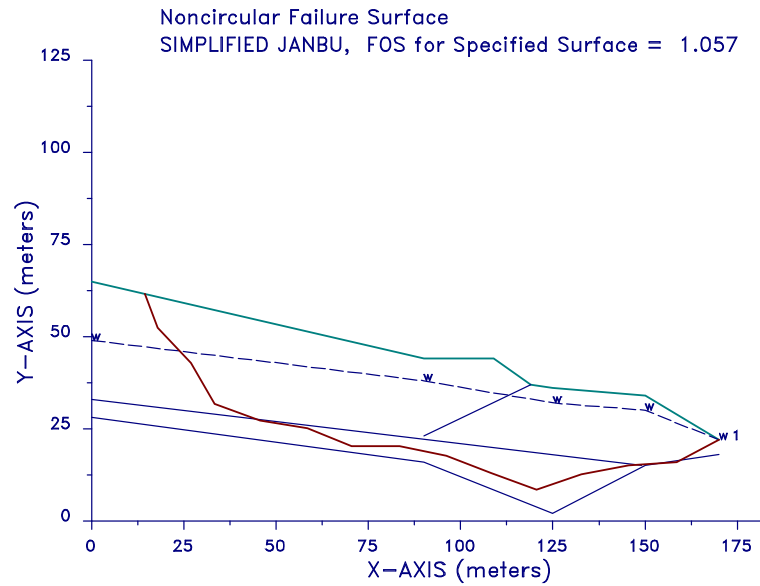


Figure 5.8: Identified larger failure surface from XSTABL

MP698_39 10-03-*** 15:24

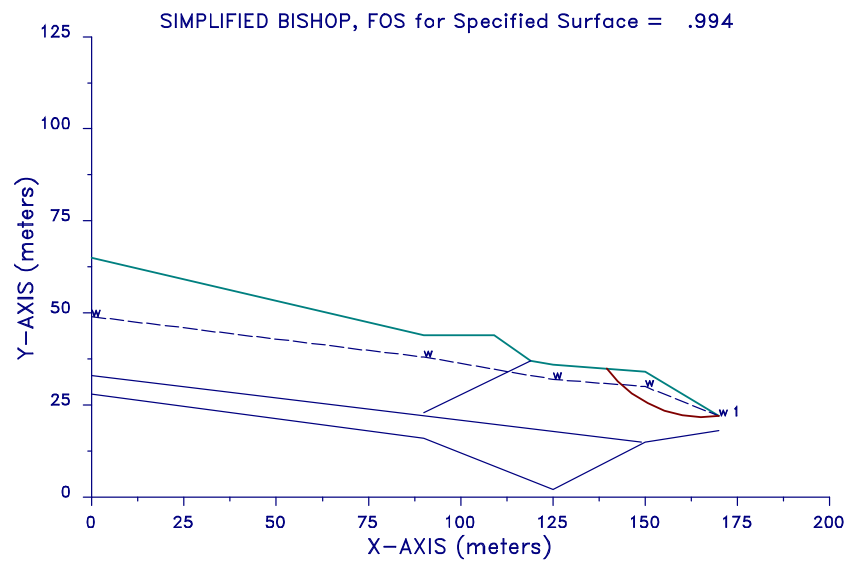


Figure 5.9: Identified smaller failure surface from XSTABL

Then FOS for the slope was calculated after installing drains for both larger and smaller failure surfaces. Porewater pressure values at the failure surface were used to input “WATER” in XSTABL. Figures 5.10 (a) and (b) show the FOS values for the identified failure surfaces. XSTABL output in these plots confirms the slope stabilized by horizontal drains. A FOS of 1.385 was obtained for the larger failure plane. Before installing drains, it was 1.057. Similarly, after adding drains, the FOS for the failure plane near the toe of the slope was 1.389. Before adding drains, it was 0.994.

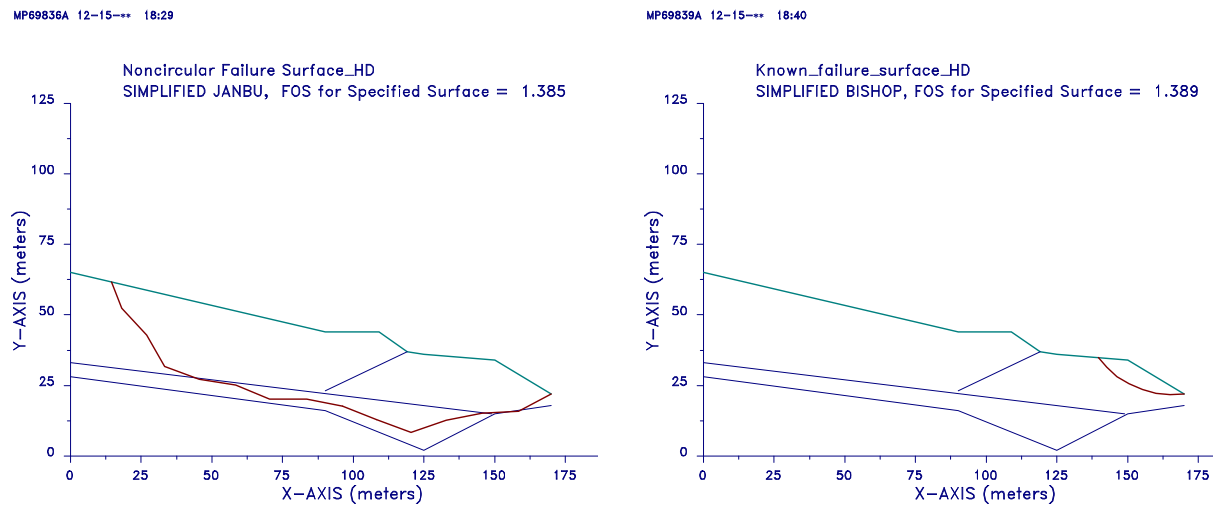


Figure 5.10(a), (b): Improved FOS after installing horizontal drains for (a) Larger failure plane, (b) Smaller failure plane.

5.7. Summary of verification results

A known failed slope near SR 101 MP69.8 was selected to verify the numerical simulation of the flow pattern using TOUGH2 and slope stability analysis using XSTABL. The site was modeled in TOUGH2 and simulated to obtain the groundwater levels and porewater pressure before and after installing horizontal drains. Simulated groundwater levels were matched to field records. Following TOUGH2 verification, critical failure surfaces were obtained using an exhaustive search using XSTABL with groundwater level from TOUGH2 as

one of the inputs. This failure surfaces were also matched to the field records. Then the FOS was calculated for the known failure planes with horizontal drains and verified to be stabilizing the slope with an improved factor of safety. The above verification process validated our modeling and simulation methodology and it can be used to model and simulate a similar site with high confidence in the future.

CHAPTER SIX

PARAMETRIC STUDY AND DESIGN CHARTS

6.1. Introduction

The ultimate aim of the design of horizontal drains on soil slopes is to ensure a certain increase in its stability. This is dependent on a number of variables, such as the drain length, spacing, and the placement location with respect to the critical failure surface. However, horizontal drains have been installed on an empirical basis, with the quantity of discharge as the main criterion of success. This approach has been criticized by a number of investigators (Nonveiller 1970; Kenney et al. 1977) who have emphasized that the primary aim of such drainage is to reduce pore water pressures which in clay slopes may be achieved with a slight yield of water. Most slopes have different soil, hydraulic, and geometric characteristics and therefore, the design of drainage systems to improve slope stability should be done on an individual basis. This is rather difficult in practice for field applications. On the other hand, numerical simulations offer an attractive alternative to model the changes in ground water level and porewater pressures as a result of drain installation. Once verified, these models can be used to study the influence of various system parameters on the increase in slope stability.

The TOUGH2 model verified with a field case study in the last chapter is used here to study the influence of various parameters on the performance of horizontal drains. A three dimensional slope with a homogeneous clay material was created and used for this study. The elevation of drains on slope, length of drains, and spacing between drains were varied to quantify their influence on the performance of horizontal drains. In addition, the influence of changes in

anisotropic permeability ratio (k_h/k_v) of the soil was also studied. The results are input into the slope stability analysis program XSTABL to determine the changes in factor of safety.

6.2. Model geometry and TOUGH2 simulations

The schematic diagram of a 3-D homogenous clay slope founded on an impermeable rock is shown in Fig. 6.1 a. The geometry was discretized in TOUGH2 and used to calculate the pore water pressures at all grid points for a given phreatic surface. The cross section of the model is defined in the XZ plane (Figure 6.1 b). The model is 150m long in the x-direction, 50m width in the y-direction and 50 m in the z-direction. Note that the dimension in y is restricted due to computer storage capacity limitations associated with TOUGH2 simulations. The compiled TOUGH2 software can support only 250,000 grid interfaces and 100,000 grid points.

The results from TOUGH2 were input into the XSTABL slope stability program to calculate the factor of safety. Note also that XSTABL is a 2-D slope stability program and it assumes that the dimension in the y-direction is infinitely wide to eliminate end effects (normal and horizontal side resisting forces along the sides of the sliding mass) (Baligh and Azzouz (1975)). Cornforth (2004) has shown that the width of the slope should be at least two times the length ($2 \times 150 = 300\text{m}$) in order to define an infinitely wide slope in practice. However, as mentioned before, due to memory limitations, and to utilize the maximum capability of TOUGH2 while keeping the unit grid size small enough to resemble a drain pipe, we are limited to a 50 m wide model. However, to ensure that the results did not change very much along the y-direction for this homogenous slope, we varied the width from 15m to 50 m and observed that

such variation had no significant change in the results. Increasing the width above 50m would have resulted in larger grid sizes, exponentially increasing simulation time and memory issues.

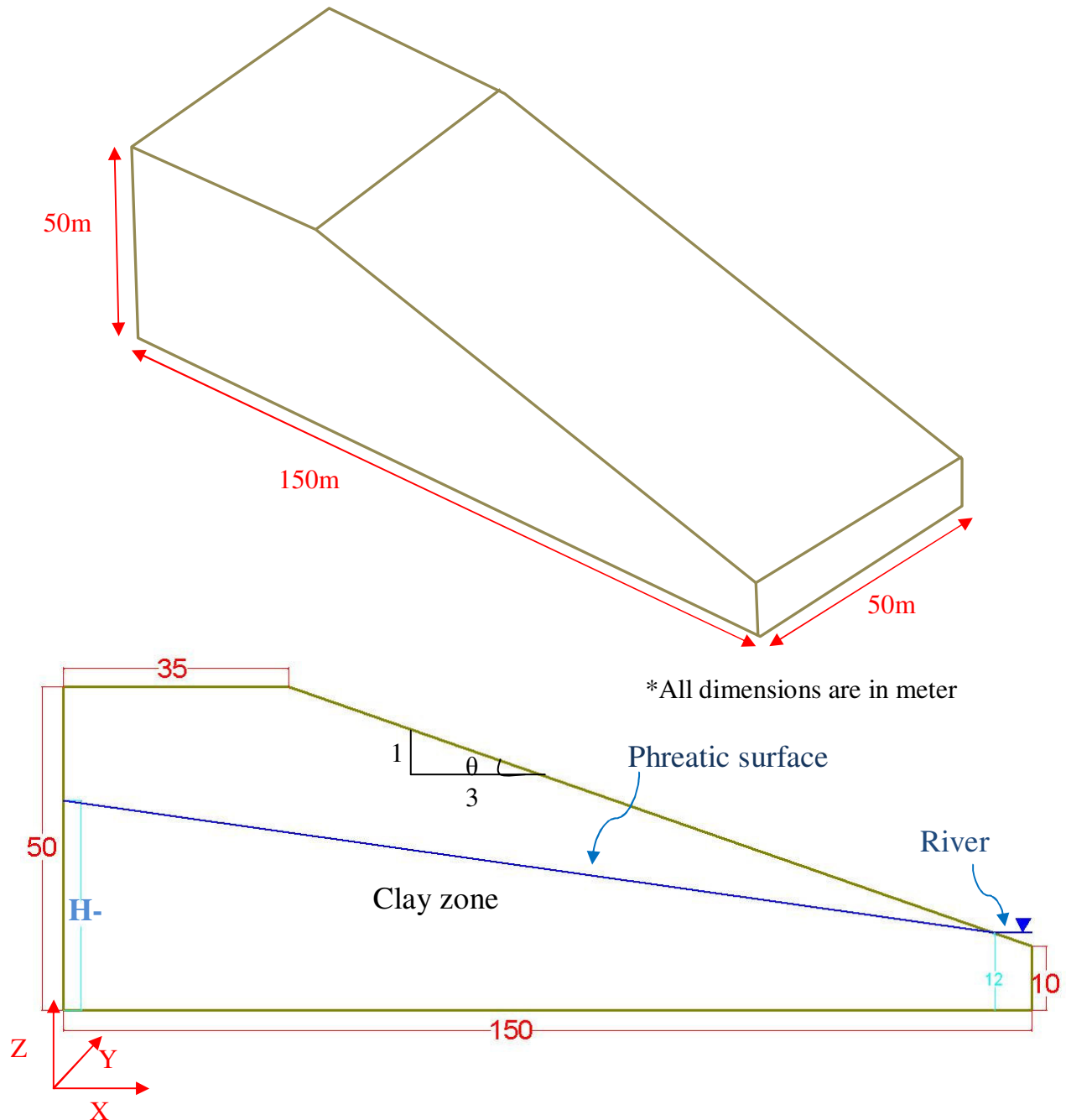


Figure 6.1(a), 6.1(b): (a)-3D geometry, (b)-2D cross-section with initial phreatic surface

The initial height of water level (H_w) was selected by changing horizontal to vertical permeability ratios. The river water level was assumed to be 12 m above the base of the model (Figure 6.1). Absolute permeability in the vertical direction was assumed to be $1 \times 10^{-12} \text{ m}^2$. The whole model was discretized into rectangular grids with a grid size of 5 m, 1 m and 1 m in the x, y and z directions, respectively, as shown in Figure 6.2(a) and (b).

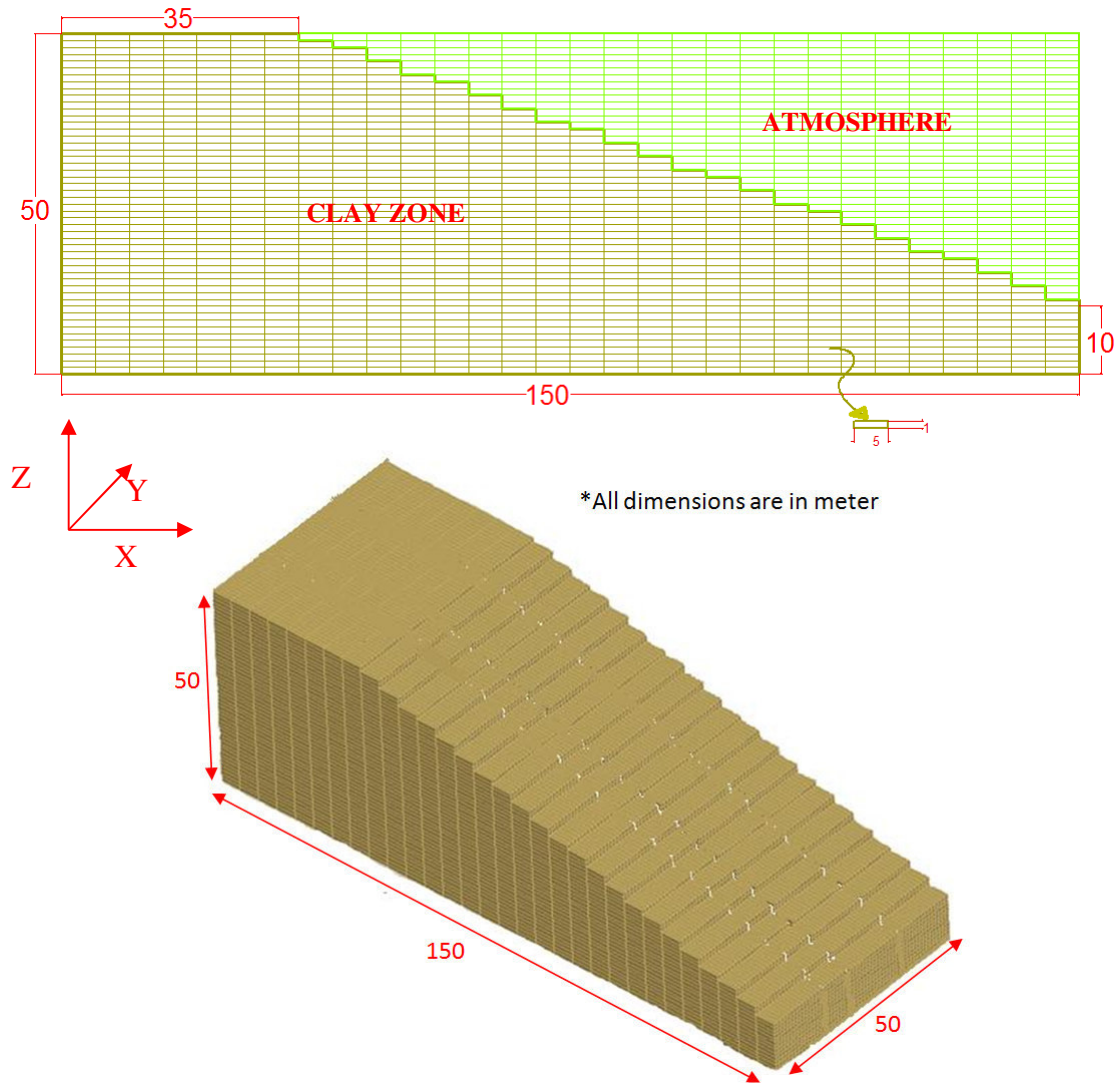


Figure 6.2(a), 6.2(b): (a) – 2D Mesh Geometry, (b) – 3D Mesh Geometry of the selected model

The clay model was numerically solved using the EOS9 module of TOUGH2 V2.0. and the resultant phreatic surface and porewater pressure distribution were determined. The changes in initial phreatic surface location with the changes in permeability ratio k_h/k_v before installation of drains are as shown in Fig. 6.3. It can be seen that the permeability ratio has a significant effect on initial steady state ground water level. The pore water pressure distribution before the drain installation with permeability ratio $k_h/k_v = 5$ is shown Figure 6.4. The plot shows the pore water contours in the interval of 50kPa.

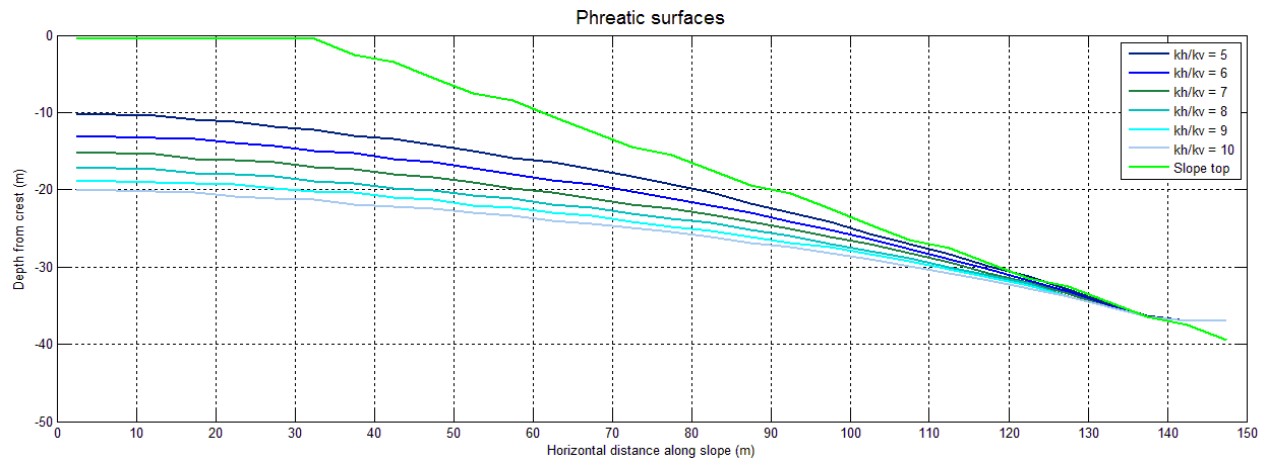


Figure 6.3: Modeled phreatic surfaces for the slope with no drains

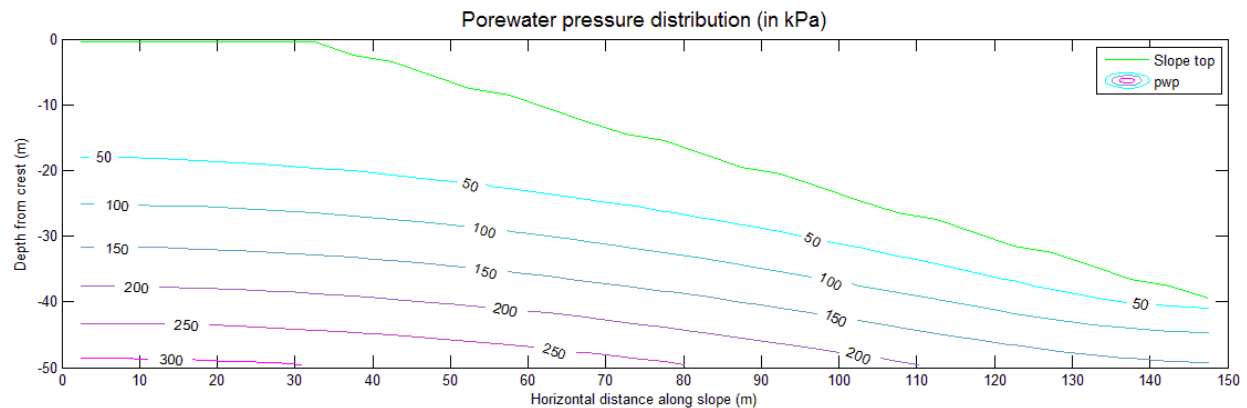


Figure 6.4: Two dimensional distribution of Pore water pressure (in kPa) of model with $k_h/k_v = 5$

6.3. Parametric Study

The schematic of the layout of the drains used in the parametric study is as shown in Figures 6.5 and 6.6 respectively. The parametric study considered the variation of the following horizontal drain parameters: (1) elevation of drain (E), (2) length of drain (L), and (3) spacing between drains (S). The analysis was performed first for five different elevations, then the length of drain was changed to cover five different lengths of drain, and finally spacing between the drains was varied for 3 different settings. The details of the variation are as shown in Table 6.1

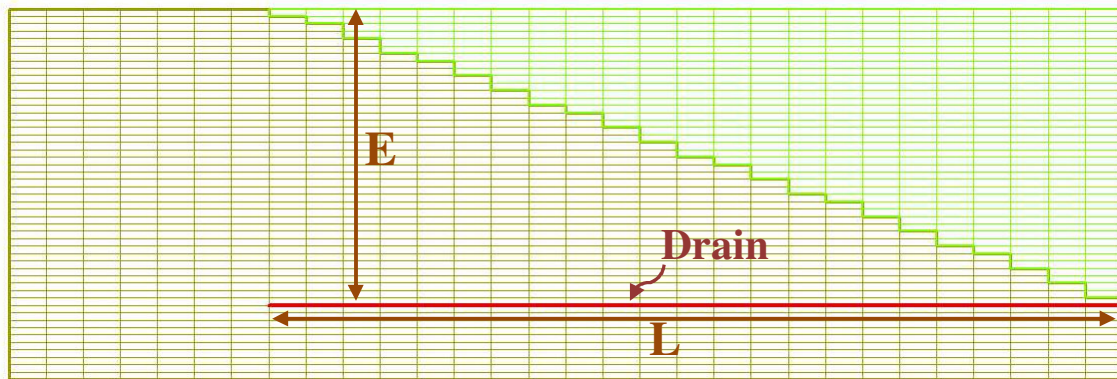


Figure 6.5: Cross section of slope with drain location and variables

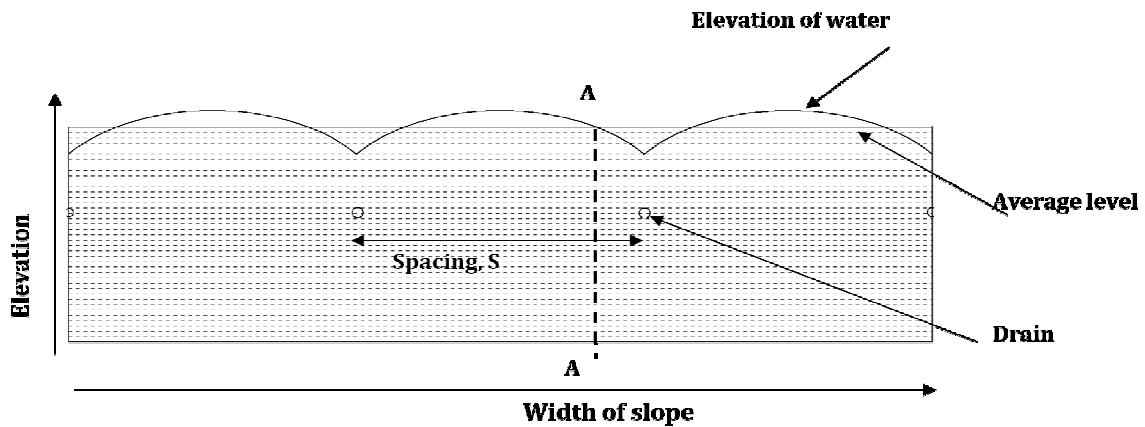


FIGURE 6.6: DRAIN LOCATION ALONG THE WIDTH OF SLOPE

Analysis for each drain system was repeated for different initial groundwater conditions based on the permeability-anisotropy ratio, as described in Table 6.1. The majority of the analyses are reported for slope inclined at a ratio of 1: 3 unless stated otherwise. In order to study the effect of slope inclination, the drain arrangement of E1 (Table 6.1) was studied for slopes with inclination 1: 2.5 and 1: 3.5.

System or Condition	Drain System (A)			Groundwater conditions (B)
	Elevation of drain (m), E L=75m, S=15m	Length of drains (m) , L E=-35m, S=15m	Spacing between drains (m), S L=125m, E=-35m	k_h/k_v ratio
1	-35	125	15	5
2	-30	100	10	8
3	-25	75	5	10
4	-20	50		
5	-15	25		

Table 6-1: Different horizontal drain arrangements and groundwater conditions

The introduction of the drains resulted in a three dimensional pore water pressure distribution from TOUGH2 that was found to be non-uniform over the width of the slope. Since XSTABL has the limitation of performing stability calculations in two dimensional spaces only, the pore water pressures taken from the cross section were averaged to an equivalent horizontal water level between crest and trough as shown on Figure 6.6. In this manner, porewater pressure in longitudinal section A-A (xz plane) was selected as input for XSTABL. It was assumed that section A-A was located at a distance of $S/4$ (m) (S = spacing between drains) from the drain to make calculations easy.

The average pore water pressure distribution for the system arrangement E1 (see table 6.1.) and $k_h/k_v = 5$ is shown in Figure 6.7. In this figure, porewater is contoured at the interval of 25kPa, and the red dotted line shows the location of the drain. When compared with Figure 6.4, porewater pressure distribution has changed after installing the drains. Porewater pressures have reduced, and they have reached a constant value below and along the drains.

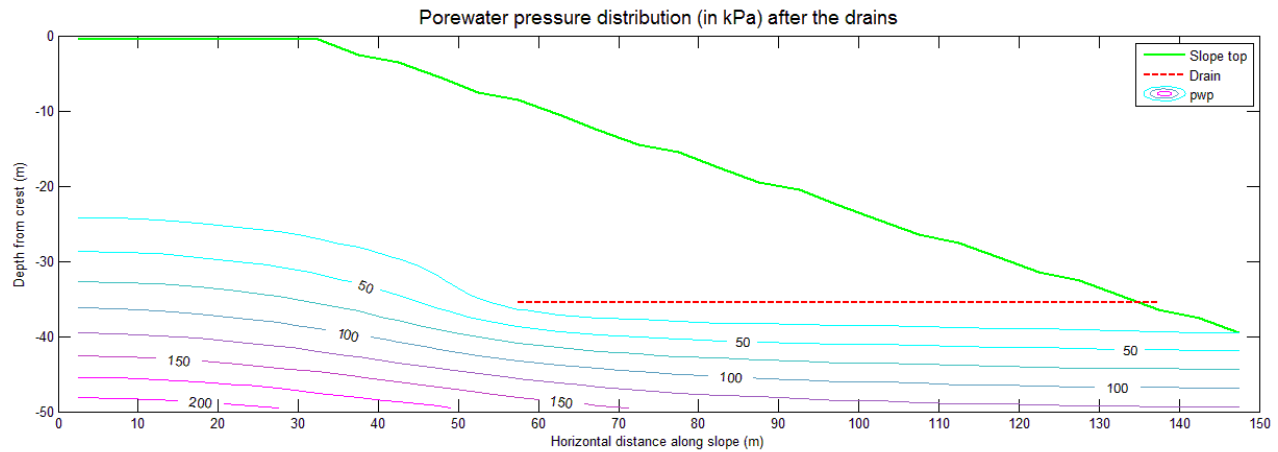


Figure 6.7: Average pore water pressure distribution of slope with drain $k_h/k_v = 5$

6.4. Stability Calculations using XSTABL.

Slope stability analysis was conducted using XSTABL for a circular failure surface based on the simplified Bishop's method. Geometry of the slope was entered as in Figure 6.1.(b) with a single soil surface. The shear strength parameters of the soil used were with cohesion as zero (cohesion less) and friction angle as 26° . TOUGH2 output was used as the phreatic surface input into XSTABL. XSTABL was configured to search for the largest critical circular failure surface. The initial XSTABL analysis was performed to find the Factor of Safety (FOS) at the extreme termination point ($x = 0$) where it is potentially the highest. If the FOS was greater than one, we refined the termination point with gradually lower values until the FOS became unity.

XSTABL also plots the corresponding failure surface for each search option. The identified failure surface and the FOS value for the case of no drains are shown in Figure 6.8.

The identified failure surface without horizontal drains from the above analysis was considered as the reference failure surface. After installing the horizontal drains, the FOS was calculated at the reference failure surface. To calculate this factor of safety, we used the “pore pressure grid” option in XSTABL. Pore pressure values at failure, which were obtained from previous TOUGH2 analysis, were used as “water input” for XSTABL.

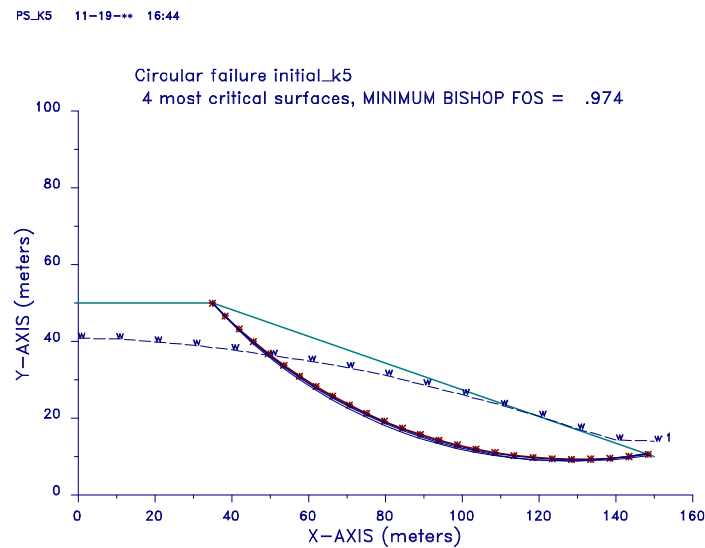


Figure 6.8: Identified failure surface for selected model

The calculated Factor of safety (FOS) for different drain systems under each initial groundwater condition (for a given permeability anisotropy ratio) is shown in Table 6.2(a), (b). Note that in this table, the FOS of the slope for the initial groundwater conditions before adding drains is denoted as F_0 , and the increase in the FOS after adding the drain is denoted as ΔF (FOS after drains – F_0). The FOS value for the various slopes with different slope angles is provided in Table 6.3.

Arrangements	$k_h/k_v = 5$ $F_0 = 0.974$ $H_w = 41\text{m}$			$k_h/k_v = 8$ $F_0 = 1.118$ $H_w = 34\text{m}$			$k_h/k_v = 10$ $F_0 = 1.174$ $H_w = 31\text{m}$		
	E	L	S	E	L	S	E	L	S
1	1.434	1.439	1.439	1.435	1.439	1.439	1.441	1.443	1.443
2	1.385	1.436	1.458	1.389	1.439	1.466	1.391	1.442	1.466
3	1.351	1.434	1.474	1.361	1.435	1.474	1.366	1.441	1.474
4	1.337	1.427		1.345	1.431		1.359	1.437	
5	1.327	1.384		1.345	1.413			1.424	

Arrangements	$k_h/k_v = 5$ $F_0 = 0.974$ $H_w = 41\text{m}$			$k_h/k_v = 8$ $F_0 = 1.118$ $H_w = 34\text{m}$			$k_h/k_v = 10$ $F_0 = 1.174$ $H_w = 31\text{m}$		
	E	L	S	E	L	S	E	L	S
1	0.46	0.465	0.368	0.317	0.321	0.321	0.267	0.269	0.269
2	0.411	0.462	0.387	0.271	0.321	0.348	0.217	0.268	0.292
3	0.377	0.46	0.403	0.243	0.317	0.356	0.192	0.267	0.3
4	0.363	0.453		0.227	0.313		0.185	0.263	
5	0.353	0.41		0.227	0.295			0.25	

Table 6-2(a), 6-2(b). (a) – FOS, (b) – difference in FOS (Δf) for different horizontal drain arrangements

Arrangements	Slope inclination	Slope angle (degree)	kh/kv = 5, $F_0 = 0.974$, Horizontal arrangement E1
1	1:3.5	15.9	1.546
2	1:3.0	18.4	1.434
3	1:2.5	21.8	1.415

Table 6-3. FOS for different slope angles

6.5. Design Charts

The results of the parametric study were used to develop design charts that could be used in the selection of system parameters for efficient horizontal drain design. The minimum safety factor for the critical slip surface was plotted against varying drain parameters in figures 6.9, 6.10, and 6.11. Figure 6.12 shows the minimum safety factor with different slope inclinations as tabulated in Table 6.3.

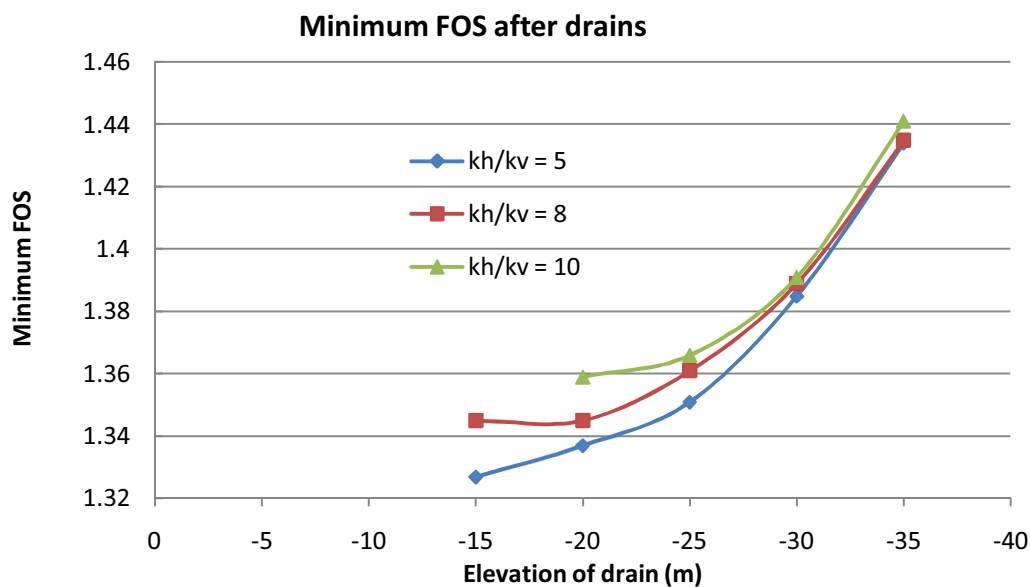


Figure 6.9: Minimum Safety Factor for critical surface against Elevation of drains

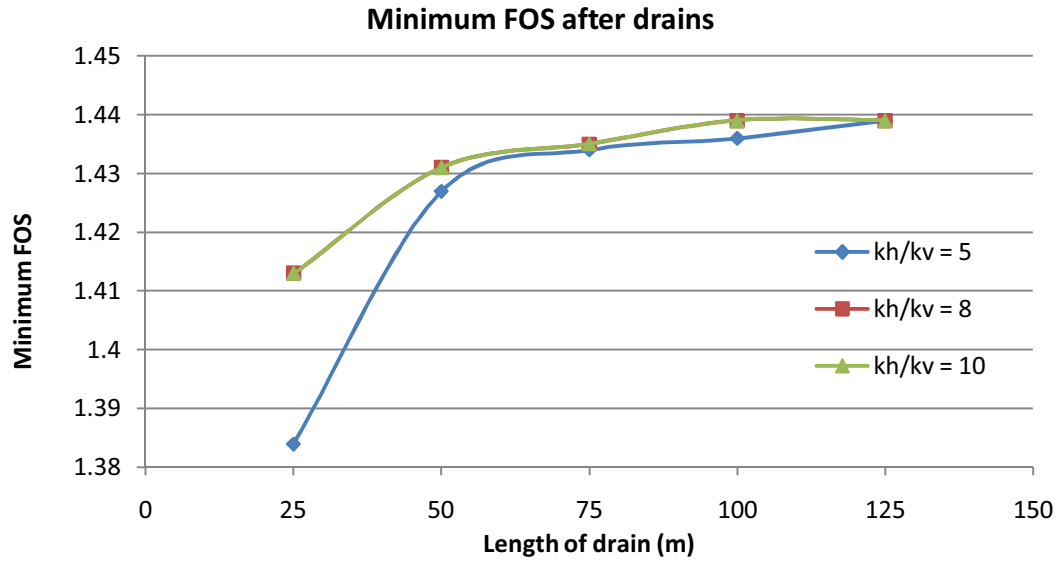


Figure 6.10: Minimum safety factor for critical surface against length of drains

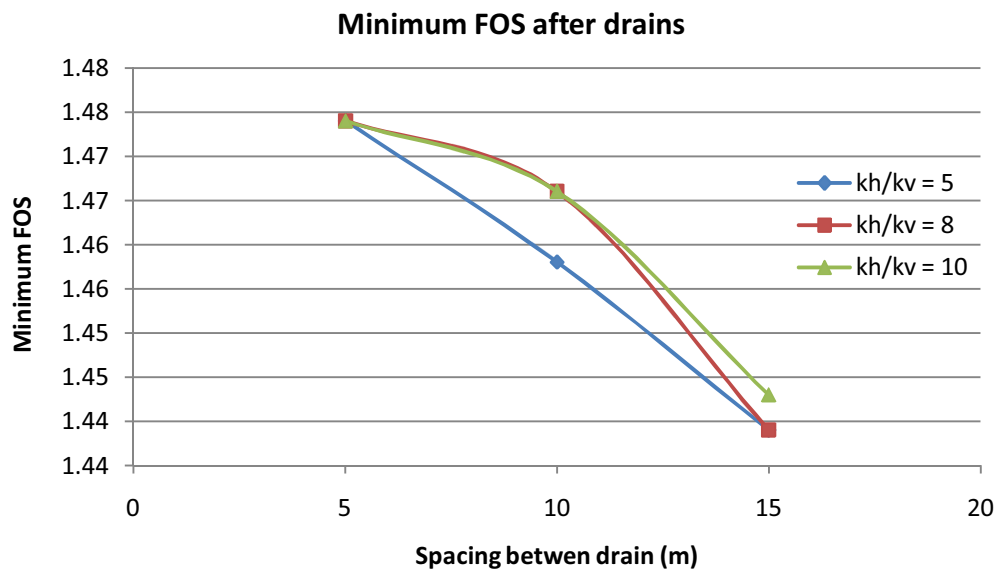


Figure 6.11: Minimum safety factor for critical surface against spacing between drains

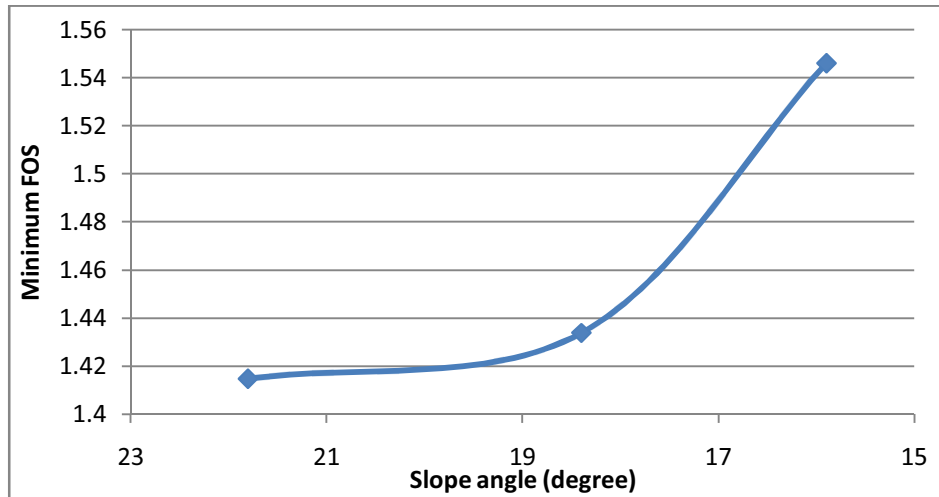


Figure 6.12: Minimum safety factor for critical surface against slope angle

The increase in factor of safety against the system parameters was plotted to obtain a pattern of horizontal drain effectiveness. The increase in FOS against the elevation of drains is shown in Figure 6.13. Similarly, the increase in FOS against length of drains is shown in Figure 6.14. Finally, the increase in FOS against varying spacing between drains is shown on Figure 6.15.

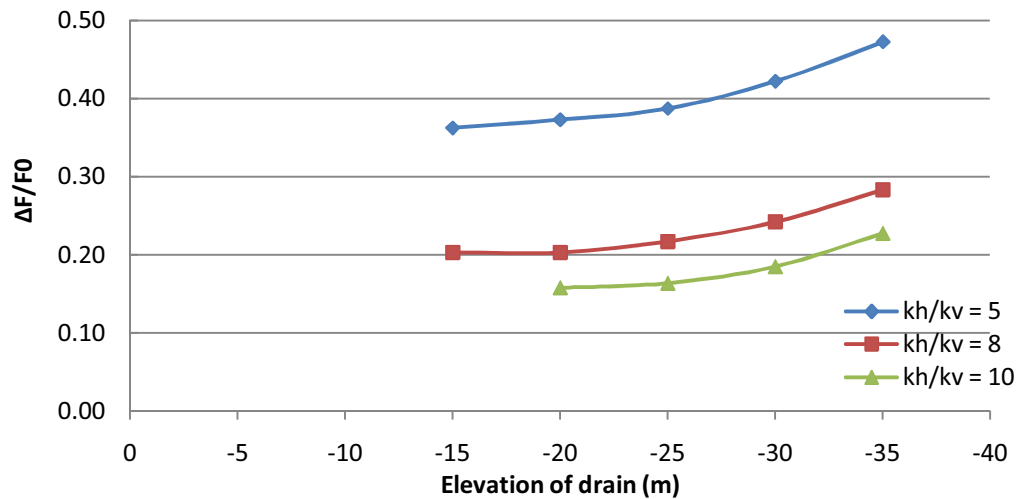


Figure 6.13: Increase in FOS ratio Versus Elevation of drains

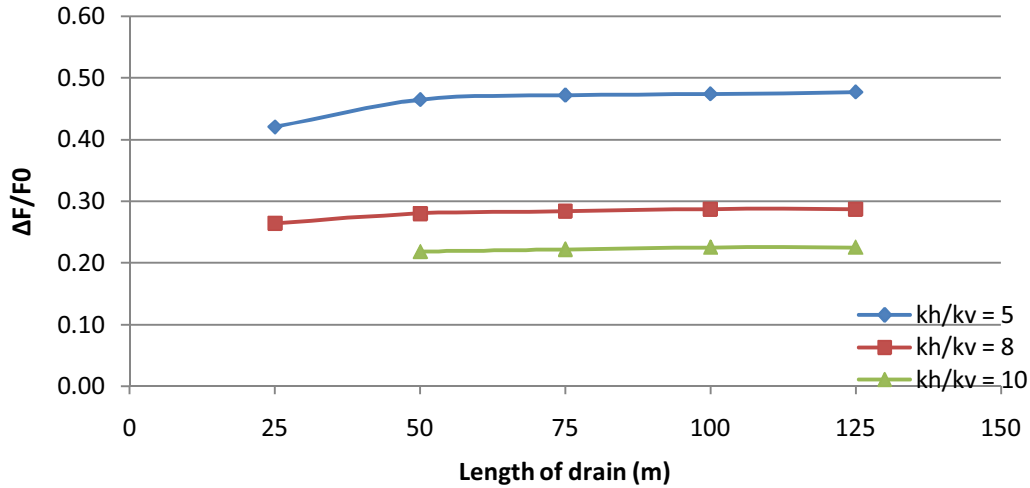


Figure 6.14: Increase in FOS ratio Versus Length of drains

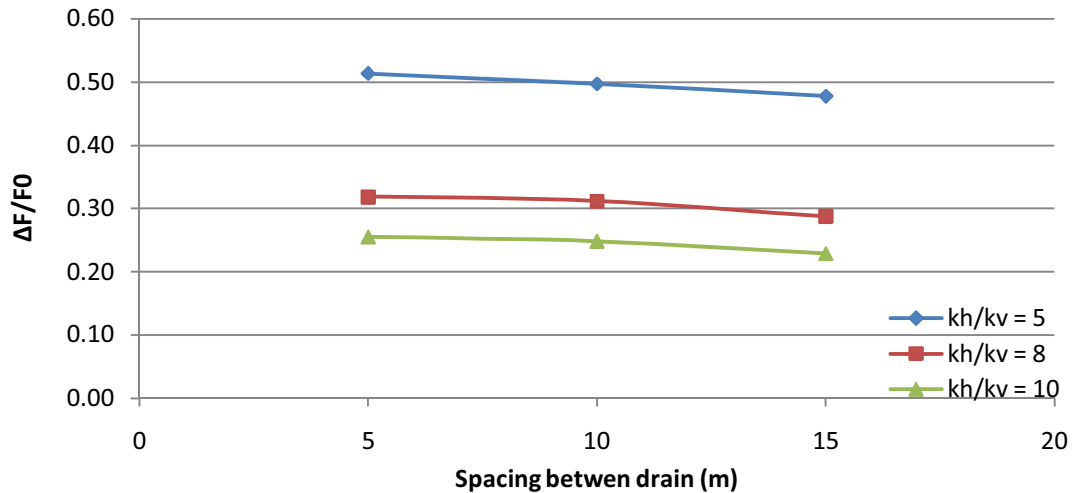


Figure 6.15: Increase in FOS Versus Spacing between drains

6.5. Results and Analysis

It is seen that drains installed along the toe of the slide give the most stability compared to those installed at higher elevations (Fig. 6.9). The FOS rapidly increases with decreasing elevations of drains with respect to slope height. The stability of the slope is also found to increase with increase in the length of drains (Figure 6.10). However, it is also seen that, regardless of the anisotropy ratio, further increase in length beyond 50m does not result in an increase in factor of

safety. This length corresponds to the location at which the drain crosses the critical slip surface. Therefore, in practice, this distance may be used as the critical length of the drain for optimal design. Beyond it, little increase in stability will be registered. As expected, use of a larger spacing between drains leads to a lower increase in FOS (Fig. 6.15). This figure also shows that change in FOS due to drain installation is dependent on the permeability anisotropic ratio.

CHAPTER SEVEN

CONCLUSIONS AND DISCUSSIONS

7.1. Conclusions

This study was focused on the numerical simulation of the performance of horizontal drains on slopes. It made use of the finite difference code TOUGH2 V2 to simulate the changes in the ground water level pattern and the pore-pressure response as a result of horizontal drain installation. The study first presented detailed examination of the field performance of horizontal drains on some selected slopes in the states of Washington and California (Chapter 3). This included the site location, details of the project, geotechnical and geologic records, drain location, instrumentation details, and performance data.

The numerical simulation of the ground water flow using TOUGH2 was verified using the field performance data from a Washington Department of Transportation project site near SR 101 MP69.8 (section 3.1). The effectiveness of the horizontal drainage system is a function of many factors including the drain location, length and spacing, as well as soil properties and slope geometry. Thus, the numerical model was used to perform a parametric study on the effect of the various system parameters on the performance of horizontal drains installed in a homogenous clay slope.

The effectiveness of a drain installation is described in terms of the increase in slope factor of safety as compared to the factor of safety without horizontal drains. The numerical result of the phreatic surface from TOUGH2 was input into the slope stability program XSTABL to perform stability calculations.

Based on an examination of the field records and the parametric study, the following conclusions can be drawn:

- (1) An examination of the field records associated with the case studies presented here showed that in all cases the installation of drains resulted in the lowering of the ground water level and increased stability. The level of the lowered ground water table remained relatively constant even with varying amounts of rainfall. Thus, it can be concluded that the horizontal drains performed well on these sites regardless of the different nature of the geological characteristics and soil profile.
- (2) The anisotropic ratio was identified as the important soil parameter influencing the horizontal drain performance because it changes the profile of the phreatic surfaces significantly (Figure 6.3). Slopes with a higher ratio of permeability (k_h/k_v) stabilized quicker than those with a lower ratio of permeability (section 6.4).
- (3) Drains installed along the toe of the slide give more stability than those installed in higher elevations (Figure 6.9).
- (4) The stability of the slope increased with increasing the length of drains, but decreased when the drains are spaced at larger intervals (Figures 6.10 and 6.11).
- (5) The length of drain extending further from its intersection with the critical failure surface does not provide any significant change in FOS (Figure 6.10).
- (6) The FOS calculated for various slope inclinations (1:2.5 to 1:3.5) confirmed that steeper slopes need more drains than shallower slopes to reach an equal level of stability (Table 6.3).

7.2. Recommendations

This study documented the sound performance of horizontal drains on selected slopes in the states of Washington and California and demonstrated the effectiveness of using numerical simulation to study the effect of system variables on horizontal drain performance. Future research may focus on extending the study in the following aspects:

- (1) It is necessary to have more instrumented sites, with instrumentation data both before and after drain installation. These will facilitate further verification of the numerical model and elicit key variables which affect its performance.
- (2) The permeability and its anisotropy in the numerical simulation were assumed to match the observed piezometric data. On the other hand, use of discharge data would be a better option to back calculate permeability and anisotropy values. This will require the use of discharge measuring devices.
- (3) While the sites documented here have performed well, it is also necessary to identify some sites where horizontal drains have not performed well. The numerical simulation could then be used to identify the conditions that resulted in poor performance.
- (4) The performance of horizontal drains was studied for a homogeneous saturated slope with a low impermeable medium. This study ignored fracture, cracks and vegetation of the slope and these effects may be included in a future analysis.

REFERENCES

- Bahner, E.E. and Jackson, G. (2007). Slope drainage improvement using wick drains installed by HDD methods, Proc. 1st North American Landslide Conference, Vail, Colorado.
- Baligh, M.M. and Azzouz, A.S. (1975). End effects on stability of cohesive slopes. ASCE, Journal of the Geotechnical Engineering Division, 101, pp: 1105-1117.
- Cai, F., Ugai, K., Wakai, A. and Li, Q. (1998). Effects of horizontal drains on slope stability under rainfall by three-dimensional finite element analysis, Computers and Geotechnics, 23: 255-275.
- CALTRANS (2001). Redtop landslide at American Canyon, Geotechnical design report.
- Choi, Y.L. (1974). Design of horizontal drains. J Eng Soc. of Hong Kong. December: 37-49.
- Crenshaw, B.A. and Santi, P.M. (2004). Water table profiles in the vicinity of horizontal drains. Environmental and Engineering Geoscience, Vol. 10, No.3, pp. 191-201.
- East, G.R.W. (1974). Remedial measures and case histories: Inclined plane slope failures in the Auckland Waitemata soils, Three cases with different remedial measures. Proc. Symp. Stability of Slopes in Natural Ground, Nelwon, New Zealand Geomechanics Society, 5.17-5.34.
- Edwards, A.L. (1972). TRUMP: A computer program for transient and steady state temperature distributions in multidimensional systems, National Technical Information Service, National Bureau of Standards, Springfield, VA.
- Golder Associates Inc. (2000). Geotechnical report, Landslide on US 101 at MP 322, Lilliwaup, WA.
- Hutchinson, J.N. (1977). Assessment of the effectiveness of corrective measures in relation to geological conditions and types of slope movement, Theme 3: General Report. Bulletin of the International Association of Engineering Geology, Vol. 16: 131-155.
- Kenney, T.C., Pazin, M., and Choi, W.S. (1976). Horizontal drains in homogeneous slopes. 29th Canadian Geotech. Conf., Vancouver, VI.1-VI.15.
- Kenney, T.C., Pazin, M., and Choi, W.S. (1977). Design of horizontal drains for soil slopes. Transp. Res. Record, Transportation Research Board, No. 749: 6-10.
- Kleinfelder Inc. (2006). Geotechnical report, Landslide on US 101 at MP 69.8, South of Aberdeen, WA.

Lamb, S.E. (1980). Embankment stabilization by use of horizontal drains. Transp. Res. Record, Transportation Research Board, No. 749:6-10.

Landau Associates Inc. (1993). Geotechnical study, SR 530, Montague Creek Bridge to Hazel Vicinity Snohomish County, WA.

Lehua Pan. (2008). User information for WinGridder Version 3.0. Lawrence Berkeley National Laboratory. Paper LBNL-273E.

Lau, K.C., and Kenney, T.C. (1983). Horizontal drains to stabilize clay slopes, 241-249.

Mallawaratchie, D.P., Thuraiamy, M., Jayamanne, J. and Attanayake, A.M.L. (1996). Stage-1 remedial measures for stabilizing landslide at Beragala Haliela Road, In: Senneset K. (ed.). Proceedings of the Seventh International Symposium on Landslides, Vol.3, Norway, Trondheim: 1759-1764.

Martin, R.P., Siu, K.L., and Premchitt, J. (1994). Performance of horizontal drains in Hong Kong. Special Project Report, SPR 11/94, Geotechnical Engineering Office, Civil Engineering Department, Hong Kong.

Moridis, G. and K. Pruess. (1998). T2SOLV: An Enhanced Package of Solvers for the TOUGH2 Family of Reservoir Simulation Codes, Geothermics, Vol. 27, No. 4, pp. 415 – 444.

Narasimhan, T.N. (1975). A unified numerical model for saturated-unsaturated groundwater flow; Ph.D. thesis. Lawrence Berkeley Laboratories, University of California.

Narasimhan, T.N. and P.A. Witherspoon. (1976). An Integrated Finite Difference Method for Analyzing Fluid Flow in Porous Media, Water Resour. Res., Vol. 12, No. 1, pp. 57 – 64.

Nonveiller, E. (1970). Stabilization of landslides by means of horizontal borings. European Civil Engineering, 5:221-228.

Pathmanathan, M.L. (2009). CD of field performance of horizontal drains on slopes, Washington State University, CEE/GEOT/2009/.

Pruess, K., Oldenburg, C., and Moridis, G. (1999). TOUGH2 USER'S GUIDE, VERSION 2.0. LBNL-43134. Earth Sciences Division, Lawrence Berkeley National Laboratory, University of California.

Rahardjo, H., Hritzuk, K.J., Leong, E.C., and Rezaur, R.B. (2002). Effectiveness of horizontal drains for slope stability, Engineering Geology, 69: 295-308.

Richards, L. (1931). Capillary conduction of liquids through porous mediums. *Physics* 1: 318–333

Samani, N., Kompani-Zare, M., Seyyedian, H., and Barry, D.A. (2005). Flow to horizontal drains in isotropic unconfined aquifers. *Journal of Hydrology*: 1-15.

Santi, P.M., Elifritis, C.D., and Liljegren, J.A. (2001). Design and installation of horizontal wick drains for landslide stabilization. *Transportation research board record* 1757, pp: 58-66.

Sharma, S. (1996), XSTABL Version 5.201. Interactive Software Designs Inc., Moscow, ID.

Smith, T.W. and Stafford, G.V. (1957). Horizontal drain on California Highways. *J Soil Mech and Found Div.* 83(3):1-26.

Stanton, T.E. (1948). California experience in stabilizing earth slopes through the installation of horizontal drains by the Hydrauger method. *Proceedings, 2nd International conference on soil mechanics and foundation engineering, Rotterdam, the Netherlands, Vol. 3* , pp: 256-260.

Tong, P.Y.L. and Maher, R.O. (1975). Horizontal drain as a slope stabilization measure. *J. Engrg Soc. of Hong Kong*: 15-27.

Tsao, T.M., Wang, M.K., Chen, M.C., Takeuchi, Y., Matsuura, S., and Ochiai, H. (2005). A case study of the pore water pressure fluctuation on the slip surface using horizontal borehole works on drainage well, *Engineering Geology*, 78: 105-118.

WSDOT (2007). Geological assessment and mitigation alternatives, Bogachiel landslide, US 101, XL-2953, Vicinity mile post 184.10 to 184.65, Jefferson county, WA.